Cellular and molecular mechanisms of cadmium neurotoxicity and cadmium interaction with *APOE4* on memory impairment

Megumi T. Matsushita

A dissertation

submitted in partial fulfillment of the

requirements for the degree of

Doctor of Philosophy

University of Washington

2022

Reading Committee:

Zhengui Xia, Chair

Julia Yue Cui

Thomas Burbacher

Program Authorized to Offer Degree:

Environmental and Occupational Health Sciences – Public Health

University of Washington

Abstract

Cellular and molecular mechanisms of cadmium neurotoxicity and cadmium interaction with *APOE4* on memory impairment

Megumi T. Matsushita

Chair of the Supervisory Committee:

Zhengui Xia, PhD., Professor

Department of Environmental and Occupational Health Sciences

Cadmium (Cd) is a ubiquitous toxic heavy metal and an emerging neurotoxicant. While Cd neurotoxicity is increasingly documented in epidemiology and toxicology studies at levels relevant to the general US population, the underlying mechanisms are not yet well understood. This dissertation describes two studies that aim to elucidate the cellular and molecular mechanisms of Cd neurotoxicity impairments of hippocampus-dependent memory.

Cd has the ability to mimic calcium ions (Ca^{2+}) and interfere with intracellular Ca^{2+} levels, Ca^{2+} binding activity, and Ca^{2+} signaling. However, little is known about Cd's effects on Ca^{2+} activity in neurons at low level exposures. In the first study, *in vivo* imaging of neuronal Ca^{2+} activity in freely behaving mice demonstrated that exposure to environmentally relevant levels of Cd inhibits calcium activity.

Environmental factors such as Cd exposure and gene-environment interactions (GxE) may increase Alzheimer's disease (AD) and accelerate cognitive decline. Apolipoprotein E4

(*APOE4*) is the strongest known genetic risk factor for late-onset AD associated with accelerated cognitive decline in carriers of E4 alleles. Our laboratory has found correlative evidence suggesting that impairment of adult neurogenesis, a process of generation of functional new neurons through adulthood with implications on hippocampus function, may be a key mechanism underlying Cd-induced impairment of hippocampus-dependent memory. The second study utilized an inducible Cre-lox recombination transgenic mouse line that genetically and conditionally stimulate adult neurogenesis with humanized ApoE4 knock-in (ApoE4-KI) background. Our results demonstrate that stimulation of adult neurogenesis after Cd exposure rescued mice from Cd-induced impairments of hippocampus-dependent memory.

The studies described in this dissertation are the first to describe Cd effects on brain Ca^{2+} activity *in vivo* in freely behaving mice and provide strong evidence for a causal link between adult neurogenesis and memory impairment in a GxE model of ApoE4 and Cd, respectively. Together, these studies describe cellular and molecular mechanisms underlying Cd neurotoxicity at exposure levels relevant to the general population.

Table of Contents

List of Figures

List of Abbreviations

AD: Alzheimer's disease
aNPCs: adult neural progenitor cells
APOE, ApoE: apolipoprotein E
APP: amyloid precursor protein
ATSDR: Agency for Toxic Substances and Disease Registry
BrdU: 5-bromo-2'-deoxyuridine
Ca^{2+}: calcium ion
CaM: calmodulin
caMEK5: constitutively active MEK5
cAMP: cyclic-AMP
CCF: cued and contextual fear conditioning
Cd: cadmium
CNMF-E: constrained non-negative matrix factorization for microendoscopic data
CS: conditioned stimulus
CREB: cAMP-response-element-binding protein
DG: dentate gyrus
DCX: doublecortin
eGFP: enhanced green fluorescent protein
EPA: Environmental Protection Agency
ERK5: extracellular signal-regulated kinase 5
FOV: field of view
GECI: genetically encoded calcium indicators
GEE: generalized estimating equations
GxE: gene-environment interaction
IARC: International Agency for Research on Cancer
ICP-MS: inductively coupled plasma mass spectrometry
IDPS: Inscopix Data Processing Software
K_D: equilibrium dissociation constant
KI: knock-in
LTD: long-term depression

LTP: long-term potentiation

MAPK: mitogen activated protein kinase

MSK1: mitogen and stress-activated kinase 1

NHANES: National Health and Nutrition Examination Survey

NOL: novel object location

NPC: neural progenitor cells

OB: olfactory bulb

OF: open field

PFA: paraformaldehyde

PKA: cAMP-dependent protein kinase

PSEN1: presenilin1

PSEN2: presenilin2

REML: restricted maximum likelihood

RfD: reference dose

RTI: Ready-to-Image

SGZ: subgranular zone

SVZ: subventricular zone

TSA: tyramide signal amplification

US: unconditioned stimulus

Acknowledgements

It is impossible for me to put to words the immense gratitude I have for everyone who has had a part in my journey through graduate school. Nonetheless, I will do my best here.

First and foremost, I would like to thank Zhengui for being an extraordinary mentor both in and out of the lab. I am one of many mentees who has had the privilege to learn and grow under your guidance and infectious passion for science. Through the countless hours you have spent with me in meetings and reviewing abstracts, manuscripts, posters, presentations, I have learned to be a better scientist, writer, and communicator both orally and visually. I owe much of my success to your generosity and unshakeable belief in me, especially at times when I felt my weakest and most vulnerable. I am here today because you saw possibilities in me as a graduate student and a scientist, and for that I am forever grateful.

I would like to thank my dissertation committee members, Julia Cui, Tom Burbacher, and Libin Xu for coming together to support my academic and professional growth. I have so much respect for each of you and your work, and appreciate all of your helpful insights and incredible support.

I am incredibly thankful for the support that I have had over the years in the Xia lab. Hao Wang has been my big brother in the lab that I have looked up to and learned from since day one—it has been inspirational to watch you grow as a scientist, and I thank you for your feedback and support with everything. Glen Abel is the real MVP of the lab who made sure everything was in order so that our experiments can go on; thank you for your friendship inside and outside the lab and numerous coffee/baked good runs. Liang Zhang shared an office space with me in my early days in the lab and challenged me to be a critical thinker both in science as well as in numerous musings about life.

I thank our collaborators, without whom none of my dissertation work would have been possible: Dan Storm, Larry Zweifel, and Richard Palmiter. I am especially grateful for the

generosity of Richard and his lab, whose collaboration enabled me to pursue my ideas for my dissertation. Jane Chen spent countless hours guiding me through surgeries and imaging to make sure my experiments went smoothly, and Sekun Park and Scott Ng-Evans helped me tremendously with troubleshooting behavior equipment.

I am thankful to be a part of the DEOHS community. Former and current toxicology faculty, as well as Tania Busch-Isaksen and Nicole Errett have taught me so much through their expertise and experiences; you are all incredible and inspirational. I am thankful for the support of DEOHS staff: OAS past and present, especially Trina Sterry, Veronica James, Janet Hang, Grace Wong, Christine Tran, and Hayley Levanthal, as well as Helen Lee and Mary Saucier—you all were there for me whenever I needed support. Lisa Hayward and BJ Cummings from UW Superfund Research Program have sparked my interest in contextualizing science in social issues and communicating my work to broader audiences. Faculty and fellow trainees in the EP/T fellowship have provided me with valuable comments. Best wishes and warmest regards to Team Tox, Team Team, and PhD cohort-ish for your support throughout graduate school—I could not have gotten through this without you.

I am also thankful for the numerous staff members at the DCM animal facilities and EH lab, as well as UW custodians, facilities workers, and librarians who work tirelessly behind the scenes to make sure my work can be carried out, especially through the uncertain times following COVID-19 related shutdowns.

Finally, thank you to my friends and family for being my constant support through graduate school and the additional isolation brought upon by the COVID-19 pandemic. I especially want to thank my parents Keiichiro and Uyen and my siblings Kenichi and Kaoru, as well as Squad, Money Mellon alums, Chili Chilly Chilies, and my queer family—thank you for reminding me of a world of beautiful things outside of school. And of course, Annie—thank you for caring for me when I forget to, and for helping me back up when I needed it the most.

Dedication

To my *obāchan*, Shōko.

Chapter 1. Introduction

1.1 Cadmium as a public health concern

Cadmium (Cd) is a naturally occurring heavy metal, present in the environment as a mineral compound in ores with zinc, copper, lead, and phosphorous (Godt et al., 2006; Méndez-Armenta and Ríos, 2007). Cd exists in only one oxidation state (+2), is highly water soluble, and forms ionic complexes with proteins, allowing for fate and transport through the biogeochemical cycle (Cullen and Maldonado, 2013) and rapid uptake in organisms (Clemens, 2006; Groten et al., 1990). While volcanos and natural weathering of rock contribute to Cd emissions, anthropogenic emission sources of Cd ultimately account for much of human exposures to Cd. Cd has been widely used in industrial manufacturing processes and commercial products, such as anticorrosive coatings, metal alloys, jewelry, nickel-Cd batteries, and vibrant yellow/orange paint pigments (Godt et al., 2006). Notable anthropogenic emission sources include industrial production of Cd-containing products, electronics recycling facilities, and through disruption of natural geochemical cycles, i.e. phosphorous rock for fertilizer (Godt et al., 2006). Its wide use and disposal have led to Cd being ranked in the top 10 of the US Agency for Toxic Substances and Disease Registry (ATSDR) Substance Priority List. This list includes substances of significance to Superfund sites that are determined to pose the most significant potential threat to human health due to their frequency, toxicity, and potential for human exposure at the sites (ATSDR, 2019).

The main sources of exposure to Cd for the general population are smoking and diet due to plant uptake from Cd-contaminated soil (Satarug and Moore, 2004). The estimated daily intakes of Cd in nonsmoking US adults are 0.35 μg Cd/kg/day for men, 0.30 μg Cd/kg/day for women (Choudhury et al., 2001). Kim et al, 2019 estimates that significant Cd intake result from consumption of common food items such as spaghetti, cereals, bread, potato chips, spinach,

lettuce, tortillas, and rice (Kim et al., 2018). An estimated 3-7% of ingested Cd is absorbed through the gastrointestinal tract and accumulates in many internal organs (Satarug et al., 2010). Smoking is a significant source of Cd exposure which almost doubles the body burden of Cd in smokers compared to non-smokers (Ellis et al., 1979). A cigarette usually contains 1-2 μg Cd, of which 10% is estimated to be absorbed (WHO 1992). The decline in smoking rates in the US population as a result of public health policies has reduced Cd exposure (measured by urine Cd levels) by 34.3% from 1988-1994 to 2003-2008, adjusted for age, sex, and race/ethnicity (Tellez-Plaza Maria et al., 2012). Nevertheless, general population exposure to Cd remains a public health concern due to the long biological half-life of 10-30 years (Suwazono et al., 2009) and the low excretion rates estimated to be 0.001% of body Cd per day (Satarug and Moore, 2004).

Epidemiological studies of the health effects of Cd exposure largely use blood and urine Cd as biomarkers of exposure for recent and chronic exposures, respectively (Adams and Newcomb, 2014). Based on a 2017-2018 National Health and Nutrition Examination Survey (NHANES), the geometric mean blood Cd levels in the general US population are 0.241μg/L (males, all ages: 0.212 μg/L; females, all ages: 0.271 μg/L; age 20+ years: 0.295 μg/L), while urine Cd levels are 0.132 μg/L (males, all ages: 0.122 μg/L; females, all ages: 0.143 μg/L; age 20+ years: 0.179 μg/L) . Compared to data from NHANES 2007-2008, for which the geometric mean blood Cd levels were 0.299 μg/L in males, 0.331 μg/L in women and urine Cd levels were 0.179μg/L in men, 0.191μg/L in women (ATSDR, 2012), there is a general decreasing trend in detected Cd levels in the general US population. In comparison, the geometric means of blood Cd levels for current smokers of ages ranging from 20 to over 70 years are 0.58-0.95μg/L in men, 0.69-1.17μg/L in women; urine Cd levels of the same group are 0.1-0.65μg/L in men and 0.17-0.91μg/L in women (Adams and Newcomb, 2014).

Major health endpoints of Cd exposure of concern include kidney toxicity as well as carcinogenicity. Cd is classified as a Group 1 human carcinogen by the International Agency for

Research on Cancer (IARC) based on occupational exposures to Cd through smelting, welding, and battery production which lead to considerably higher exposures, predominantly through inhalation, than the general population (ATSDR, 2012). The US Environmental Protection Agency (EPA) established an oral reference dose (RfD; estimate of daily oral exposure to human populations including sensitive subgroups that is likely to be without an appreciable risk of health effects during a lifetime) of 1 µg Cd/kg/day based on a chronic oral exposure that would result in a kidney Cd concentration of 200µg/g ww (ATSDR, 2012). More recent studies have found that environmental Cd exposure at levels found in the general population is associated with liver disease such as hepatic necroinflammation, non-alcoholic fatty liver disease, and non-alcoholic steatohepatitis, with individuals in the top quartile of urinary Cd having over a threefold increased risk of liver disease mortality but not liver cancer related mortality (Hyder et al., 2013).

1.2 Neurotoxicity of cadmium

Increasing evidence in the last few decades in humans and model organisms suggests that Cd is a potent neurotoxicant. Recent epidemiological studies suggest that Cd is neurotoxic at much lower levels than safe levels established through risk assessment based on renal and carcinogenic toxicity end points, and more significantly, at levels present in the general population. Epidemiological studies using data from the US National Health and Nutrition Examination Survey (NHANES) report associations between Cd levels and cognitive function in children aged 6-15 years (Ciesielski et al., 2012), adults age 20-59 (Ciesielski et al., 2013), and adults older than 60 years (Li et al., 2018).

An increasing body of literature in rodents, including studies from our laboratory, have demonstrated brain Cd accumulation, cellular dysfunction, and behavioral effects following repeated doses (subacute, subchronic, and chronic) through oral, intranasal, and intraperitoneal

exposure routes (Choudhuri et al., 1996; Czarnecki et al., 2011; Kim et al., 2016; Namgyal et al., 2020; Wang et al., 2017, 2019; Zhang et al., 2019b). High level exposures through intraperitoneal routes and 10 mg/L or higher $CdCl_2$ through drinking water have been commonly used to study the neurological effects of Cd exposure in mice (Antonio et al., 1998; Chen et al., 2014; Gonçalves et al., 2010; Honda et al., 2013; Marini et al., 2018; Qu et al., 2018). Only one of these studies report Cd levels, approximately 30-60 ng/g tissue in the brain and 5-10 µg/L in plasma with 10, 25, and 50 mg/L Cd exposures through drinking water for 6 weeks (Chen et al., 2014). Previous publications from our laboratory reported significant and persistent hippocampus-dependent learning and memory effects in mice of different genetic backgrounds exposed to environmentally relevant levels of Cd (0.6 mg/L $CdCl_2$ and 3 mg/L Cd as $CdCl_2$) through drinking water (Wang et al., 2017, 2020b; Zhang et al., 2019b), providing direct evidence of Cd neurotoxicity in controlled laboratory experiments. We reported blood Cd levels of approximately 0.3µg/L, within the range of the general US population.

While some reports of neurological effects of Cd have been published, Cd has not been generally associated with neurotoxicity due to a paucity of strong epidemiological evidence (ATSDR, 2012). It is critical to note that epidemiological studies mentioned here investigating Cd neurotoxicity were not included in the ATSDR toxicological review, which was released for public comment in 2008 and published in 2012.

1.3 Calcium signaling in learning and memory

The brain can adapt to new stimuli and associations, thus allowing the organism to learn and remember environmental cues and adapt to changing environments. The acquisition, storage, and retrieval of memory is critical to our daily lives as functional humans. The hippocampus is a key brain region for the integration of somatosensory information and required

for the formation of memory (Dudai et al., 2015; Squire et al., 2015; Yonelinas et al., 2019). The hippocampus is comprised of distinct structures and highly defined neuronal circuits (Knierim, 2015). Recent work suggest that dorsal and ventral hippocampus contribute differentially to learning and memory due to their distinct neuronal connections, with dorsal hippocampus CA1 region being responsive to spatial contexts (Besnard et al., 2020; Izquierdo et al., 2016; Jimenez et al., 2020; Riaz et al., 2017).

Neuron activity causes rapid changes in intracellular free calcium ion (Ca^{2+}) concentrations. Neuronal plasticity is largely dependent on Ca^{2+} signaling pathways that strengthen or weaken synaptic transmission through physical changes in individual neurons that lead to long-term potentiation (LTP) or depression (LTD) (Whitlock, 2006). The modulation of synaptic transmission through LTP and LTD is a critical process affecting cognitive health and disease (Heck et al., 2015). There are two major timescales of plasticity. Short term plasticity is initiated by the influx of Ca^{2+} through glutamate receptors and voltage-gated Ca^{2+} channels. The resulting transient increase in cytosolic Ca^{2+} activates Ca^{2+} dependent pathways which results in enhancement of membrane conductance (postsynaptic) and increase of transmitter release probability (presynaptic) (Bliss and Cooke, 2011; Zucker and Regehr, 2002). Long term plasticity requires regulation of synaptic protein transcription through the cyclic-AMP (cAMP) dependent signaling cascade mediated by cAMP-dependent protein kinase (PKA) and various mitogen activated protein kinases (MAPK). Ultimately, cAMP-response-element-binding protein (CREB) binds to specific DNA sequences to up- or downregulate synaptic proteins, required for long-term memory (Wang and Storm, 2003). Ca^{2+} stimulation of CREB-mediated transcription downstream of MEK1/2, ERK1/2, and mitogen and stress-activated kinase 1 (MSK1) during contextual memory formation is mediated by cAMP and regulated by Ca^{2+}-stimulated adenylyl cyclases (Sindreu et al., 2007). Contextual memory training and retrieval specifically activates and

reactivates ERK 1/2 in excitatory neurons in the CA1 region of the hippocampus (Sindreu et al., 2011, 2007; Zamorano et al., 2018).

Ca^{2+} indicators such as genetically encoded Ca^{2+} indicator GCaMP6 have been developed over the years to visualize Ca^{2+} activity *in vivo*. Ca^{2+} activity has been reported in numerous *in vivo* imaging studies during learning and memory tasks in the hippocampus (Jimenez et al., 2020; Sheintuch et al., 2017; Ziv et al., 2013). Work in our lab and others have further demonstrated that subsets of cells are consistently activated in learning and memory tasks, suggesting the presence of memory engrams that rely on Ca^{2+}-dependent signaling to consolidate memory (Josselyn et al., 2015; Josselyn and Tonegawa, 2020; Zhang et al., 2019a).

1.4 Cadmium potential to impair calcium signaling

Biochemically, Cd is a soft ion that mimics Ca^{2+} ions, and its lack of oxidation reduction reactivity limits its interactions to proteins with metal binding sites rich in soft ligands such as sulfhydryl groups (Lund et al., 2018). A large body of evidence (reviewed in Thévenod et al., 2018) suggest that Cd can be transported into cells through mimicry and disrupt cytosolic Ca^{2+} levels (Biagioli et al., 2008; Choong et al., 2014) as well as direct and indirect effects on various Ca^{2+}-binding proteins, kinases, growth factors, and second messengers (Templeton and Liu, 2018; Thévenod et al., 2018). Notably, the only studies referenced in neurons or acute slices were related to Cd block effects of voltage-gated Ca^{2+} dependent channels (Fox et al., 1987; Huguenard, 1996; Liu et al., 2001; Thévenod and Jones, 1992) in concentrations ranging from tens of uM to mM level Cd.

There is a research gap in understanding the molecular mechanisms underlying the neurotoxic effects of Cd *in vivo*. *In vivo* Ca^{2+} imaging using GCaMP6 provides an effective method to investigate the effects of Cd on Ca^{2+} activity, thus leading to Specific Aim 1 to record single-

cell resolution Ca^{2+} transients in the hippocampal CA1 region to investigate the effects of Cd exposure on Ca^{2+} activity *in vivo* during the acquisition and retrieval of contextual memory.

1.5 Alzheimer's disease and gene-environment interaction

Dementia is characterized by impairment of cognition, function, and behavior with a high and costly burden of disease (Reitz et al., 2011). Alzheimer's disease (AD) is the most common cause of dementia, accounting for an estimated 60-80% of cases and $305 billion in health care costs in 2020 (Alzheimer's Association, 2020). In 2022, an estimated 6.5 million people in the United States live with AD (Alzheimer's Association, 2022). With increasing population aging and growth, the national disease burden is expected to rise with an annual number of new AD cases projected to reach 13.8 million by 2060 (Rajan et al., 2021). The pathological hallmarks of AD are amyloid plaques and neurofibrillary tangles (Ballard et al., 2011). Accumulation and aggregation of mutant form of the amyloid-β peptide (Aβ-42) from improper cleavage of the amyloid precursor protein (APP) is hypothesized to initiate a cascade that progresses into neuronal loss, synaptic loss, brain atrophy, and inflammation, leading to AD (Ballard et al., 2011; Kim et al., 2009).

Numerous epidemiology studies have identified various risk and protective factors, including comorbidities with cerebrovascular disease, blood pressure, type 2 diabetes, genetics, and lifestyle factors such as diet, physical activity, and intellectual activity (Alzheimer's Association, 2020; Ballard et al., 2011; Bartolotti and Lazarov, 2016). Well established genetic mutations associated with AD include autosomal dominant mutations of genes encoding *APP* and presenilin (*PSEN1*, *PSEN2*) which lead to increased production of Aβ-42. Specifically, *APP* and *PSEN* mutations are mechanistic causes of early-onset familial AD (Ballard et al., 2011). These autosomal dominant mutations are estimated to account for less than 6% of all AD cases or about 110 of every 100,000 people in the United States (Bateman et al., 2011; Bekris et al., 2010).

In stark contrast, approximately 1 in every 9 people older than 65 years of age have Alzheimer's dementia in the United States (Alzheimer's Association, 2022). The strongest known genetic risk factor for late-onset AD is the Apolipoprotein E (*APOE*) gene, which encodes for a lipid transporter that regulates lipid homeostasis (Mahley and Rall, 2000). Compared to ε4-non carriers, one allele of ε4 increases AD risk 2-3 fold while two ε4 alleles increases AD risk 12 fold even in the absence of AD pathology (Kim et al., 2009; Liu et al., 2013).

There has been increasing research interest in understanding the contribution of combinations of genetic and non-genetic risk factors in AD pathogenesis (Finch and Kulminski, 2019). Environmental factors are of particular interest to AD researchers and clinicians as environmental exposures are modifiable through behavioral and policy changes. It is possible that a **gene-environment interaction (GxE)**—combination of adverse effects from genetic risk factors and environmental exposures—can contribute to AD onset and/or severity through common mechanisms. However, little is known about the effects of GxE on cognitive function or the underlying mechanisms. Studies of postmortem brain Cd concentrations in AD patients and nondemented controls report contradicting findings (Szabo et al., 2016; Ward and Mason, 1987; Xu et al., 2018). A recent study of 4064 participants aged >60 years old with available Cd data and no other missing information at baseline from the 1999-2004 NHANES found a significant association between blood Cd levels and AD mortality. Specifically, participants with high Cd levels (> 0.6μg/L) exhibited a 3.83-fold increased risk of AD mortality compared with participants with low blood Cd levels (< 0.3μg/L) (Min and Min, 2016). In another study, urinary Cd was associated with a 58% higher rate of AD mortality per 0.51μg/L increase in urinary Cd (Peng et al., 2017). While these studies suggest a possible link between Cd levels and AD in human patients, both studies are highly limited by possible misclassification of AD cases, as well as numerous confounding factors. Furthermore, they lack any insight into the interaction of genetics

with environmental exposure, their potentially synergistic effect on cognitive function, and underlying mechanisms.

1.6 Adult neurogenesis

Neurogenesis is the process of stem cell proliferation, neuronal differentiation, and migration and integration in the nervous system. While neurogenesis is ubiquitous in the developing brain, the process persists through adulthood, albeit restricted to a few discrete brain regions with tight regulation of molecular and network inputs. The process of adult neurogenesis describes the generation of neurons from a subset of neural progenitor/ cells (NPCs) in a quiescence state into fully differentiated neurons that integrate into existing neuronal circuits (Aimone et al., 2014; Gonçalves et al., 2016). In the adult mammalian brain, the NPC population is restricted to two neurogenic regions: the subventricular zone (SVZ), which gives rise to new inhibitory neurons in the olfactory bulb, and the subgranular zone (SGZ) of the hippocampal dentate gyrus (DG), which gives rise to excitatory granular cells DG (Aimone et al., 2014; Gage, 2000). Hippocampal adult neurogenesis plays an important role in hippocampus-dependent learning and memory. The reduction or suppression of adult neurogenesis has been observed to cause decline in the performance of spatial learning and memory in mice (Denny et al., 2014; Dupret et al., 2007) as well as impairment in pattern separation (Pan et al., 2012). Likewise, the activation of adult neurogenesis has been observed to enhance spatial pattern discrimination and spatial learning and memory as well as hippocampus-dependent long-term memory (Choi et al., 2018; Wang et al., 2014).

While adult neurogenesis has been observed in numerous mammals including non-human primates and humans (Eriksson et al., 1998) in the decades following its discovery (Altman and Das, 1965), there has been skepticism and controversy over whether adult neurogenesis is

relevant to the human brain. Two notable studies of hippocampal adult neurogenesis presented findings directly contradicting each other (Boldrini et al., 2018; Sorrells et al., 2018). Much of this controversy has been speculated to be from differences in methodological (i.e. duration of postmortem delay, fixation methods, and staining protocols) and analysis criteria between studies while both utilized immunostaining techniques in postmortem tissue (Gage, 2019; Kuhn et al., 2018). Nevertheless, strong evidence supporting persistent adult neurogenesis into the ninth decade of life in the human hippocampus have been presented in cell birth dating studies utilizing synthetic thymidine analog 5-bromo-2'-deoxyuridine (BrdU) (Eriksson et al., 1998) and radiocarbon dating (Ernst et al., 2014; Spalding et al., 2013).

Adult neurogenesis is highly regulated and can be modulated by numerous stimuli over the course of maturation. The neurogenic niche in the SGZ provides a microenvironment that permits and supports neurogenesis, regulated by surrounding astrocytes, and vasculature through network inputs and neuromodulation, local signaling, and external stimuli (Aimone et al., 2014). Adult neurogenesis has been reported to be affected by age (Kuhn et al., 1996) as well as activities such as mating and exercise (Aimone et al., 2014; Ming and Song, 2011). Extrinsic factors such as stress (Schoenfeld and Gould, 2012), diet (Stangl and Thuret, 2009) can also impact neurogenesis levels. Furthermore, environmental toxicants including heavy metals have been observed to impair neurogenesis (Adamson et al., 2018; Engstrom and Xia, 2017; Wang et al., 2019). A recent study in our laboratory reported a functional rescue of impairment of hippocampus-dependent memory (Wang et al., 2020b) and olfaction (Wang et al., 2020a) upon stimulation of adult neurogenesis, suggesting that impairment of adult neurogenesis underlies Cd-induced impairments in both cognition and olfaction.

There is also evidence that adult neurogenesis is impaired in AD patients, implicating a potential role of adult neurogenesis in neurodegeneration in AD. A recent study of postmortem brain tissue from AD patients and cognitively normal controls found that severity of AD as

characterized by Braak stage is associated with a sharp decline of adult neurogenesis levels (Moreno-Jiménez et al., 2019). In two recent studies utilizing a humanized knock-in (KI) mouse model of AD expressing human ε4 (ApoE4-KI) or human ε3 alleles (ApoE3-KI) under the control of the endogenous mouse ApoE promoter, we reported a GxE effect of ApoE4 on hippocampus-dependent learning and memory in mice exposed to lead (Engstrom and Xia, 2017) as well as Cd (Zhang et al., 2019b). Furthermore, Cd impaired neuronal differentiation of adult-born neurons in the hippocampus of ApoE4-KI mice (Zhang et al., 2019b). Combined, these data suggest that impairment of adult hippocampal neurogenesis may be one of the underlying mechanisms of the GxE effect of ApoE4 and Cd on cognitive function. However, these findings were correlative. This leads to Specific Aim 2, where I aim to establish a direct link between GxE effect of ApoE4 and Cd on cognition and impairment in adult neurogenesis by utilizing a tamoxifen-mediated Cre-Lox transgenic mouse line in an ApoE4-KI background that allows for conditional and genetic stimulation of adult neurogenesis.

1.7 Goals of dissertation research

While research results reported over the last 20 years are converging to suggest that Cd is a potent neurotoxin, the cellular and molecular mechanisms underlying hippocampus-dependent memory impairments at exposure levels relevant to the general US population are not yet well understood. *The overall goal of my work is to elucidate the underlying cellular and molecular mechanisms of Cd neurotoxicity*.

As reviewed in Sections 1.3 and 1.4, there is some evidence of Cd impairment of intracellular Ca^{2+} levels and disruption of Ca^{2+}-dependent signaling pathways. The molecular mechanisms of learning and memory are known to be dependent on transient increases in intracellular Ca^{2+}. We identified a research gap in understanding the molecular mechanisms

underlying neurotoxic effects of Cd. We hypothesized that Cd impairs Ca^{2+} activity in the hippocampus, contributing to impairments in learning and memory.

As reviewed in Sections 1.5 and 1.6, there is emerging evidence of a GxE interaction effect of Cd and *APOE4* on cognitive impairment. Our recent study reported a correlation between a GxE effect on impairment of hippocampus-dependent memory and impairment of adult neurogenesis. Here I hypothesized that the GxE effect of ApoE4 and Cd on hippocampal adult neurogenesis contributes to impairment of cognitive function. To test these hypotheses, I proposed the following specific aims:

Specific Aim 1: Determine if Cd disrupts Ca^{2+} transients of neurons in CA1 region of the hippocampus during an associative learning paradigm. I utilize *in vivo* Ca^{2+} imaging in awake, freely moving C57BL/6 mice to measure Ca^{2+} activity in neurons virally transfected with engineered Ca^{2+} sensor GCaMP6.

Specific Aim 2: Determine if the GxE impairment of learning and memory can be reversed by a conditional genetic enhancement of adult neurogenesis. This functional recovery study aims to establish a direct link between Cd-induced impairment in adult neurogenesis and cognition in a rodent GxE model.

Chapter 1 introduced the context of the dissertation. Chapter 2 describes Cd effects on Ca^{2+} activity *in vivo* in mice during an associative learning paradigm. Chapter 3 describes the functional recovery study. Chapter 4 provides a summary and conclusions of the dissertation.

1.8 References

Adams SV, Newcomb PA. 2014. Cadmium blood and urine concentrations as measures of exposure: NHANES 1999–2010. *J Expo Sci Environ Epidemiol* **24**:163–170. doi:10.1038/jes.2013.55

Adamson SX-F, Shen X, Jiang W, Lai V, Wang X, Shannahan JH, Cannon JR, Chen J, Zheng W. 2018. Subchronic Manganese Exposure Impairs Neurogenesis in the Adult Rat Hippocampus. *Toxicol Sci* **163**:592–608. doi:10.1093/toxsci/kfy062

Aimone JB, Li Y, Lee SW, Clemenson GD, Deng W, Gage FH. 2014. Regulation and Function of Adult Neurogenesis: From Genes to Cognition. *Physiol Rev* **94**:991–1026. doi:10.1152/physrev.00004.2014

Altman J, Das GD. 1965. Autoradiographic and histological evidence of postnatal hippocampal neurogenesis in rats. *J Comp Neurol* **124**:319–335. doi:https://doi.org/10.1002/cne.901240303

Alzheimer's Association. 2022. 2022 Alzheimer's Disease Facts and Figures. *Alzheimers Dement* **18**.

Alzheimer's Association. 2020. 2020 Alzheimer's disease facts and figures. *Alzheimers Dement* **16**:391+.

Antonio MT, Benito MJ, Leret ML, Corpas I. 1998. Gestational administration of cadmium alters the neurotransmitter levels in newborn rat brains. *J Appl Toxicol* **18**:83–88. doi:https://doi.org/10.1002/(SICI)1099-1263(199803/04)18:2<83::AID-JAT480>3.0.CO;2-1

ATSDR. 2019. 2019 Substance Priority List. https://www.atsdr.cdc.gov/spl/index.html

ATSDR (Agency for Toxic Substances and Disease Registry). 2012. Toxicological Profile for Cadmium.

Ballard C, Gauthier S, Corbett A, Brayne C, Aarsland D, Jones E. 2011. Alzheimer's disease. *The Lancet* **377**:1019–1031. doi:10.1016/S0140-6736(10)61349-9

Bartolotti N, Lazarov O. 2016. Lifestyle and Alzheimer's DiseaseGenes, Environment and Alzheimer's Disease. Elsevier. pp. 197–237. doi:10.1016/B978-0-12-802851-3.00007-3

Bateman RJ, Aisen PS, De Strooper B, Fox NC, Lemere CA, Ringman JM, Salloway S, Sperling RA, Windisch M, Xiong C. 2011. Autosomal-dominant Alzheimer's disease: a review and proposal for the prevention of Alzheimer's disease. *Alzheimers Res Ther* **3**:1. doi:10.1186/alzrt59

Bekris LM, Yu C-E, Bird TD, Tsuang DW. 2010. Genetics of Alzheimer disease. *J Geriatr Psychiatry Neurol* **23**:213–227. doi:10.1177/0891988710383571

Besnard A, Miller SM, Sahay A. 2020. Distinct Dorsal and Ventral Hippocampal CA3 Outputs Govern Contextual Fear Discrimination. *Cell Rep* **30**:2360-2373.e5. doi:10.1016/j.celrep.2020.01.055

Biagioli M, Pifferi S, Ragghianti M, Bucci S, Rizzuto R, Pinton P. 2008. Endoplasmic reticulum stress and alteration in calcium homeostasis are involved in cadmium-induced apoptosis. *Cell Calcium* **43**:184–195. doi:10.1016/j.ceca.2007.05.003

Bliss TVP, Cooke SF. 2011. Long-term potentiation and long-term depression: a clinical perspective. *Clinics* **66**:3–17. doi:10.1590/S1807-59322011001300002

Boldrini M, Fulmore CA, Tartt AN, Simeon LR, Pavlova I, Poposka V, Rosoklija GB, Stankov A, Arango V, Dwork AJ, Hen R, Mann JJ. 2018. Human Hippocampal Neurogenesis Persists throughout Aging. *Cell Stem Cell* **22**:589-599.e5. doi:10.1016/j.stem.2018.03.015

Chen S, Ren Q, Zhang J, Ye Y, Zhang Z, Xu Y, Guo M, Ji H, Xu C, Gu C, Gao W, Huang S, Chen L. 2014. N-acetyl-L-cysteine protects against cadmium-induced neuronal apoptosis by inhibiting ROS-dependent activation of Akt/mTOR pathway in mouse brain. *Neuropathol Appl Neurobiol* **40**:759–777. doi:10.1111/nan.12103

Choi SH, Bylykbashi E, Chatila ZK, Lee SW, Pulli B, Clemenson GD, Kim E, Rompala A, Oram MK, Asselin C, Aronson J, Zhang C, Miller SJ, Lesinski A, Chen JW, Kim DY, Praag H van, Spiegelman BM, Gage FH, Tanzi RE. 2018. Combined adult neurogenesis and BDNF mimic exercise effects on cognition in an Alzheimer's mouse model. *Science* **361**. doi:10.1126/science.aan8821

Choong G, Liu Y, Templeton DM. 2014. Interplay of calcium and cadmium in mediating cadmium toxicity. *Chem Biol Interact* **211**:54–65. doi:10.1016/j.cbi.2014.01.007

Choudhuri S, Li Liu W, Berman NEJ, Klaassen CD. 1996. Cadmium accumulation and metallothionein expression in brain of mice at different stages of development. *Toxicol Lett* **84**:127–133. doi:10.1016/0378-4274(95)03444-7

Choudhury H, Harvey T, Thayer WC, Lockwood TF, Stiteler WM, Goodrum PE, Hassett JM, Diamond GL. 2001. Urinary cadmium elimination as a biomarker of exposure for evaluating a cadmium dietary exposure--biokinetics model. *J Toxicol Environ Health A* **63**:321–350. doi:10.1080/15287390152103643

Ciesielski T, Bellinger DC, Schwartz J, Hauser R, Wright RO. 2013. Associations between cadmium exposure and neurocognitive test scores in a cross-sectional study of US adults. *Environ Health* **12**. doi:10.1186/1476-069X-12-13

Ciesielski T, Weuve J, Bellinger DC, Schwartz J, Lanphear B, Wright RO. 2012. Cadmium Exposure and Neurodevelopmental Outcomes in U.S. Children. *Environ Health Perspect* **120**:758–763. doi:10.1289/ehp.1104152

Clemens S. 2006. Toxic metal accumulation, responses to exposure and mechanisms of tolerance in plants. *Biochimie*, Facets of Environmental Nuclear Toxicology **88**:1707–1719. doi:10.1016/j.biochi.2006.07.003

Cullen JT, Maldonado MT. 2013. Biogeochemistry of Cadmium and Its Release to the Environment In: Sigel A, Sigel H, Sigel RK, editors. Cadmium: From Toxicity to Essentiality, Metal Ions in Life Sciences. Dordrecht: Springer Netherlands. pp. 31–62. doi:10.1007/978-94-007-5179-8_2

Czarnecki LA, Moberly AH, Rubinstein T, Turkel DJ, Pottackal J, McGann JP. 2011. In vivo visualization of olfactory pathophysiology induced by intranasal cadmium instillation in mice. *NeuroToxicology* **32**:441–449. doi:10.1016/j.neuro.2011.03.007

Denny CA, Kheirbek MA, Alba EL, Tanaka KF, Brachman RA, Laughman KB, Tomm NK, Turi GF, Losonczy A, Hen R. 2014. Hippocampal Memory Traces Are Differentially Modulated by Experience, Time, and Adult Neurogenesis. *Neuron* **83**:189–201. doi:10.1016/j.neuron.2014.05.018

Dudai Y, Karni A, Born J. 2015. The Consolidation and Transformation of Memory. *Neuron* **88**:20–32. doi:10.1016/j.neuron.2015.09.004

Dupret D, Fabre A, Döbrössy MD, Panatier A, Rodríguez JJ, Lamarque S, Lemaire V, Oliet SHR, Piazza P-V, Abrous DN. 2007. Spatial Learning Depends on Both the Addition and Removal of New Hippocampal Neurons. *PLoS Biol* **5**. doi:10.1371/journal.pbio.0050214

Ellis KJ, Vartsky D, Zanzi I, Cohn SH, Yasumura S. 1979. Cadmium: in vivo measurement in smokers and nonsmokers. *Science* **205**:323–325. doi:10.1126/science.377488

Engstrom AK, Xia Z. 2017. Lead exposure in late adolescence through adulthood impairs short-term spatial memory and the neuronal differentiation of adult-born cells in C57BL/6 male mice. *Neurosci Lett* **661**:108–113. doi:10.1016/j.neulet.2017.09.060

Eriksson PS, Perfilieva E, Björk-Eriksson T, Alborn AM, Nordborg C, Peterson DA, Gage FH. 1998. Neurogenesis in the adult human hippocampus. *Nat Med* **4**:1313–1317. doi:10.1038/3305

Ernst A, Alkass K, Bernard S, Salehpour M, Perl S, Tisdale J, Possnert G, Druid H, Frisén J. 2014. Neurogenesis in the striatum of the adult human brain. *Cell* **156**:1072–1083. doi:10.1016/j.cell.2014.01.044

Finch CE, Kulminski AM. 2019. The Alzheimer's Disease Exposome. *Alzheimers Dement* **15**:1123–1132. doi:10.1016/j.jalz.2019.06.3914

Fox AP, Nowycky MC, Tsien RW. 1987. Kinetic and pharmacological properties distinguishing three types of calcium currents in chick sensory neurones. *J Physiol* **394**:149–172. doi:10.1113/jphysiol.1987.sp016864

Gage FH. 2019. Adult neurogenesis in mammals. *Science* **364**:827–828. doi:10.1126/science.aav6885

Gage FH. 2000. Mammalian Neural Stem Cells. *Science* **287**:1433–1438. doi:10.1126/science.287.5457.1433

Godt J, Scheidig F, Grosse-Siestrup C, Esche V, Brandenburg P, Reich A, Groneberg DA. 2006. The toxicity of cadmium and resulting hazards for human health. *J Occup Med Toxicol Lond Engl* **1**:22. doi:10.1186/1745-6673-1-22

Gonçalves JF, Fiorenza AM, Spanevello RM, Mazzanti CM, Bochi GV, Antes FG, Stefanello N, Rubin MA, Dressler VL, Morsch VM, Schetinger MRC. 2010. N-acetylcysteine prevents memory deficits, the decrease in acetylcholinesterase activity and oxidative stress in rats exposed to cadmium. *Chem Biol Interact* **186**:53–60. doi:10.1016/j.cbi.2010.04.011

Gonçalves JT, Schafer ST, Gage FH. 2016. Adult Neurogenesis in the Hippocampus: From Stem Cells to Behavior. *Cell* **167**:897–914. doi:10.1016/j.cell.2016.10.021

Groten JP, Sinkeldam EJ, Luten JB, van Bladeren PJ. 1990. Comparison of the toxicity of inorganic and liver-incorporated cadmium: A 4-wk feeding study in rats. *Food Chem Toxicol* **28**:435–441. doi:10.1016/0278-6915(90)90090-A

Heck A, Fastenrath M, Coynel D, Auschra B, Bickel H, Freytag V, Gschwind L, Hartmann F, Jessen F, Kaduszkiewicz H, Maier W, Milnik A, Pentzek M, Riedel-Heller SG, Spalek K, Vogler C, Wagner M, Weyerer S, Wolfsgruber S, Quervain DJ-F de, Papassotiropoulos A. 2015. Genetic Analysis of Association Between Calcium Signaling and Hippocampal Activation, Memory Performance in the Young and Old, and Risk for Sporadic Alzheimer Disease. *JAMA Psychiatry* **72**:1029–1036. doi:10.1001/jamapsychiatry.2015.1309

Honda A, Watanabe C, Yoshida M, Nagase H, Satoh M. 2013. Microarray analysis of neonatal brain exposed to cadmium during gestation and lactation. *J Toxicol Sci* **38**:151–153.

Huguenard JR. 1996. Low-threshold calcium currents in central nervous system neurons. *Annu Rev Physiol* **58**:329–348. doi:10.1146/annurev.ph.58.030196.001553

Hyder O, Chung M, Cosgrove D, Herman JM, Li Z, Firoozmand A, Gurakar A, Koteish A, Pawlik TM. 2013. Cadmium exposure and liver disease among US adults. *J Gastrointest Surg Off J Soc Surg Aliment Tract* **17**:1265–1273. doi:10.1007/s11605-013-2210-9

Izquierdo I, Furini CRG, Myskiw JC. 2016. Fear Memory. *Physiol Rev* **96**:695–750. doi:10.1152/physrev.00018.2015

Jimenez JC, Berry JE, Lim SC, Ong SK, Kheirbek MA, Hen R. 2020. Contextual fear memory retrieval by correlated ensembles of ventral CA1 neurons. *Nat Commun* **11**:3492. doi:10.1038/s41467-020-17270-w

Josselyn SA, Köhler S, Frankland PW. 2015. Finding the engram. *Nat Rev Neurosci* **16**:521–534. doi:10.1038/nrn4000

Josselyn SA, Tonegawa S. 2020. Memory engrams: Recalling the past and imagining the future. *Science* **367**:eaaw4325. doi:10.1126/science.aaw4325

Kim J, Basak JM, Holtzman DM. 2009. The Role of Apolipoprotein E in Alzheimer's Disease. *Neuron* **63**:287–303. doi:10.1016/j.neuron.2009.06.026

Kim K, Melough MM, Vance TM, Noh H, Koo SI, Chun OK. 2018. Dietary Cadmium Intake and Sources in the US. *Nutrients* **11**. doi:10.3390/nu11010002

Kim W, Yim HS, Yoo DY, Jung HY, Kim JW, Choi JH, Yoon YS, Kim DW, Hwang IK. 2016. Dendropanax morbifera Léveille extract ameliorates cadmium-induced impairment in memory and hippocampal neurogenesis in rats. *BMC Complement Altern Med* **16**. doi:10.1186/s12906-016-1435-z

Knierim JJ. 2015. The hippocampus. *Curr Biol* **25**:R1116–R1121. doi:10.1016/j.cub.2015.10.049

Kuhn HG, Dickinson-Anson H, Gage FH. 1996. Neurogenesis in the dentate gyrus of the adult rat: age-related decrease of neuronal progenitor proliferation. *J Neurosci* **16**:2027–2033. doi:10.1523/JNEUROSCI.16-06-02027.1996

Kuhn HG, Toda T, Gage FH. 2018. Adult Hippocampal Neurogenesis: A Coming-of-Age Story. *J Neurosci* **38**:10401–10410. doi:10.1523/JNEUROSCI.2144-18.2018

Li H, Wang Z, Fu Z, Yan M, Wu N, Wu H, Yin P. 2018. Associations between blood cadmium levels and cognitive function in a cross-sectional study of US adults aged 60 years or older. *BMJ Open* **8**. doi:10.1136/bmjopen-2017-020533

Liu C-C, Kanekiyo T, Xu H, Bu G. 2013. Apolipoprotein E and Alzheimer disease: risk, mechanisms and therapy. *Nat Rev Neurol* **9**:106–118. doi:10.1038/nrneurol.2012.263

Liu X, Zhou J-L, Chung K, Chung JM. 2001. Ion channels associated with the ectopic discharges generated after segmental spinal nerve injury in the rat. *Brain Res* **900**:119–127. doi:10.1016/S0006-8993(01)02274-0

Lund E, Krezoski S, Petering D. 2018. The Chemical Biology of Cadmium In: Thévenod F, Petering D, M. Templeton D, Lee W-K, Hartwig A, editors. Cadmium Interaction with Animal Cells. Cham: Springer International Publishing. pp. 23–52. doi:10.1007/978-3-319-89623-6_2

Mahley RW, Rall SC. 2000. Apolipoprotein E: Far More Than a Lipid Transport Protein. *Annu Rev Genomics Hum Genet* **1**:507–537. doi:10.1146/annurev.genom.1.1.507

Marini HR, Puzzolo D, Micali A, Adamo EB, Irrera N, Pisani A, Pallio G, Trichilo V, Malta C, Bitto A, Squadrito F, Altavilla D, Minutoli L. 2018. Neuroprotective Effects of Polydeoxyribonucleotide in a Murine Model of Cadmium Toxicity. *Oxid Med Cell Longev* **2018**:4285694. doi:10.1155/2018/4285694

Méndez-Armenta M, Ríos C. 2007. Cadmium neurotoxicity. *Environ Toxicol Pharmacol* **23**:350–358. doi:10.1016/j.etap.2006.11.009

Min J, Min K. 2016. Blood cadmium levels and Alzheimer's disease mortality risk in older US adults. *Environ Health* **15**. doi:10.1186/s12940-016-0155-7

Ming G, Song H. 2011. Adult Neurogenesis in the Mammalian Brain: Significant Answers and Significant Questions. *Neuron* **70**:687–702. doi:10.1016/j.neuron.2011.05.001

Moreno-Jiménez EP, Flor-García M, Terreros-Roncal J, Rábano A, Cafini F, Pallas-Bazarra N, Ávila J, Llorens-Martín M. 2019. Adult hippocampal neurogenesis is abundant in neurologically healthy subjects and drops sharply in patients with Alzheimer's disease. *Nat Med* **25**:554–560. doi:10.1038/s41591-019-0375-9

Namgyal D, Ali S, Mehta R, Sarwat M. 2020. The neuroprotective effect of curcumin against Cd-induced neurotoxicity and hippocampal neurogenesis promotion through CREB-BDNF signaling pathway. *Toxicology* **442**:152542. doi:10.1016/j.tox.2020.152542

Pan Y-W, Chan GCK, Kuo CT, Storm DR, Xia Z. 2012. Inhibition of Adult Neurogenesis by Inducible and Targeted Deletion of ERK5 Mitogen-Activated Protein Kinase Specifically in Adult Neurogenic Regions Impairs Contextual Fear Extinction and Remote Fear Memory. *J Neurosci* **32**:6444–6455. doi:10.1523/JNEUROSCI.6076-11.2012

Peng Q, Bakulski KM, Nan B, Park SK. 2017. Cadmium and Alzheimer's disease mortality in U.S. adults: Updated evidence with a urinary biomarker and extended follow-up time. *Environ Res* **157**:44–51. doi:10.1016/j.envres.2017.05.011

Qu Y, Liu Y, Chen L, Zhu Yanmei, Xiao X, Wang D, Zhu Yulan. 2018. Nobiletin prevents cadmium-induced neuronal apoptosis by inhibiting reactive oxygen species and modulating JNK/ERK1/2 and Akt/mTOR networks in rats. *Neurol Res* **40**:211–220. doi:10.1080/01616412.2018.1424685

Rajan KB, Weuve J, Barnes LL, McAninch EA, Wilson RS, Evans DA. 2021. Population estimate of people with clinical Alzheimer's disease and mild cognitive impairment in the United States (2020–2060). *Alzheimers Dement* **17**:1966–1975. doi:10.1002/alz.12362

Reitz C, Brayne C, Mayeux R. 2011. Epidemiology of Alzheimer disease. *Nat Rev Neurol* **7**:137–152. doi:10.1038/nrneurol.2011.2

Riaz S, Schumacher A, Sivagurunathan S, Van Der Meer M, Ito R. 2017. Ventral, but not dorsal, hippocampus inactivation impairs reward memory expression and retrieval in contexts defined by proximal cues. *Hippocampus* **27**:822–836. doi:10.1002/hipo.22734

Satarug S, Garrett SH, Sens MA, Sens DA. 2010. Cadmium, Environmental Exposure, and Health Outcomes. *Environ Health Perspect* **118**:182–190. doi:10.1289/ehp.0901234

Satarug S, Moore MR. 2004. Adverse Health Effects of Chronic Exposure to Low-Level Cadmium in Foodstuffs and Cigarette Smoke. *Environ Health Perspect* **112**:1099–1103. doi:10.1289/ehp.6751

Schoenfeld TJ, Gould E. 2012. Stress, stress hormones, and adult neurogenesis. *Exp Neurol*, Special Issue: Stress and neurological disease **233**:12–21. doi:10.1016/j.expneurol.2011.01.008

Sheintuch L, Rubin A, Brande-Eilat N, Geva N, Sadeh N, Pinchasof O, Ziv Y. 2017. Tracking the Same Neurons across Multiple Days in Ca2+ Imaging Data. *Cell Rep* **21**:1102–1115. doi:10.1016/j.celrep.2017.10.013

Sindreu C, Palmiter RD, Storm DR. 2011. Zinc transporter ZnT-3 regulates presynaptic Erk1/2 signaling and hippocampus-dependent memory. *Proc Natl Acad Sci* **108**:3366–3370. doi:10.1073/pnas.1019166108

Sindreu CB, Scheiner ZS, Storm DR. 2007. Ca2+-Stimulated Adenylyl Cyclases Regulate ERK-Dependent Activation of MSK1 during Fear Conditioning. *Neuron* **53**:79–89. doi:10.1016/j.neuron.2006.11.024

Sorrells SF, Paredes MF, Cebrian-Silla A, Sandoval K, Qi D, Kelley KW, James D, Mayer S, Chang J, Auguste KI, Chang EF, Gutierrez AJ, Kriegstein AR, Mathern GW, Oldham MC,

Huang EJ, Garcia-Verdugo JM, Yang Z, Alvarez-Buylla A. 2018. Human hippocampal neurogenesis drops sharply in children to undetectable levels in adults. *Nature* **555**:377–381. doi:10.1038/nature25975

Spalding KL, Bergmann O, Alkass K, Bernard S, Salehpour M, Huttner HB, Boström E, Westerlund I, Vial C, Buchholz BA, Possnert G, Mash DC, Druid H, Frisén J. 2013. Dynamics of Hippocampal Neurogenesis in Adult Humans. *Cell* **153**:1219–1227. doi:10.1016/j.cell.2013.05.002

Squire LR, Genzel L, Wixted JT, Morris RG. 2015. Memory Consolidation. *Cold Spring Harb Perspect Biol* **7**. doi:10.1101/cshperspect.a021766

Stangl D, Thuret S. 2009. Impact of diet on adult hippocampal neurogenesis. *Genes Nutr* **4**:271–282. doi:10.1007/s12263-009-0134-5

Suwazono Y, Kido T, Nakagawa H, Nishijo M, Honda R, Kobayashi E, Dochi M, Nogawa K. 2009. Biological half-life of cadmium in the urine of inhabitants after cessation of cadmium exposure. *Biomarkers* **14**:77–81. doi:10.1080/13547500902730698

Szabo ST, Harry GJ, Hayden KM, Szabo DT, Birnbaum L. 2016. Comparison of Metal Levels between Postmortem Brain and Ventricular Fluid in Alzheimer's Disease and Nondemented Elderly Controls. *Toxicol Sci* **150**:292–300. doi:10.1093/toxsci/kfv325

Tellez-Plaza Maria, Navas-Acien Ana, Caldwell Kathleen L., Menke Andy, Muntner Paul, Guallar Eliseo. 2012. Reduction in Cadmium Exposure in the United States Population, 1988–2008: The Contribution of Declining Smoking Rates. *Environ Health Perspect* **120**:204–209. doi:10.1289/ehp.1104020

Templeton DM, Liu Y. 2018. Interactions of Cadmium with Signaling Molecules In: Thévenod F, Petering D, M. Templeton D, Lee W-K, Hartwig A, editors. Cadmium Interaction with Animal Cells. Cham: Springer International Publishing. pp. 53–81. doi:10.1007/978-3-319-89623-6_3

Thévenod F, Jones SW. 1992. Cadmium block of calcium current in frog sympathetic neurons. *Biophys J* **63**:162–168. doi:10.1016/S0006-3495(92)81575-8

Thévenod F, Petering D, M. Templeton D, Lee W-K, Hartwig A, editors. 2018. Cadmium Interaction with Animal Cells. Cham: Springer International Publishing. doi:10.1007/978-3-319-89623-6

Wang H, Abel GM, Storm DR, Xia Z. 2019. Cadmium Exposure Impairs Adult Hippocampal Neurogenesis. *Toxicol Sci* **171**:501–514. doi:10.1093/toxsci/kfz152

Wang H, Matsushita MT, Abel GM, Storm DR, Xia Z. 2020a. Inducible and conditional activation of ERK5 MAP kinase rescues mice from cadmium-induced olfactory memory deficits. *NeuroToxicology* **81**:127–136. doi:10.1016/j.neuro.2020.09.038

Wang H, Matsushita MT, Zhang L, Abel GM, Mommer BC, Huddy TF, Storm DR, Xia Z. 2020b. Inducible and Conditional Stimulation of Adult Hippocampal Neurogenesis Rescues Cadmium-Induced Impairments of Adult Hippocampal Neurogenesis and Hippocampus-

Dependent Memory in Mice. *Toxicol Sci Off J Soc Toxicol* **177**:263–280. doi:10.1093/toxsci/kfaa104

Wang H, Storm DR. 2003. Calmodulin-Regulated Adenylyl Cyclases: Cross-Talk and Plasticity in the Central Nervous System. *Mol Pharmacol* **63**:463–468. doi:10.1124/mol.63.3.463

Wang H, Zhang L, Abel GM, Storm DR, Xia Z. 2017. Cadmium Exposure Impairs Cognition and Olfactory Memory in Male C57BL/6 Mice. *Toxicol Sci*. doi:10.1093/toxsci/kfx202

Wang W, Pan Y-W, Zou J, Li T, Abel GM, Palmiter RD, Storm DR, Xia Z. 2014. Genetic Activation of ERK5 MAP Kinase Enhances Adult Neurogenesis and Extends Hippocampus-Dependent Long-Term Memory. *J Neurosci* **34**:2130–2147. doi:10.1523/JNEUROSCI.3324-13.2014

Ward NI, Mason JA. 1987. Neutron activation analysis techniques for identifying elemental status in Alzheimer's disease. *J Radioanal Nucl Chem* **113**:515–526. doi:10.1007/BF02050527

Whitlock JR. 2006. Learning Induces Long-Term Potentiation in the Hippocampus. *Science* **313**:1093–1097. doi:10.1126/science.1128134

Xu L, Zhang W, Liu X, Zhang C, Wang P, Zhao X. 2018. Circulatory Levels of Toxic Metals (Aluminum, Cadmium, Mercury, Lead) in Patients with Alzheimer's Disease: A Quantitative Meta-Analysis and Systematic Review. *J Alzheimers Dis* **62**:361–372. doi:10.3233/JAD-170811

Yonelinas AP, Ranganath C, Ekstrom AD, Wiltgen BJ. 2019. A contextual binding theory of episodic memory: systems consolidation reconsidered. *Nat Rev Neurosci* **20**:364–375. doi:10.1038/s41583-019-0150-4

Zamorano C, Fernández-Albert J, Storm DR, Carné X, Sindreu C. 2018. Memory Retrieval Re-Activates Erk1/2 Signaling in the Same Set of CA1 Neurons Recruited During Conditioning. *Neuroscience*, Molecular and Cellular Mechanisms of Cognitive Function **370**:101–111. doi:10.1016/j.neuroscience.2017.03.034

Zhang L, Chen X, Sindreu C, Lu S, Storm DR, Zweifel LS, Xia Z. 2019a. Dynamics of a hippocampal neuronal ensemble encoding trace fear memory revealed by in vivo Ca2+ imaging. *PLoS ONE* **14**. doi:10.1371/journal.pone.0219152

Zhang L, Wang H, Abel GM, Storm DR, Xia Z. 2019b. The Effects of Gene-Environment Interactions Between Cadmium Exposure and Apolipoprotein E4 on Memory in a Mouse Model of Alzheimer's Disease. *Toxicol Sci* kfz218. doi:10.1093/toxsci/kfz218

Ziv Y, Burns LD, Cocker ED, Hamel EO, Ghosh KK, Kitch LJ, Gamal AE, Schnitzer MJ. 2013. Long-term dynamics of CA1 hippocampal place codes. *Nat Neurosci* **16**:264–266. doi:10.1038/nn.3329

Zucker RS, Regehr WG. 2002. Short-Term Synaptic Plasticity. *Annu Rev Physiol* **64**:355–405. doi:10.1146/annurev.physiol.64.092501.114547

Chapter 2. Cadmium inhibits calcium activity in hippocampal CA1 in C57BL/6 mice

2.1 Introduction

Cadmium (Cd) is a toxic heavy metal that has been widely used in industrial manufacturing processes and commercial products, including fertilizers (Godt et al., 2006). Due to high transfer rates from contaminated soil, the main sources of exposure for the general population is smoking and diet (Satarug and Moore, 2004). Increasing evidence in the last decade in humans and model organisms suggest that Cd may be a potent neurotoxicant at levels relevant to the general population. Epidemiological studies using data from the US National Health and Nutrition Examination Survey (NHANES) have found associations between Cd levels and cognitive function in children aged 6-15 years (Ciesielski et al., 2012), adults age 20-59 (Ciesielski et al., 2013), and adults older than 60 years (Li et al., 2018). We previously established an environmentally relevant model of Cd exposure of 3 mg/L Cd (as $CdCl_2$) through drinking water, resulting in blood Cd levels of approximately 0.3 µg/L and within the range of blood Cd levels in the general US population (Wang et al., 2018). Mice exposed to 3 mg/L and a lower dose of 0.6 mg/L Cd in drinking water exhibited impairments in spontaneous alternation, novel object location test, and contextual fear memory, suggesting that environmentally relevant Cd exposure cause significant and persistent hippocampus-dependent learning and memory effects (Wang et al., 2018, 2020; Zhang et al., 2019b). While we described impairment of adult neurogenesis as a cellular mechanism of low-level Cd neurotoxicity previously (Wang et al., 2020, 2019), the underlying molecular mechanisms are not yet well understood.

Cd is a soft ion that can mimic calcium ions (Ca^{2+}) and interact with proteins with metal binding sites rich in soft ligands such as sulfhydryl groups (Lund et al., 2018). Cd can be transported into cells through mimicry and disrupt cytosolic Ca^{2+} levels (Biagioli et al., 2008; Choong et al., 2014) causing both direct and indirect effects on various Ca^{2+}-binding proteins,

kinases, growth factors, and second messengers (Templeton and Liu, 2018; Thévenod et al., 2018). In neurons, rapid changes in intracellular Ca^{2+}concentrations during activity lead to Ca^{2+}-dependent signaling pathways that are critical in learning and memory consolidation (Heck et al., 2015; Sabatini et al., 2002; Whitlock, 2006). Ca^{2+}-binding proteins in the brain such as calmodulin (CaM) have binding affinity for Cd comparable to affinity for Ca^{2+} (Suzuki et al., 1985) and it has been posited that Cd may displace Ca^{2+} and affect cellular functions (Thévenod and Lee, 2013). However, existing evidence for Cd interference with Ca^{2+} in neurons describe Cd block effects of voltage-gated Ca^{2+} dependent channels (Fox et al., 1987; Huguenard, 1996; Liu et al., 2001; Thévenod and Jones, 1992) at high concentrations ranging from tens of μM to mM in cell culture or acute slices. Thus, there is a research gap in the understanding of the effects of environmentally relevant levels of Cd on Ca^{2+} activity in neurons.

Genetically encoded calcium indicators (GECI) such as GCaMP6 have been developed over the years to enable visualization of intracellular Ca^{2+} activity *in vivo* as a proxy for neuronal activity. Combined with miniature microscopy, Ca^{2+} activity can be recorded in the hippocampus in a large field of view *in vivo* during learning and memory tasks (Jimenez et al., 2020; Sheintuch et al., 2017; Ziv et al., 2013). Work in our lab and others have further demonstrated that subsets of cells in the CA1 region of the hippocampus are persistently reactivated in learning and memory tasks, demonstrating that transient increases in Ca^{2+} levels are associated with memory acquisition and retrieval *in vivo* (Josselyn et al., 2015; Josselyn and Tonegawa, 2020; Zhang et al., 2019a).

In vivo Ca^{2+} imaging in GCaMP6 expressing neurons provides an effective approach to investigate the effects of Cd exposure on Ca^{2+} activity during animal behavior. We hypothesized that environmentally relevant Cd exposure impairs Ca^{2+} activity in the hippocampus *in vivo*, which contributes to impairments in learning and memory. To test this hypothesis, we recorded single-cell resolution Ca^{2+} transients in the hippocampal CA1 region to investigate the effects of Cd

exposure on Ca^{2+} activity *in vivo* in freely moving mice during the acquisition and retrieval of contextual memory.

2.2 Materials and Methods

Animals

5-week-old male C57BL/6J mice were purchased from Charles River Laboratories and housed (5 animals per cage; individually housed after surgical procedures) in standard conditions (12 h light/dark cycle) with food and water provided *ad libitum*. The mice were acclimated to bottled water starting at 7 weeks of age, then received 0 or 3 mg/L Cd (in the form of $CdCl_2$) starting at 8 weeks of age. Cd drinking water was prepared from a stock solution (Cat. 202908, Sigma-Aldrich, St. Louis, MO) and replaced every week. Water consumption was monitored every week during the exposure period by the weight of the bottle before placement in the cage and after removal from the cage. Animals were exposed to Cd for 10 weeks. At the end of 10 weeks, animals were allowed to drink water from a valve drinking system. All experiments were conducted during the light cycle. The preparation, use, and disposal of hazardous reagents were conducted according to the guidelines set forth by the office of Environmental Health and Safety at the University of Washington. All animal care, treatments, and procedures were approved by the University of Washington Institutional Animal Care and Use Committee.

GCaMP6 virus

Adeno-associated viruses (AAV1.CaMK2a.GCaMP6f.WPRE.bGHpA) used for visualizing excitatory cells for Ca^{2+} imaging were supplied by Inscopix, Inc (Palo Alto, CA) as the Ready-to-Image (RTI) virus for mouse dorsal CA1 hippocampus at titer 1.34×10^{12} vG/ml.

Stereotaxic surgeries

All surgical procedures were performed using a sterile technique. For all procedures, mice were anesthetized (4% induction, 1.5-2.0% maintenance with isoflurane, 0.8-1.0 L/min O_2) and head-fixed in a stereotax (David Kopf, Tujunga, CA). Ophthalmic ointment (Dechra Veterinary Products, Overland Park, KS) was applied for eye lubrication, fur was shaved, incision site sterilized, and body temperature maintained with a covered heating plate controlled by a TCAT-2 temperature controller (Harvard Apparatus, Holliston, MA) set to 37.0 degrees. Each mouse was leveled in the medial-lateral and anterior-posterior directions prior to all procedures. All surgical procedures targeted the right hemisphere. Subcutaneous injection of ketoprofen (5 mg/kg b.w.) was provided 15-30 minutes prior to the end of surgery for analgesia. Animals were returned to a clean cage with a heating pad under half of the cage until the animal was fully recovered from anesthesia. Animals were group housed in the original home cages following the virus injections, and individually housed in a clean home cage from just before the lens implantation surgery the day of the procedure until the end of the experiment. Wire racks were removed from the cage to prevent injury to the animal or damage to lens components.

All GCaMP6 virus injections targeted the dorsal CA1 hippocampus to visualize cells in the CA1 cell layer. All injection surgeries were performed in experimental week 11. After leveling the skull, a craniotomy was made using a dental drill and dura removed from the brain surface. Mice were injected unilaterally (in mm, from bregma at 1.35 ML, -1.95 AP, -1.55 DV) with 500 nl of RTI virus with a microsyringe pump (World Precision Instruments, Sarasota, FL) at 100 nl/min. The microsyringe was raised slowly following a 5-min period after the completion of the injection. The incision site was sutured, and animals were allowed to recover for at least 1 week. After recovery, each animal underwent a second surgery for mini-microscope lens implantation, in experimental weeks 12-14. 1 skull screw was inserted on the left parietal skull and a 1.1-1.2 mm craniotomy (craniotomy center at 1.35 ML, -1.95 AP) was made using a handheld dental drill, and the skull

was removed carefully using fine forceps. The brain tissue above the hippocampus was aspirated slowly with constant irrigation with sterile saline to where striations of white matter tracts were visible. Throughout brain aspiration, bleeding was controlled with small pieces of gelfoam saturated with sterile saline. Once bleeding was controlled, a 1.0 mm x 4.0 mm GRIN lens (ProView^{TM} Integrated Lens; Inscopix, Inc) was lowered slowly into the craniotomy by approximately 0.1 mm increments to the target (-1.35 DV). C&B Metabond (Parkell, Edgewood, NY) was applied to cure an initial layer on the skull with the lens, then dental acrylic (Lang Dental Manufacturing, Wheeling, IL) was used to further fix the lens to the skull. A baseplate cover (Inscopix, Inc) was installed to protect the lens, and animals were allowed to recover for at least 2 weeks before habituation to the dummy and mini-microscopes and 3 weeks before behavioral experiments.

In vivo image acquisition

In vivo brain imaging data were acquired using a miniature microscope system (nVista 3.0 system, Inscopix, Inc) at 1280 x 800 pixels and a 20 Hz sample rate. Following recovery from lens implant surgery for at least 2 weeks, each animal was handled twice daily for five days in the home cage to habituate to handling by the experimenter, slowly building up to gentle scruffing. The following week, each animal was habituated to a dummy microscope attached to a dummy attachment cable for 20 minutes in a 10 x 10 x 16 inch (width x depth x height) open field arena (Coulbourn Instruments, Whitehall, PA) at least once a day for three days. At the end of this habituation period, animals were gently scruffed, a mini-microscope was attached onto the implanted lens, and imaged for 2-5 minutes to inspect the field of view (FOV) and imaging parameters for each animal (gain, EX-LED power, lens focus) were recorded as a reference focal plane that visualizes the greatest number of cells in focus. For each imaging session, the lens

focus was adjusted as needed from the initial imaging parameters to visually ensure consistent FOV to account for small shifts in focal plane between different imaging sessions.

For each behavioral imaging session, animals were gently scruffed and a mini-microscope was attached to the implanted lens, then the mouse was immediately moved to the behavioral chamber. Imaging parameters were quickly selected to check for FOV consistency prior to initiating image acquisition. The mini-miscroscope lens was cleaned with 70% ethanol on lens paper and checked for surface dust between every animal. All imaging sessions were limited to 10 minutes to avoid bleaching of fluorescence signal.

In vivo image processing

All images were processed using Inscopix Data Processing Software (IDPS version 1.8.0.0; Inscopix, Inc). Images were spatially and temporally downsampled by a factor of 4 and 2 respectively, cropped to an image size of 800 x 800 pixels, processed through a spatial band-pass filter to reduce low and high frequency information, then motion corrected. Constrained non-negative matrix factorization for microendoscopic data (CNMF-E) (Zhou et al., 2018) with an estimated cell diameter of 6 pixels was used to identify neurons, then identified neurons were manually confirmed both by the identified cell outline as well as Ca^{2+} trace.

To identify cells that were imaged across all imaging days, we utilized the longitudinal registration algorithm on IDPS. The algorithm creates cell maps for each recording and aligns cell sets to a reference (cell map from day 1) to match cells. Cells were registered across days with minimum correlation of 0.50, and only cells that were registered across all relevant days of an experiment were included in further analyses. Ca^{2+} transient events were identified using an algorithm that detects a fast increase in amplitude followed by an exponential decay back to baseline level, using a conservative threshold factor of 12.0 mean absolute deviation from baseline to avoid misclassification of Ca^{2+} events and smallest decay time of 200 ms based on

GCaMP6f fluorescence (Chen et al., 2013). While mean firing rates of 0.01 Hz is a common cutoff for inclusion in analysis in the dorsal CA1 (Rubin et al., 2019; Sheintuch et al., 2020), we did not exclude cells from analysis based on firing rates due to the conservative threshold used to identify Ca^{2+} transient events. For Ca^{2+} traces, we converted dF/noise trace outputs extracted by CNMF-E to z-score by normalization to the baseline mean of the population. dF/noise is used over dF/F because estimated noise is a more robust measure of variance in a temporal trace in fluorescence images compared to the standard deviation.

Open field

The open field test was first used to assess locomotor activity and anxiety prior to survival surgeries at baseline (before Cd exposure) and at 10 weeks of exposure. Mice were placed into a 10” x 10” x 16” TruScan Photo Beam Tracking arena (Coulbourn Instruments) with clear Plexiglas sidewalls. Their movements were monitored by 2 sets of infrared beams spaced 0.6 in apart. Mice were allowed to explore the arena without prehabituation for 20 min, and the data were collected and analyzed by TruScan 2.0 software (Coulbourn Instruments). The arena was cleaned with 5% acetic acid between experimental animals. The total number of moves, moving time, and moving distance were used to assess the effects of Cd and tamoxifen on locomotor activity. The number of center entries, time spent in the center and margin, and distance traveled in the center and margin were used to assess the effects of Cd and tamoxifen on anxiety. The margin was defined as the area within 1.5 inches of the arena wall.

Following stereotaxic surgeries and after the cued and contextual fear test, the open field test was paired with simultaneous Ca^{2+} recording to assess baseline Ca^{2+} activity. Mice were placed into a 40 x 40 cm arena with white Plexiglas walls and allowed to explore freely for 10 minutes. A USB camera was connected to a computer and video tracking software (EthoVision XT10, Noldus, Leesburg, VA) recorded the data, video, and synchronized Ca^{2+} recording with a

TTL trigger. The experiment and recording started 1 s after detection of an animal in the open field arena.

Novel object location test

The novel object location (NOL) test was used to assess the effects of Cd on hippocampus-dependent spatial working memory throughout the exposure period (experiment weeks 0, 4, 7, and 10). This assay was performed as previously described (Wang et al., 2020, Zhang et al., 2019). Briefly, each mouse was placed into an open field arena (Coulbourn Instruments) with 2 identical objects placed in 2 different corners. During the training session, the mouse was allowed to freely explore the arena and objects, then returned to its home cage. 1 h after training, the animal was returned to the arena with the same 2 objects with one object in the original location and the other moved to a novel location. For each week of NOL test, object locations were randomized to exclude preference of specific locations. Training and test session were recorded by video cameras for later quantification. The time each animal spent actively investigating each object was scored and analyzed by an experimenter blinded to the animal's treatment. The data inclusion criteria for NOL assays were a minimum of 1 s total exploration time.

Following stereotaxic surgeries and following the open field test, the NOL test was paired with simultaneous Ca^{2+} recording to assess Ca^{2+} activity during training and test sessions. Mice were placed into the same 40 x 40 cm open field arena with white Plexiglas walls. Two plastic guides (4 cm wide) were used to ensure object placement was consistent for every session and between subjects. A USB camera was connected to a computer and EthoVision XT10 (Noldus) recorded the data, video, and synchronized Ca^{2+} recording with a TTL trigger. The experiment and recording started 1 s after detection of an animal in the open field arena. Videos from experimental sessions were reanalyzed with EthoVision XT13 (Noldus) to better identify the nose

and tail positions in the presence of shadows created by the NOL objects. Circular zones were created approximately 1 cm around the object and object exploration was defined as the nose point being inside the zone and the mouse head directed toward the zone.

Cued and contextual fear conditioning

We utilized cued and contextual fear conditioning to test for contextual fear, which is hippocampus-dependent and found to be impaired in Cd-treated animals and, and cued fear, which is amygdala dependent and found to be unimpaired in Cd-treated animals (Wang et al., 2020, 2018). Mice underwent a 3-day contextual fear conditioning paradigm, modified from a 2-day contextual fear conditioning paradigm described previously (Engstrom et al., 2017; Pan et al., 2012). On each experimental day, mice in their home cages were placed in a separate room across from the experimental room, and each mouse was placed in the experimental room for at least 5 minutes. On day 1, mice were conditioned in a modified, sound-attenuated chamber (Med-Associates, Fairfax, VT) with a 120 s free exploration period followed by three cue pairings (conditioned stimulus, CS; 3 kHz, 80 dB, 30 s duration) that co-terminated with a foot shock (unconditioned stimulus, US; 0.3 mA, 2 s duration) with 120 s ISI and a final 120 s post-training period. Chambers were cleaned before sessions with 70% ethanol. On day 2, mice were placed back into the conditioning context for 2 min without CS or US to assess for freezing for contextual fear. On day 3, mice were placed in a modified fear conditioning box with metal bar floors and 3 walls covered with a smooth, white plastic insert, cleaned with 2.5% acetic acid before sessions to freely explore for 2 min, then presented with CS tone-cue for 2 min to assess freezing for cued fear. For all sessions, a small fan provided white noise inside the sound attenuation box (approximately 65 dB) and dim overhead lighting illuminated the inside of the chamber.

For each session, one or two behavioral chambers were controlled by MED-PC software to start at identical times. Ca^{2+} recording was synchronized with the behavioral experiment with a

TTL trigger. Animal behavior was recorded at with an overhead infrared camera, aligned to a house light flash at the beginning of the experiment, and analyzed using EthoVision XT13 software using activity analysis. A mobility score output (binary variable: 1 = motionless, 0 = moving, time bin = 0.1 s) was used to calculate percent of time spent freezing in 30 s bins.

Blood and hipppocampus sample collection and analysis

A subset of animals (n = 4 per treatment) was sacrificed at the end of the experiment for collection of blood and hippocampus samples. Mice were anesthetized with ketamine/xylazine and checked for limb reflexes prior to cardiac puncture for blood collection (> 0.3 ml/animal). Following cervical dislocation, brain samples were dissected out, separated by hemisphere using a glass slide cover, then the hippocampus was dissected out. Hippocampus from both hemispheres were combined, snap frozen, and stored in -80 °C until further analysis. Blood samples were stored in -20 °C until further analysis. Whole blood and hippocampus samples were analyzed for Cd by the Environmental Health Laboratory at the University of Washington using inductively coupled plasma mass spectrometry (ICP-MS). The experimenter who performed Cd analysis was blinded to the treatment and genotype of animals. The Agilent 7900 (Agilent Technologies, Santa Clara, CA) has a detection limit of approximately 0.3 ng/g per sample.

Histology and microscopy

All other mice were perfused transcardially with PBS followed by 4% paraformaldehyde (PFA) in PBS. Whole heads with the lens implant were removed, skulls partially opened, and post-fixed in 4% PFA to allow fixation of tissue with the probe attached. Up to 24 h later, brains were removed and cryoprotected in 30% sucrose until the brains were saturated and sank to the bottom (1-2 days). Brains were cut down the midline and the right hemispheres (ipsilateral to virus injection and probe implantation) were embedded in OCT medium and stored in -80 °C. 30 µm

coronal sections were cut on a cryostat (Leica Microsystems, Buffalo Grove, IL), collected in cryoprotectant, and stored in -20 °C. Sections were washed 3x in PBS, incubated in 2.5 µg/ml Hoechst 33342 (Invitrogen, Carlsbad, CA) for 30 min, then washed 3x in PBS prior to mounting onto slides with anti-fade Aqua Poly/Mount (Polysciences, Warrington, PA). No signal enhancement was performed to capture GCaMP6 fluorescence at levels comparable to *in vivo* imaging.

Fluorescent images for confirming injection sites and probe placement were captured using a Leica SP8X confocal microscope (Leica Microsystems) with 10x (air) or 20x (air) lenses or a fluorescent microscope (Zeiss, Germany) equipped with a camera and 4x and 10x objectives. Images were stitched using the stitching plugin, then adjusted for color, brightness, and contrast uniformly with ImageJ (NIH, Bethesda, MA).

Statistical analysis

All means are reported as means ± standard error unless otherwise stated. All analyses were performed using R statistical analysis software. Wilcoxon rank sum exact tests were conducted for comparisons of blood and hippocampus Cd levels. Welch's two-tailed t-test was used for pairwise comparisons of open field and NOL test behavior. Repeated-measures designs were analyzed using the mixed-effects restricted maximum likelihood (REML) model (R packages *lme4, lmerTest*). The following random effects were included in the REML model to account for correlated data points in time series data: animal weight: animal ID; water consumption: cage ID; fear conditioning: animal ID.

We used generalized estimating equations (GEE), a semiparametric method for longitudinal correlated data, to understand if there is a significant difference in the odds of activation comparing control and Cd separately at each time point and over time. GEE allows for inferences about the population when accounting for within-subject correlation (Ballinger, 2004).

We employed a logistic regression and assumde an independent correlation structure and used robust standard errors.

Our model is: $logit(M_{ij}) = \beta_0 + \beta_1 treatment + \beta_2 time + \beta_3 treatment * phase + \varepsilon$, where M_{ij} is the probability of activation for cell *i* at phase *j*. We are interested in comparing the odds of activation between Cd and control: $OR = e^{\beta_1} + e^{\beta_3 phase}$

2.3 Results

Mouse body weight, water consumption

We exposed 8 wk old male C57BL/6 mice to 0 or 3 mg/L Cd for 10 weeks and conducted behavior tests before and throughout exposure prior to Ca^{2+} imaging (Figure 2.1A). The 3 mg/L dose was chosen based on our previous study that achieved human relevant blood Cd levels of 0.3-0.4 µg/L in C57BL/6 mice treated with 3 mg/L Cd for 20 weeks (Wang et al., 2018). Mouse body weights were recorded every week through Cd treatment. We did not observe any weight differences between Cd-treated animals compared to controls (Figure 2.1B). Mouse water consumption was calculated from weights of water bottles before and after installation in cages. We did not observe any differences in water consumption between control and Cd treated cages (Figure 2.1C: mixed-effects REML, Cd main effect: p = 0.13). These data suggest that Cd treatment had no effect on animal weights or water consumption.

Cd concentrations in blood and hippocampus

We collected blood and hippocampus for Cd analysis from a subset of animals (n = 4 per treatment) to assess Cd exposure levels at the end of the experiment at 10 weeks after end of Cd exposure. All samples except two blood samples from control treatment had Cd levels above the detection limit. Cd levels in blood samples from Cd-treated animals were elevated (control:

median: 0.0265 µg/L, mean ± SD: 0.134 ± 0.229 µg/L; Cd: median: 0.307 µg/L, mean ± SD: 0.329 ± 0.161 µg/L), although these differences were not statistically significant (Figure 2.2A; Wilcoxon rank sum exact test: p = 0.2). Cd levels in hippocampus samples from Cd-treated animals were also elevated (control: median: 0.780 pg/mg, mean ± SD: 0.913 ± 0.800 pg/mg; Cd: median: 3.325 pg/mg, mean ± SD: 3.645 ± 1.39 pg/mg). These differences were statistically significant (Figure 2.2B; Wilcoxon rank sum exact test: p = 0.029).

Locomotor activity and anxiety

To assess effects of Cd on locomotor activity, we performed an open field test both before and after Cd treatment and analyzed for general movement. We observed increased moving time and moving distance before Cd treatment in the Cd treatment group (Figure 2.3A, Welch's two-tailed t-test: moving time: p = 0.026, moving distance: p = 0.0079), selected *a priori*. We also observed increased moving distance after Cd treatment in the Cd-treated group (Figure 2.3A: Welch's two-tailed t-test: moving distance: p = 0.013), consistent with results from before Cd treatment. These results suggest that the higher locomotor activity of Cd-treated mice is a consistent behavior difference between the two groups of mice rather than from Cd treatment.

We further analyzed open field data to screen for anxiety behavior based on movement in the margin, in the center, and into the center of the open field arena. We observed an increase in the distance moved in the arena margin before Cd treatment in the Cd treatment group (Figure 2.3B: Welch's two-tailed t-test: margin distance: p = 0.04), suggesting that mice in the Cd-treatment group were potentially exhibiting elevated levels of anxiety prior to Cd treatment. We did not observe any differences in anxiety behavior after Cd treatment. Taken together, these data suggest that 10-week exposure to 3 mg/L Cd did not affect locomotor or anxiety behavior in C57BL/6 mice.

NOL test during Cd treatment

We performed 1-h NOL tests to assess the effects of Cd treatment on hippocampus-dependent spatial memory. Prior to Cd exposure, all groups of mice spent significantly more time exploring the object in the novel location (location C) compared to the old location (location A) in the test session, suggesting that mice in both groups had memory for the original object locations and were able to discriminate between old and novel locations (Figure 2.4A). Cd-treated animals showed spatial memory deficits at 7 and 10 weeks of Cd exposure, indicated by a failure to discriminate between old and novel locations (Figure 2.4C, D). These data suggest that a 10-week Cd treatment was sufficient to impair hippocampus dependent spatial memory.

Cued and contextual fear conditioning - behavior

At the end of 10 weeks of Cd exposure, Cd treatment was stopped, and each animal underwent survival surgeries to first inject GCaMP6 virus in the dorsal hippocampal CA1 (week 11), then implant a GRIN lens above the hippocampus CA1 region (experimental weeks 12-14) (see Methods: Stereotaxic Surgeries). All mice were habituated to handling with dummy mini-microscopes as well as the Inscopix nVista mini-microscope system by the experimenter prior to further behavior tests or image acquisition.

To investigate the effect of prior Cd exposure on Ca^{2+} activity during fear memory acquisition and recall, we conducted cued and contextual fear conditioning tests while recording Ca^{2+} activity *in vivo*. A modified 3-day contextual fear conditioning paradigm with 3 x 0.3 mA foot shock in conditioning (Figure 2.5A) was used because we previously reported higher sensitivity to changes in contextual memory (Engstrom et al., 2017; Pan et al., 2012; Wang et al., 2018). During training, the average freezing level increased over the three conditioning trials, ending at around 50% freezing at the last trial, suggesting that animals were learning to associate CS-US pairs (Figure 2.5B). There were no differences in freezing between Ctrl and Cd treated groups

during conditioning (mixed-effects REML: Cd-effect: $F_{(1, 19)}$ = 3.72, p = 0.07). There were no differences between groups in contextual fear, novel context fear, or auditory cued fear tests (Figure 2.5C-D, mixed-effects REML: contextual fear: Cd effect: p = 0.70; novel/cued fear: Cd effect: p = 0.25). Together, these data suggest that a prior 10-week Cd treatment had no effect on fear memory acquisition and recall of context or cue.

Cued and contextual fear conditioning – Ca^{2+} activity

We investigated the effects of prior Cd exposure on Ca^{2+} activity during this fear memory acquisition and recall by recording Ca^{2+} activity of excitatory neurons in the CA1 region from fluorescent signals of Ca^{2+} indicator GCaMP6f through the implanted GRIN lens using a mini-microscope. The expression of GCaMP6f in the CA1 at endogenous fluorescence levels was confirmed by histology to be restricted to the cell layer in the CA1 (Figure 2.6A). Cells were identified from raw images using CNMF-E (Zhou et al., 2018) and registered longitudinally across the three experimental days to obtain Ca^{2+} traces as well as detected Ca^{2+} events (Figure 2.6B). Of the 21 animals (n = 11 control; n = 10 Cd) included in the behavior tests, only 4 animals per treatment had cells that were registered across all three experimental days. From these animals, we recorded Ca^{2+} activity across all three experimental days in 150 cells from control mice and 76 cells from Cd-exposed mice. Representative cells showed moderately increased noise (i.e. fluorescence signal not classified as Ca^{2+} events) in Ca^{2+} traces in cells from Cd exposed groups compared to control (Figure 2.6C) and these differences in fluorescence levels were observed in cell population averages (Supplementary Figure 2.1A). While Ca^{2+} transients can have wide ranges of fluorescence activity at any given point, we observed that on average, cells had low fluorescence levels (Figure 2.6D, Supplementary Figure 2.1B, and Supplementary Figure 2.2), consistent with other reports of Ca^{2+} activity in CA1 (Jimenez et al., 2020; Ziv et al., 2013). Next, we asked how Cd exposure affected fluorescence signals of the overall cell populations

throughout the three-day experiment. Cells from Cd-exposed mice exhibited a lower range in fluorescence activity and subtly increased median and IQR (Z-scores, Cd: min: -14.1, Q1: -1.76, median: -0.927, Q3: 0.180, max: 92.8, IQR: 1.94; Ctrl: min: -11.7, Q1: -1.70, median: -0.40, Q3: 0.0440, max: 139.0, IQR: 1.744). Cd-treatment significantly altered the distribution of fluorescence signals (Filgner-Killeen test: $p < 2.2e-16$; Wilcoxon rank sum test: $p = 4.58e-14$). These results suggest an overall inhibiting effect of Cd on Ca^{2+} activity of CA1 neurons.

To investigate whether Cd exposure affected activity of neurons in each phase of the experiment, we used Ca^{2+} events to calculate activity frequency (Figure 2.7A). Ca^{2+} events were identified using a conservative threshold factor of 12.0 mean absolute deviation from individual cell trace baseline. At experiment baseline, the distributions of Ca^{2+} event frequencies were similar between cells from control and Cd treated mice (Figure 2.7B). We observed that Cd-treated cells had increased distribution of cells during certain phases of the experiment (Figure 2.7C). To quantify these possible differences, we classified cells as activated (or not activated) compared to the mean baseline frequency by 2SD within each treatment groups. Lower proportion of cells were activated in Cd treated animals compared to control animals in nearly every phase (Figure 2.7D). We used a GEE to test for significant differences in the odds of activation comparing treatment groups. We found that the ratio of odds of activation comparing Cd to control was significantly different from 0 (or the odds ratio is significantly different from 1) ($p < 0.001$), where the odds of activation was significantly higher for control compared to Cd. We also found that the ratio of the odds of activation comparing the two groups was significantly different from 0 at each time point ($p < 0.001$), where the odds of activation was significantly higher for the control group. Additionally, we observed that activated cells were not always consistent across phases: cells that are activated during the first conditioning trial were not necessarily reactivated in later trials, although fewer percent of cells were reactivated consistently in Cd groups than control

(Figure 2.8). Overall, these findings suggest that Cd impairs the transient increases in Ca^{2+} activity in CA1 neurons during fear memory acquisition and recall.

2.4 Discussion

In this study we aimed to investigate the effects of a 10-week Cd exposure at 3 mg/L Cd in drinking water on Ca^{2+} activity *in vivo* during behavior paradigms involving the hippocampus. We used an *in vivo* Ca^{2+} imaging technique to monitor CA1 excitatory neuron activity in freely moving mice during fear conditioning and cued and contextual fear tests to investigate the effects of environmentally relevant Cd exposure on Ca^{2+} activity. Following the confirmation of a hippocampus-dependent memory impairment in the NOL test, Cd exposure was stopped for stereotaxic surgeries to inject GCaMP6f virus into hippocampus CA1 and to implant a GRIN lens to facilitate visualization of CA1 excitatory neurons. Cage wire racks were removed following stereotaxic surgeries to avoid animal injury or probe damage, therefore continued Cd exposure was not feasible due to the logistical limitations with housing cages, which cannot hold water bottles without wire racks.

We first observed that Ca^{2+} traces from Cd-exposed group appear to have higher noise (i.e. fluorescence activity that is not classified as a Ca^{2+} event) compared to control overall (Figure 2.6C and Supplementary Figure 2.1A). Biochemically, Cd can mimic Ca^{2+} and interact with proteins with metal binding sites (Lund et al., 2018). Cd can also enter cells through Ca^{2+} channels through mimicry (Bridges and Zalups, 2005; Choong et al., 2014; Hinkle et al., 1987). GCaMP6 is a CaM-based GECI. In one reference, Cd's binding affinity to CaM was reported to be high (equilibrium dissociation constant, K_D = 4.5 μM) (Suzuki et al., 1985), though the relative affinities for CaM is higher for Ca^{2+} than Cd (Richardt et al., 1986; Shirran and Barran, 2009). Based on previous brain Cd concentrations (Wang et al., 2018; Zhang et al., 2019b), we estimate

extracellular Cd concentration in the brain at 3 mg/L Cd exposure to be approximately 0.05 μM. Our observation of higher noise in fluorescence in Cd-treated groups supports the idea that Cd enters the brain and impacts Ca^{2+} binding to GCaMP6. The dF/noise calculation normalizes for baseline differences in noise between cells from Cd and control animals, thus it is likely that Cd influences Ca^{2+} binding kinetics to GCaMP6. While tens to 500 μM Cd treatments have been observed to block voltage-dependent Ca^{2+} channels in slice electrophysiology experiments (Fox et al., 1987; Huguenard, 1996; Thévenod and Jones, 1992), we observed rapid GCaMP6 fluorescence level changes *in vivo*, suggesting that our exposure paradigm resulted in low brain Cd levels that permit Ca^{2+} influxes. However, we observed a significant effect in the distribution of fluorescence level (z-score) with cells from Cd-exposed animals having decreased range of fluorescence levels overall. This finding suggests that there may be a partial block of voltage-gated Ca^{2+} channels with our exposure paradigm, although a dose-response will be necessary to clarify whether this is a block effect or related to GCaMP6.

Next, we investigated cell-level effects on Ca^{2+} activity of Cd exposure during each phase of the experiment. We observed that distributions of frequencies of Ca^{2+} events of each cell were further right skewed in the Cd-exposed group without complete elimination of higher event frequency responses. To quantify these differences, we classified cells as activated or not activated based on increased frequency compared to baseline (2SD). We found that Cd significantly decreased the proportion of activated cells during conditioning, as well as during contextual, novel, and cued fear memory tests. Our findings provide the first evidence in mice *in vivo* supporting the idea that exposure to environmentally relevant Cd may interfere with Ca^{2+} signaling in the hippocampus.

Our finding also suggests that on an individual neuron level, fewer proportion of neurons are undergoing significant Ca^{2+} influxes. One possible consequence is that the decreased activity directly results in lower activity of the signal transduction pathways implicated in memory

acquisition and consolidation, such as the Ca^{2+}/cAMP/ERK 1/2 MAP kinases/MSK1/CREB transcriptional pathway (Sindreu et al., 2007). Intracellular Ca^{2+} concentrations rapidly increase during activation of neurons, facilitating signaling pathways critical in learning and memory (Heck et al., 2015; Sabatini et al., 2002). Transient increase in cytosolic Ca^{2+} from influx through glutamate receptors and voltage-gated Ca^{2+} channels activates Ca^{2+}-dependent pathways that enhance membrane conductance and increase transmitter release probability, resulting in physical changes that strengthen or weaken synaptic transmission in a short time scale (Bliss and Cooke, 2011; Whitlock, 2006; Zucker and Regehr, 2002). Furthermore, this transient increase in Ca^{2+} is critical in regulation of synaptic protein transcription through the cyclic-AMP (cAMP) dependent signaling cascade mediated by cAMP-dependent protein kinase (PKA) and various mitogen activated protein kinases (MAPK). Ultimately, cAMP-response-element-binding protein (CREB) binds to specific DNA sequences to up- or down-regulate synaptic proteins, required for long-term memory (Wang and Storm, 2003). Ca^{2+} stimulation of CREB-mediated transcription downstream of MEK1/2, ERK1/2, and MSK1 during contextual memory formation is mediated by cAMP and regulated by Ca^{2+}-stimulated adenylyl cyclases (Sindreu et al., 2007). Contextual memory training and retrieval specifically activates and reactivates ERK 1/2 in excitatory neurons in the CA1 region of the hippocampus (Sindreu et al., 2011, 2007; Zamorano et al., 2018). While additional experiments are needed to clarify the relationship between decreased activity and downstream signaling, it is nevertheless an interesting finding that suggests a molecular mechanism for Cd impairment of memory.

Although we found inhibiting effects of Cd exposure on Ca^{2+} activity, we nevertheless observed no differences in fear conditioning, contextual fear memory, novel context fear, or cued fear memory between Cd and control groups 7 weeks after a 10-week exposure at 3 mg/L. Consistent with this finding, we observed that Cd exposure no longer had short term spatial memory impairments in the NOL test at 8 weeks after the end of exposure (data not shown).

These are both unexpected and inconsistent with previous reports using identical or near-identical behavior paradigms. In one study of C57BL/6 mice exposed to 3 mg/L Cd for 20 weeks, contextual fear memory was impaired 14 weeks after the end of exposure, consistent with other impairments in hippocampus-dependent memory including NOL test (9 weeks after exposure) and spontaneous alteration (10 weeks after exposure) (Wang et al., 2018). In another study of Nestin-CreER^{TM}:caMEK5-eGFP$^{loxP/loxP}$ mice exposed to 0.6 mg/L Cd for 38 weeks, impairment of contextual fear was observed 23 weeks after end of exposure (Wang et al., 2020). Because impairment was observed in both studies long after exposure, we did not expect to see a recovery in impairment from decreased Cd body burden. There are several possible explanations for these discrepancies. First, all scoring of behavioral data with *in vivo* imaging was done using EthoVision software. While EthoVision and other software-based behavior analysis is commonly used for higher throughput and unbiased behavioral analyses by automated animal tracking, their performance can lack flexibility and accuracy, leading to human scoring remaining as the gold standard (Sturman et al., 2020). It is possible that despite best efforts to optimize automated animal tracking and manual review of automated scoring data, that we are limited by the software. Second, although all mice were extensively handled and habituated to restraint and mini-microscope weight to reduce stress and anxiety, it is possible that freezing behavior was elevated in both groups of mice due to the brief restraint process prior to imaging. The high freezing in the novel context test, which typically results in <10% freezing (Wang et al., 2020, 2018) is consistent with this possibility.

Conclusion

In summary, we report that environmentally relevant Cd exposure impairs Ca^{2+} activity in neurons *in vivo* in the mouse hippocampus. We found that while this low-level Cd exposure continues to permit Ca^{2+} influx through Ca^{2+} channels, Cd exposure significantly decreased the

proportion of activated cells during acquisition and retrieval of contextual memory. To our knowledge, this is the first investigation of Cd's effects on brain Ca^{2+} activity *in vivo* in freely behaving mice and our findings provides a plausible molecular mechanism underlying Cd-induced impairment of hippocampus-dependent learning and memory. These findings provide new and exciting mechanistic insights of Cd neurotoxicity.

2.5 Future directions

Correlation of Ca^{2+} activity and freezing behavior

Our behavior data suggest that prior Cd treatment did not have significant effects on contextual fear memory. It would be interesting to see how Cd treatment affect how cells encode for context-specific (or tone-specific) fear response. To answer this question, we hope to investigate the correlation between freezing behavior and Ca^{2+} events by comparing Ca^{2+} events by freezing behavior, experiment phase, and treatment, with random effects variable accounting for cell ID. We hope to use these data to discern between general fear and context/tone-specific fear.

Cd effects on spatial representations in CA1

Neurons in the hippocampus respond to spatial cues, with particularly distinct cells, aptly named place cells, firing in the CA1 region when the rodent was in a certain place in the local environment (Moser et al., 2008, 2015). Because Cd effects are observed in spatial memory at levels relevant to the general population, we hypothesized that spatial representations in CA1 neurons is impaired in Cd-treated animals. In addition to the cued and contextual fear conditioning test, we habituated a subset of animals (n = 8 per treatment) in a new open field arena, then performed the 1-h NOL test in this arena to assess the effects of prior Cd exposure on

hippocampus-dependent spatial memory and *in vivo* Ca^{2+} activity. We hope to use these data to understand the effects of Cd exposure on spatial representations in CA1 place cells in the open field, as well as in NOL test.

2.6 Funding Statement

This work was supported in part by the University of Washington Superfund Research Program (NIEHS P42-ES-004696 to Z.X.) and the University of Washington Environmental Pathology/Toxicology Training Program (T32-ES-007032-42 to M.T.M.). We also acknowledge support from the NIH (S10 OD016240) to the W. M. Keck Center.

2.7 Acknowledgements

We thank Glen Abel, Dr. Hao Wang, and Dr. Liang Zhang for helpful discussion on experimental design. We thank the members of Dr. Richard Palmiter's laboratory, especially Drs. Jane Chen and Sekun Park for their guidance with methodology. We thank the University of Washington Environmental Health Laboratory for technical assistance with metals analysis, and for staff at the University of Washington Department of Comparative Medicine for expert animal care. We also thank the Statistical Consulting Program in the Department of Biostatistics at the University of Washington for statistical advice. All schematic figures were made using BioRender (biorender.com).

2.8 References

Ballinger GA. 2004. Using Generalized Estimating Equations for Longitudinal Data Analysis. *Organ Res Methods* **7**:127–150. doi:10.1177/1094428104263672

Biagioli M, Pifferi S, Ragghianti M, Bucci S, Rizzuto R, Pinton P. 2008. Endoplasmic reticulum stress and alteration in calcium homeostasis are involved in cadmium-induced apoptosis. *Cell Calcium* **43**:184–195. doi:10.1016/j.ceca.2007.05.003

Bliss TVP, Cooke SF. 2011. Long-term potentiation and long-term depression: a clinical perspective. *Clinics* **66**:3–17. doi:10.1590/S1807-59322011001300002

Bridges C, Zalups R. 2005. Molecular and ionic mimicry and the transport of toxic metals. *Toxicol Appl Pharmacol* **204**:274–308. doi:10.1016/j.taap.2004.09.007

Chen T-W, Wardill TJ, Sun Y, Pulver SR, Renninger SL, Baohan A, Schreiter ER, Kerr RA, Orger MB, Jayaraman V, Looger LL, Svoboda K, Kim DS. 2013. Ultrasensitive fluorescent proteins for imaging neuronal activity. *Nature* **499**:295–300. doi:10.1038/nature12354

Choong G, Liu Y, Templeton DM. 2014. Interplay of calcium and cadmium in mediating cadmium toxicity. *Chem Biol Interact* **211**:54–65. doi:10.1016/j.cbi.2014.01.007

Ciesielski T, Bellinger DC, Schwartz J, Hauser R, Wright RO. 2013. Associations between cadmium exposure and neurocognitive test scores in a cross-sectional study of US adults. *Environ Health* **12**. doi:10.1186/1476-069X-12-13

Ciesielski T, Weuve J, Bellinger DC, Schwartz J, Lanphear B, Wright RO. 2012. Cadmium Exposure and Neurodevelopmental Outcomes in U.S. Children. *Environ Health Perspect* **120**:758–763. doi:10.1289/ehp.1104152

Engstrom AK, Snyder JM, Maeda N, Xia Z. 2017. Gene-environment interaction between lead and Apolipoprotein E4 causes cognitive behavior deficits in mice. *Mol Neurodegener* **12**. doi:10.1186/s13024-017-0155-2

Fox AP, Nowycky MC, Tsien RW. 1987. Kinetic and pharmacological properties distinguishing three types of calcium currents in chick sensory neurones. *J Physiol* **394**:149–172. doi:10.1113/jphysiol.1987.sp016864

Godt J, Scheidig F, Grosse-Siestrup C, Esche V, Brandenburg P, Reich A, Groneberg DA. 2006. The toxicity of cadmium and resulting hazards for human health. *J Occup Med Toxicol Lond Engl* **1**:22. doi:10.1186/1745-6673-1-22

Heck A, Fastenrath M, Coynel D, Auschra B, Bickel H, Freytag V, Gschwind L, Hartmann F, Jessen F, Kaduszkiewicz H, Maier W, Milnik A, Pentzek M, Riedel-Heller SG, Spalek K, Vogler C, Wagner M, Weyerer S, Wolfsgruber S, Quervain DJ-F de, Papassotiropoulos A. 2015. Genetic Analysis of Association Between Calcium Signaling and Hippocampal Activation, Memory Performance in the Young and Old, and Risk for Sporadic Alzheimer Disease. *JAMA Psychiatry* **72**:1029–1036. doi:10.1001/jamapsychiatry.2015.1309

Hinkle PM, Kinsella PA, Osterhoudt KC. 1987. Cadmium uptake and toxicity via voltage-sensitive calcium channels. *J Biol Chem* **262**:16333–16337.

Huguenard JR. 1996. Low-threshold calcium currents in central nervous system neurons. *Annu Rev Physiol* **58**:329–348. doi:10.1146/annurev.ph.58.030196.001553

Jimenez JC, Berry JE, Lim SC, Ong SK, Kheirbek MA, Hen R. 2020. Contextual fear memory retrieval by correlated ensembles of ventral CA1 neurons. *Nat Commun* **11**:3492. doi:10.1038/s41467-020-17270-w

Josselyn SA, Köhler S, Frankland PW. 2015. Finding the engram. *Nat Rev Neurosci* **16**:521–534. doi:10.1038/nrn4000

Josselyn SA, Tonegawa S. 2020. Memory engrams: Recalling the past and imagining the future. *Science* **367**:eaaw4325. doi:10.1126/science.aaw4325

Li H, Wang Z, Fu Z, Yan M, Wu N, Wu H, Yin P. 2018. Associations between blood cadmium levels and cognitive function in a cross-sectional study of US adults aged 60 years or older. *BMJ Open* **8**. doi:10.1136/bmjopen-2017-020533

Liu X, Zhou J-L, Chung K, Chung JM. 2001. Ion channels associated with the ectopic discharges generated after segmental spinal nerve injury in the rat. *Brain Res* **900**:119–127. doi:10.1016/S0006-8993(01)02274-0

Lund E, Krezoski S, Petering D. 2018. The Chemical Biology of Cadmium In: Thévenod F, Petering D, M. Templeton D, Lee W-K, Hartwig A, editors. Cadmium Interaction with Animal Cells. Cham: Springer International Publishing. pp. 23–52. doi:10.1007/978-3-319-89623-6_2

Moser EI, Kropff E, Moser M-B. 2008. Place Cells, Grid Cells, and the Brain's Spatial Representation System. *Annu Rev Neurosci* **31**:69–89. doi:10.1146/annurev.neuro.31.061307.090723

Moser M-B, Rowland DC, Moser EI. 2015. Place Cells, Grid Cells, and Memory. *Cold Spring Harb Perspect Biol* **7**:a021808. doi:10.1101/cshperspect.a021808

Pan Y-W, Chan GCK, Kuo CT, Storm DR, Xia Z. 2012. Inhibition of Adult Neurogenesis by Inducible and Targeted Deletion of ERK5 Mitogen-Activated Protein Kinase Specifically in Adult Neurogenic Regions Impairs Contextual Fear Extinction and Remote Fear Memory. *J Neurosci* **32**:6444–6455. doi:10.1523/JNEUROSCI.6076-11.2012

Richardt G, Federolf G, Habermann E. 1986. Affinity of heavy metal ions to intracellular Ca2+-binding proteins. *Biochem Pharmacol* **35**:1331–1335. doi:10.1016/0006-2952(86)90278-9

Rubin A, Sheintuch L, Brande-Eilat N, Pinchasof O, Rechavi Y, Geva N, Ziv Y. 2019. Revealing neural correlates of behavior without behavioral measurements. *Nat Commun* **10**. doi:10.1038/s41467-019-12724-2

Sabatini BL, Oertner TG, Svoboda K. 2002. The Life Cycle of Ca2+ Ions in Dendritic Spines. *Neuron* **33**:439–452. doi:10.1016/S0896-6273(02)00573-1

Satarug S, Moore MR. 2004. Adverse Health Effects of Chronic Exposure to Low-Level Cadmium in Foodstuffs and Cigarette Smoke. *Environ Health Perspect* **112**:1099–1103. doi:10.1289/ehp.6751

Sheintuch L, Geva N, Baumer H, Rechavi Y, Rubin A, Ziv Y. 2020. Multiple Maps of the Same Spatial Context Can Stably Coexist in the Mouse Hippocampus. *Curr Biol* **30**:1467-1476.e6. doi:10.1016/j.cub.2020.02.018

Sheintuch L, Rubin A, Brande-Eilat N, Geva N, Sadeh N, Pinchasof O, Ziv Y. 2017. Tracking the Same Neurons across Multiple Days in Ca2+ Imaging Data. *Cell Rep* **21**:1102–1115. doi:10.1016/j.celrep.2017.10.013

Shirran SL, Barran PE. 2009. The use of ESI-MS to probe the binding of divalent cations to calmodulin. *J Am Soc Mass Spectrom* **20**:1159–1171. doi:10.1016/j.jasms.2009.02.008

Sindreu C, Palmiter RD, Storm DR. 2011. Zinc transporter ZnT-3 regulates presynaptic Erk1/2 signaling and hippocampus-dependent memory. *Proc Natl Acad Sci* **108**:3366–3370. doi:10.1073/pnas.1019166108

Sindreu CB, Scheiner ZS, Storm DR. 2007. Ca2+-Stimulated Adenylyl Cyclases Regulate ERK-Dependent Activation of MSK1 during Fear Conditioning. *Neuron* **53**:79–89. doi:10.1016/j.neuron.2006.11.024

Sturman O, von Ziegler L, Schläppi C, Akyol F, Privitera M, Slominski D, Grimm C, Thieren L, Zerbi V, Grewe B, Bohacek J. 2020. Deep learning-based behavioral analysis reaches human accuracy and is capable of outperforming commercial solutions. *Neuropsychopharmacology* **45**:1942–1952. doi:10.1038/s41386-020-0776-y

Suzuki Y, Chao S-H, Zysk JR, Cheung WY. 1985. Stimulation of calmodulin by cadmium ion. *Arch Toxicol* **57**:205–211. doi:10.1007/BF00290889

Templeton DM, Liu Y. 2018. Interactions of Cadmium with Signaling Molecules In: Thévenod F, Petering D, M. Templeton D, Lee W-K, Hartwig A, editors. Cadmium Interaction with Animal Cells. Cham: Springer International Publishing. pp. 53–81. doi:10.1007/978-3-319-89623-6_3

Thévenod F, Jones SW. 1992. Cadmium block of calcium current in frog sympathetic neurons. *Biophys J* **63**:162–168. doi:10.1016/S0006-3495(92)81575-8

Thévenod F, Lee W-K. 2013. Cadmium and cellular signaling cascades: interactions between cell death and survival pathways. *Arch Toxicol* **87**:1743–1786. doi:10.1007/s00204-013-1110-9

Thévenod F, Petering D, M. Templeton D, Lee W-K, Hartwig A, editors. 2018. Cadmium Interaction with Animal Cells. Cham: Springer International Publishing. doi:10.1007/978-3-319-89623-6

Wang H, Abel GM, Storm DR, Xia Z. 2019. Cadmium Exposure Impairs Adult Hippocampal Neurogenesis. *Toxicol Sci* **171**:501–514. doi:10.1093/toxsci/kfz152

Wang H, Matsushita MT, Zhang L, Abel GM, Mommer BC, Huddy TF, Storm DR, Xia Z. 2020. Inducible and Conditional Stimulation of Adult Hippocampal Neurogenesis Rescues Cadmium-Induced Impairments of Adult Hippocampal Neurogenesis and Hippocampus-Dependent Memory in Mice. *Toxicol Sci Off J Soc Toxicol* **177**:263–280. doi:10.1093/toxsci/kfaa104

Wang H, Storm DR. 2003. Calmodulin-Regulated Adenylyl Cyclases: Cross-Talk and Plasticity in the Central Nervous System. *Mol Pharmacol* **63**:463–468. doi:10.1124/mol.63.3.463

Wang H, Zhang L, Abel GM, Storm DR, Xia Z. 2018. Cadmium Exposure Impairs Cognition and Olfactory Memory in Male C57BL/6 Mice. *Toxicol Sci Off J Soc Toxicol* **161**:87–102. doi:10.1093/toxsci/kfx202

Whitlock JR. 2006. Learning Induces Long-Term Potentiation in the Hippocampus. *Science* **313**:1093–1097. doi:10.1126/science.1128134

Zamorano C, Fernández-Albert J, Storm DR, Carné X, Sindreu C. 2018. Memory Retrieval Re-Activates Erk1/2 Signaling in the Same Set of CA1 Neurons Recruited During Conditioning. *Neuroscience*, Molecular and Cellular Mechanisms of Cognitive Function **370**:101–111. doi:10.1016/j.neuroscience.2017.03.034

Zhang L, Chen X, Sindreu C, Lu S, Storm DR, Zweifel LS, Xia Z. 2019a. Dynamics of a hippocampal neuronal ensemble encoding trace fear memory revealed by in vivo Ca2+ imaging. *PLoS ONE* **14**. doi:10.1371/journal.pone.0219152

Zhang L, Wang H, Abel GM, Storm DR, Xia Z. 2019b. The Effects of Gene-Environment Interactions Between Cadmium Exposure and Apolipoprotein E4 on Memory in a Mouse Model of Alzheimer's Disease. *Toxicol Sci* kfz218. doi:10.1093/toxsci/kfz218

Zhou P, Resendez SL, Rodriguez-Romaguera J, Jimenez JC, Neufeld SQ, Giovannucci A, Friedrich J, Pnevmatikakis EA, Stuber GD, Hen R, Kheirbek MA, Sabatini BL, Kass RE, Paninski L. 2018. Efficient and accurate extraction of in vivo calcium signals from microendoscopic video data. *eLife* **7**:e28728. doi:10.7554/eLife.28728

Ziv Y, Burns LD, Cocker ED, Hamel EO, Ghosh KK, Kitch LJ, Gamal AE, Schnitzer MJ. 2013. Long-term dynamics of CA1 hippocampal place codes. *Nat Neurosci* **16**:264–266. doi:10.1038/nn.3329

Zucker RS, Regehr WG. 2002. Short-Term Synaptic Plasticity. *Annu Rev Physiol* **64**:355–405. doi:10.1146/annurev.physiol.64.092501.114547

2.9 Figures

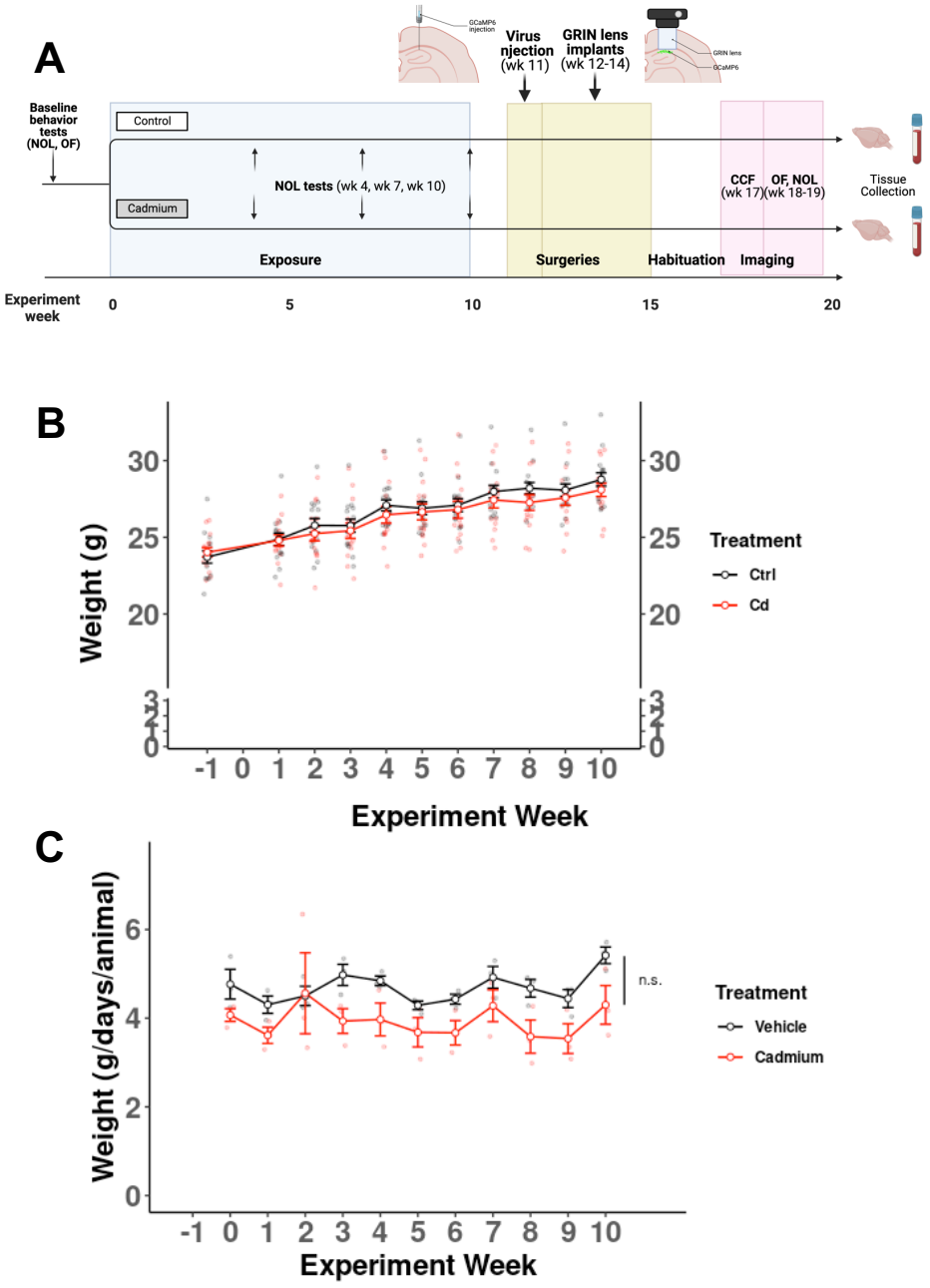

Figure 2.1: Experimental design and timeline. (A) Schematic of the experimental design with Cd exposure (3 mg/L Cd as $CdCl_2$), stereotaxic surgeries, and imaging. Animals were 8 weeks of age at the start of Cd treatment. n = 15 animals per treatment. (B) Body weight of each mouse was measured every 1-2 weeks during and after Cd exposure. n = 3 cages per treatment. (C) Water consumption was estimated from water bottle weights of each cage, measured every week. n = 5 animals per cage. Data are presented as mean ± SEM. NOL = novel object location, OF = open field, CCF = Cued and context fear conditioning.

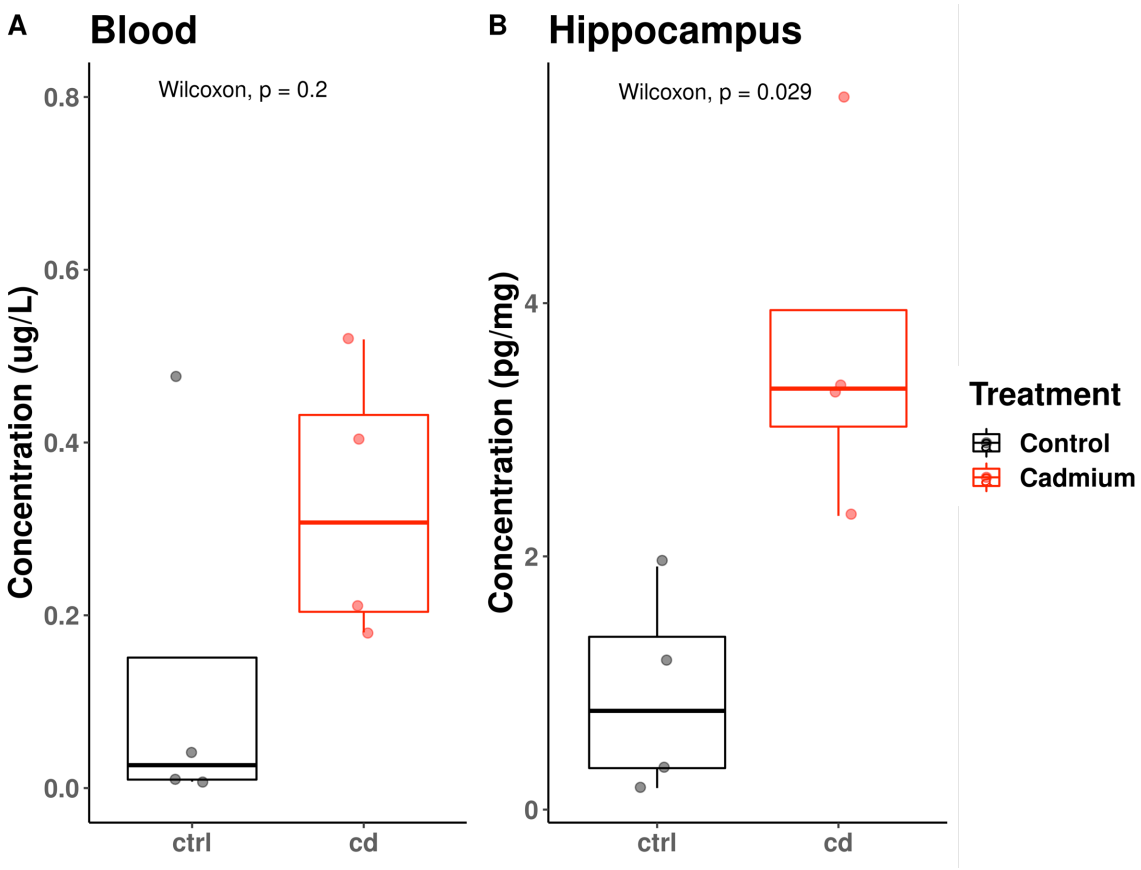

Figure 2.2: Cd levels in collected tissue measured by ICP-MS. (A) Blood Cd levels. (B) Brain Cd levels in the hippocampus. n = 4 per group. Data are presented as box plots with median + IQR.

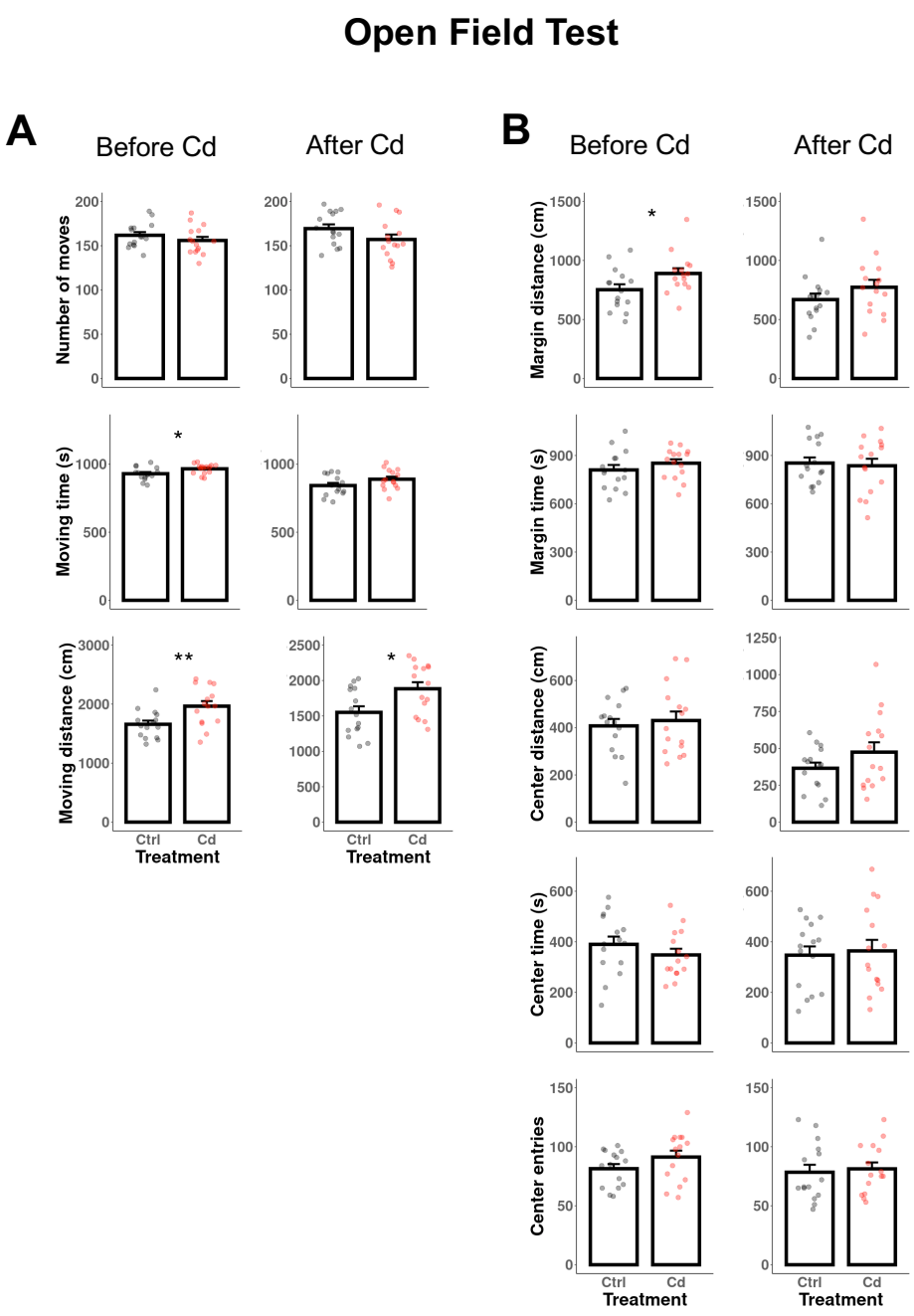

Figure 2.3: Locomotor and anxiety activity of control and Cd treated mice measured in the open field test. (A) Locomotor activity. Before Cd treatment, the Cd group (selected *a priori*) showed higher moving time and moving distance. After Cd treatment, the Cd group still showed higher moving distance. (B) Anxiety activity. Before Cd treatment, the Cd group showed higher distance traveled in the margin. There were no differences in included metrics after Cd treatment. n = 15 animals per treatment. Welch's two-tailed t-test: *p < 0.05, **p < 0.01.

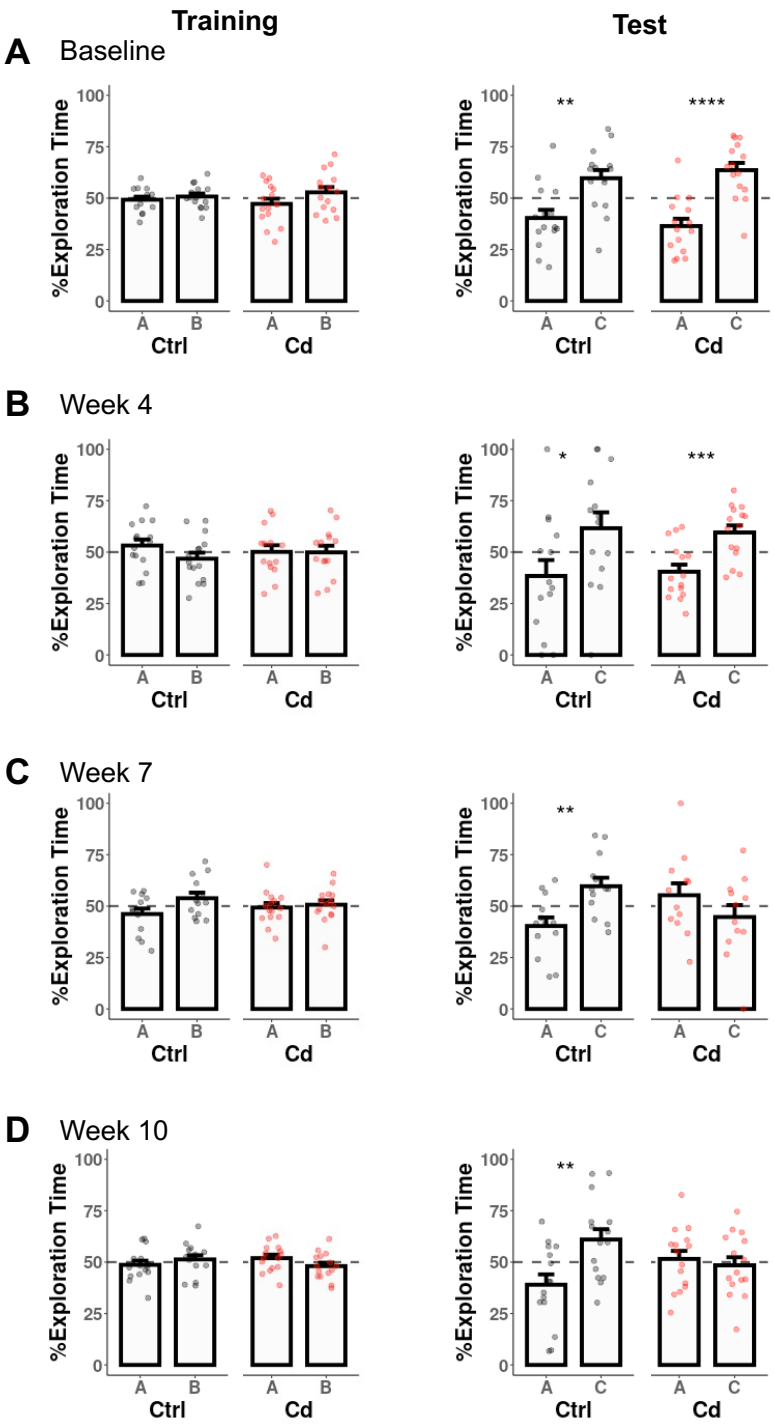

Figure 2.4: The effects of Cd exposure on hippocampus-dependent short-term spatial memory in the NOL test. The time each mouse spent exploring objects in the old location (location A) and a novel location (location C) was quantified and compared. (A, B) Both treatment groups were able to distinguish between old and novel locations at baseline and at week 4. (C, D) Cd-treated mice no longer distinguish between the old and novel locations at weeks 7 and 10. Data are presented as mean ± SEM. n = 15 animals per treatment. Welch's two-tailed t-test, *p < 0.05, **p < 0.01, ***p < 0.001, ****p < 0.0001.

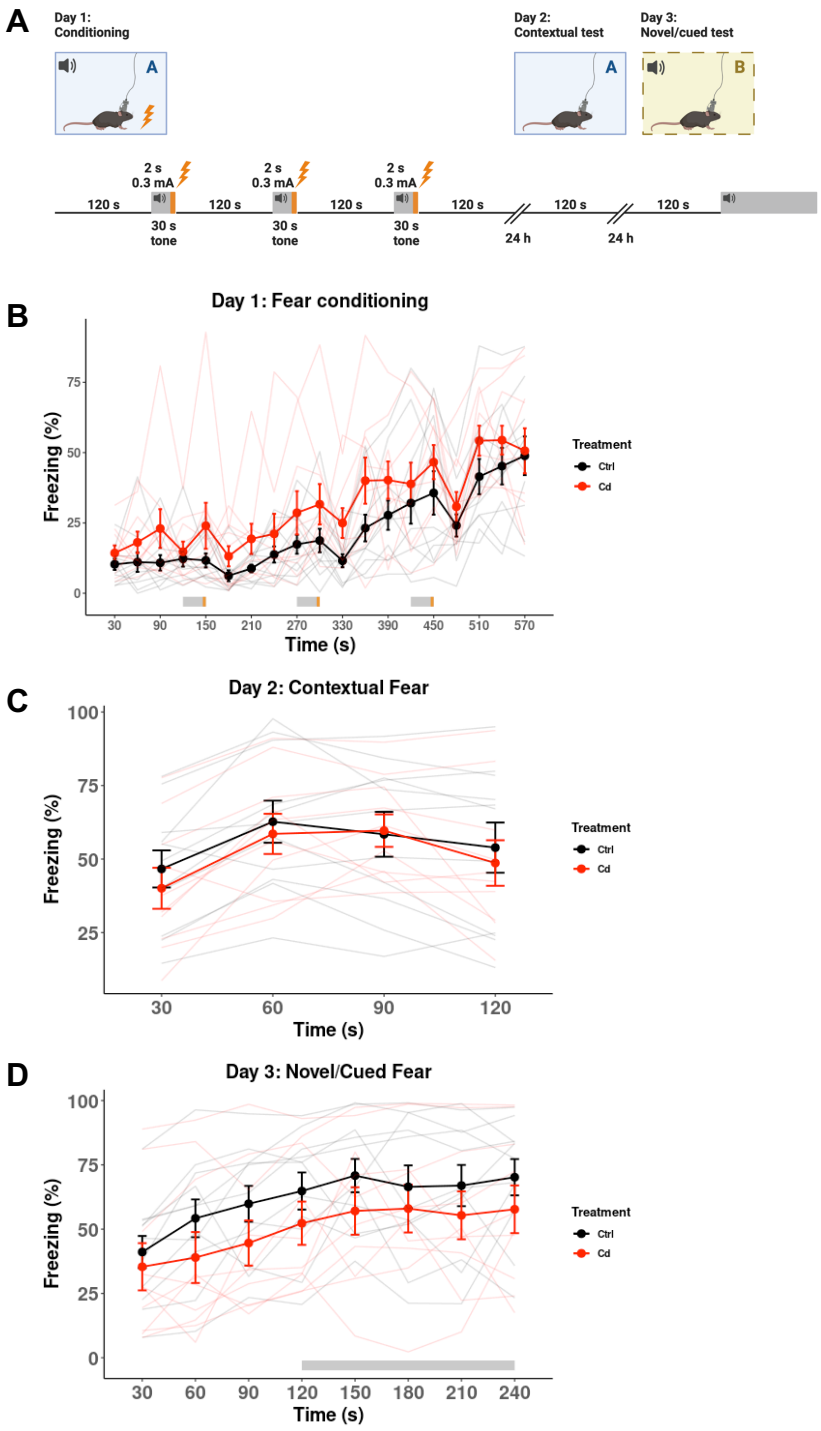

Figure 2.5: Cued and contextual fear conditioning. (A) Illustrated schematic of the 3-day cued and contextual fear conditioning. Conditioning with 0.3 mA x3 foot shock presentations with 30 s tone makes this fear paradigm challenging and sensitive to changes in contextual memory. (B) Mice in both groups exhibit increased freezing over conditioning. (C). Both groups exhibit high level of freezing in contextual fear test. Cd treated animals did not show any difference in freezing at any 30-s bins. (D) Cd treated animals did not show any difference in freezing at any 30-s bins during novel context or cued tests. n = 11 control; n = 10 Cd.

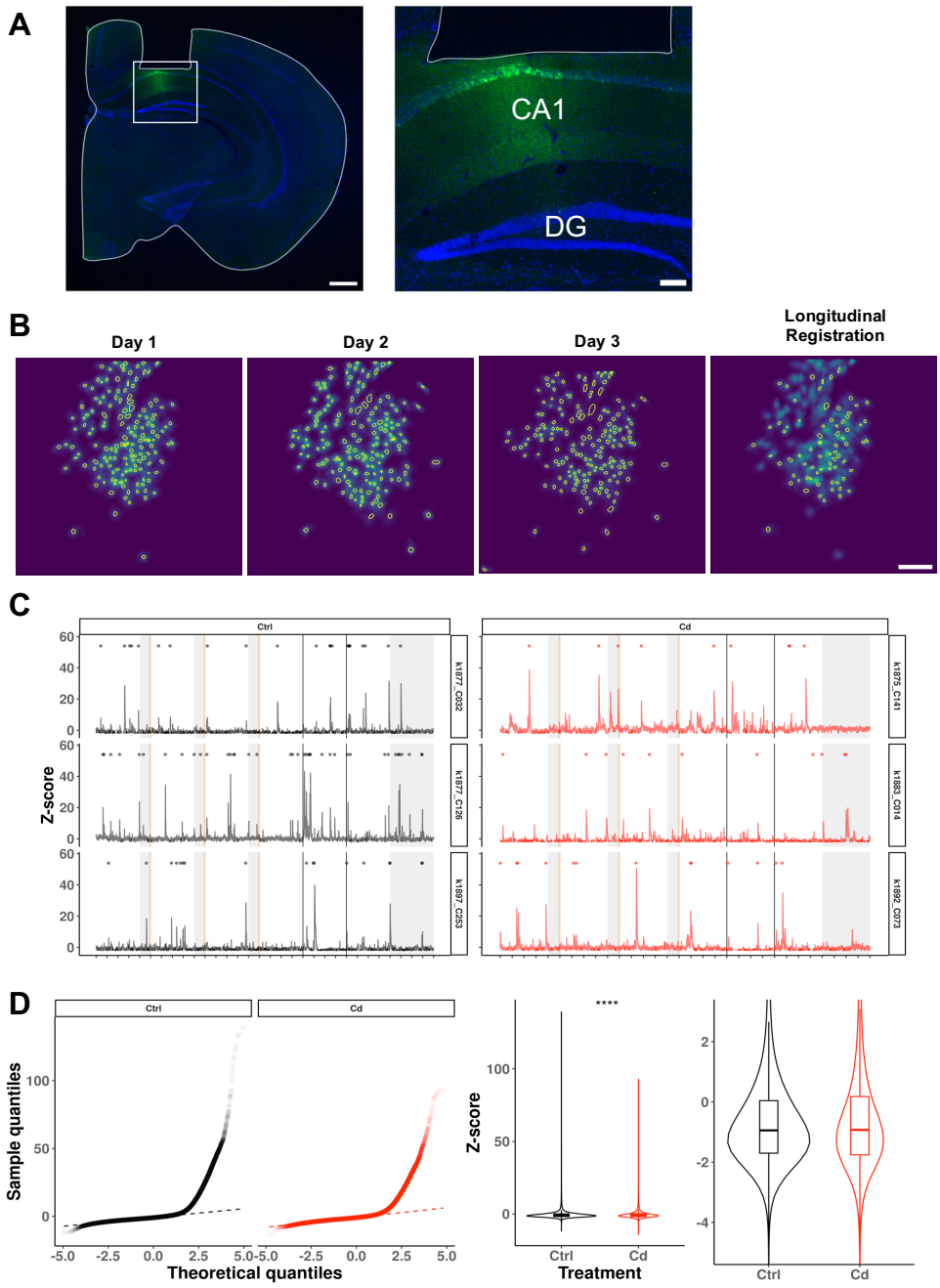

Figure 2.6: Fluorescence activity monitored by GCaMP6f. (A) Representative image of GCaMP6f virus injection site in CA1 and GRIN lens placement above the CA1 in a coronal section (left) and zoom (right). Endogenous GCaMP6f fluorescence (green), DAPI counterstain (blue). Scale bar, 500um (left), 100um (right). (B) Representative image of cells identified by CNMF-E on each experimental day and longitudinal registration. (C) Representative traces in cells from control (left) and Cd-exposed (right) mice. Dots represent Ca^{2+} events. (D) Left: Fluorescence data are non-normally distributed for both treatment groups. Right: Distributions of fluorescence signals are significantly different between treatments. Zoom in violin plot shows higher median, larger IQR, and smaller range in Cd treatment. n = 150, control; n = 76, Cd. Wilcoxon rank sum test: ****p <= 0.0001.

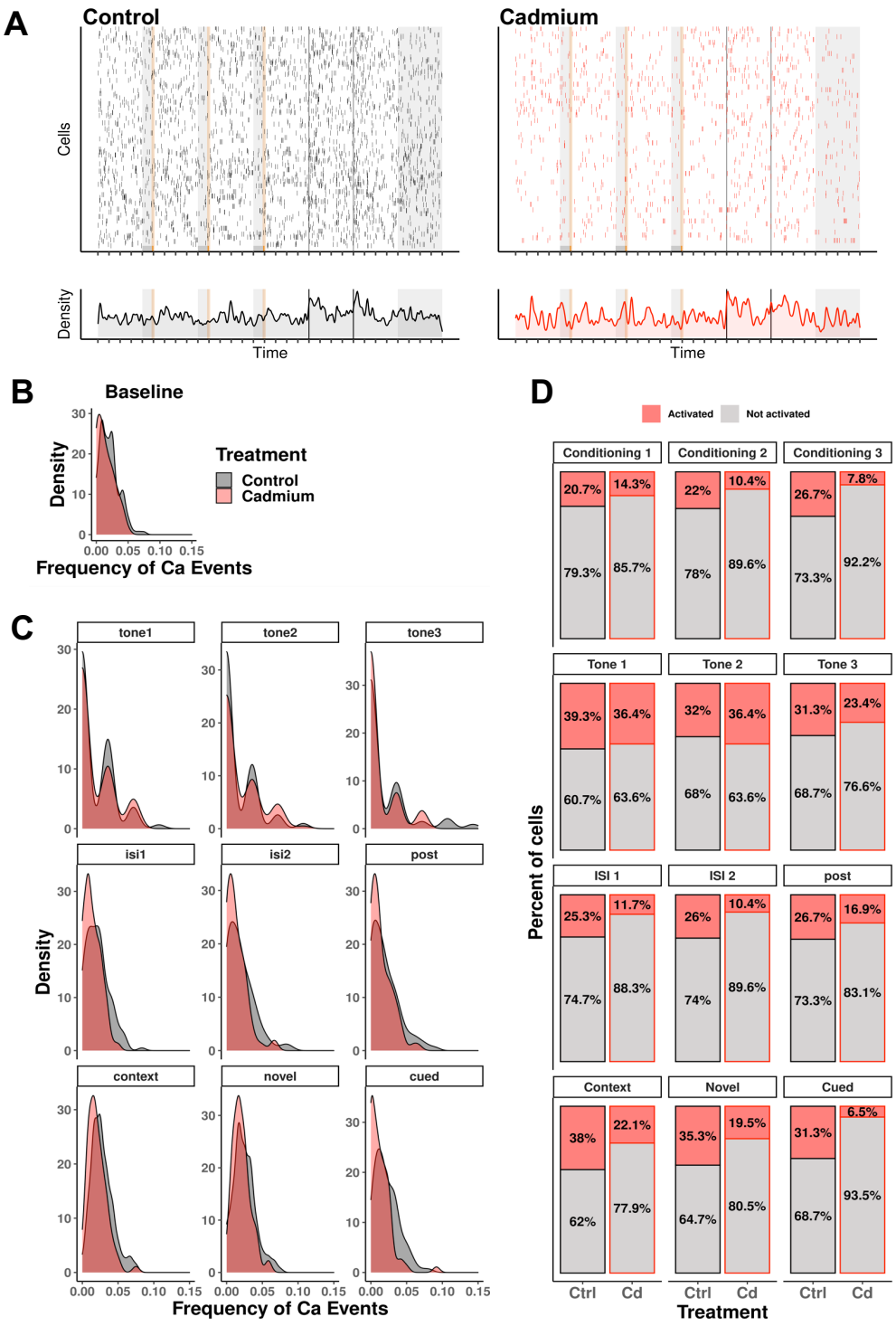

Figure 2.7: Ca^{2+} events and event frequency during the 3-day CCF test. (A) Raster plot of Ca^{2+} events during the experiment (top) and density plots for cells in control (n = 150, black) and Cd (n = 76, red) exposed animals. (B) Distributions of frequency of Ca^{2+} events during baseline. (C) Distributions of frequency of Ca^{2+} events during each phase of the CCF test. (D) Cells were classified as activated or not activated compared to the period (2SD). Lower percent of cells were activated in Cd-treated mice.

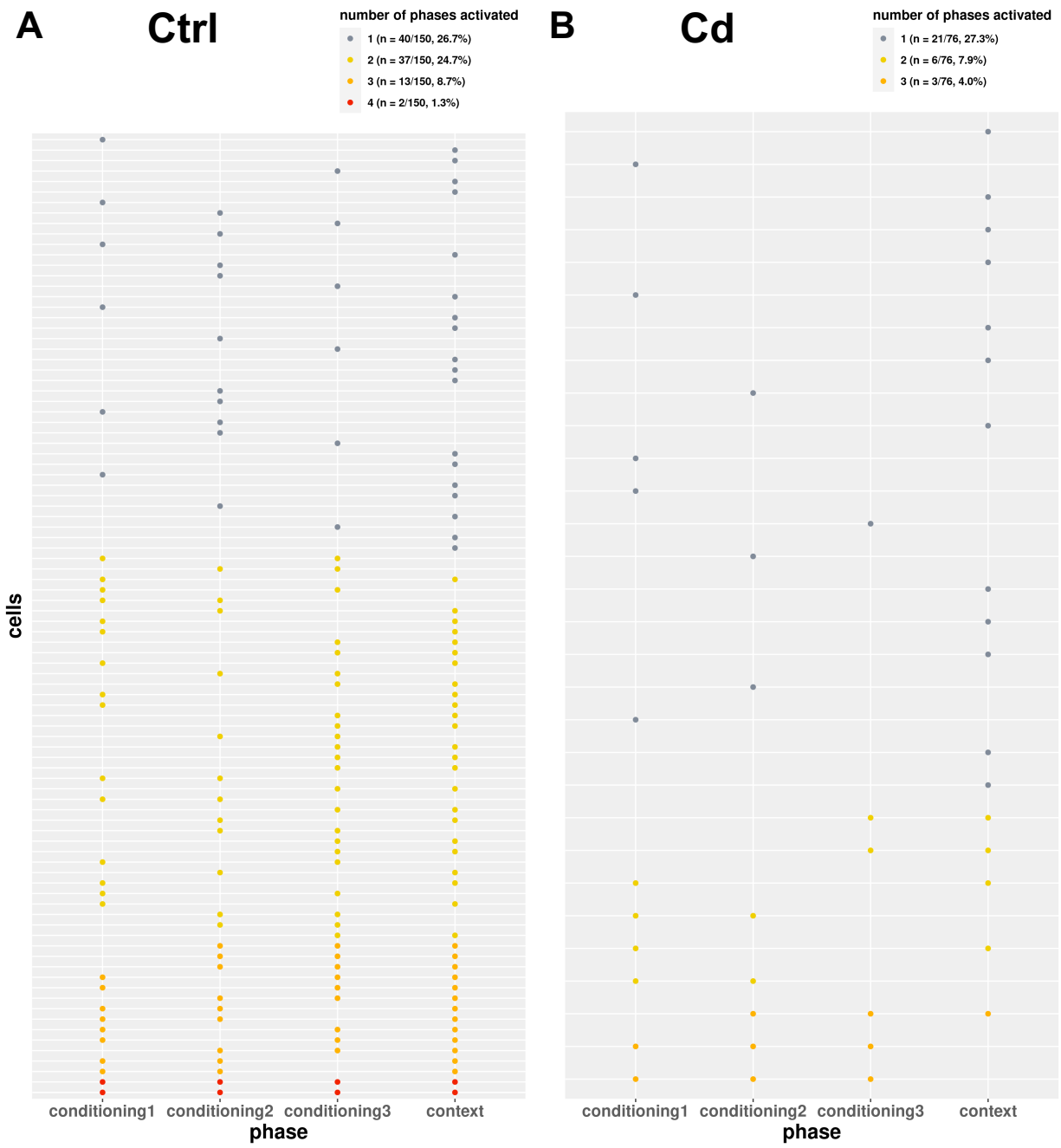

Figure 2.8: Activated cells during conditioning phases and context test. Each row corresponds to a unique cell, with activation during a phase indicated by the presence of data points. Data point color corresponds to the number of phases (1-4) each cell is activated. Cells from the control treatment group (A) have higher percentage of cells that are activated across multiple phases compared to Cd treatment group (B).

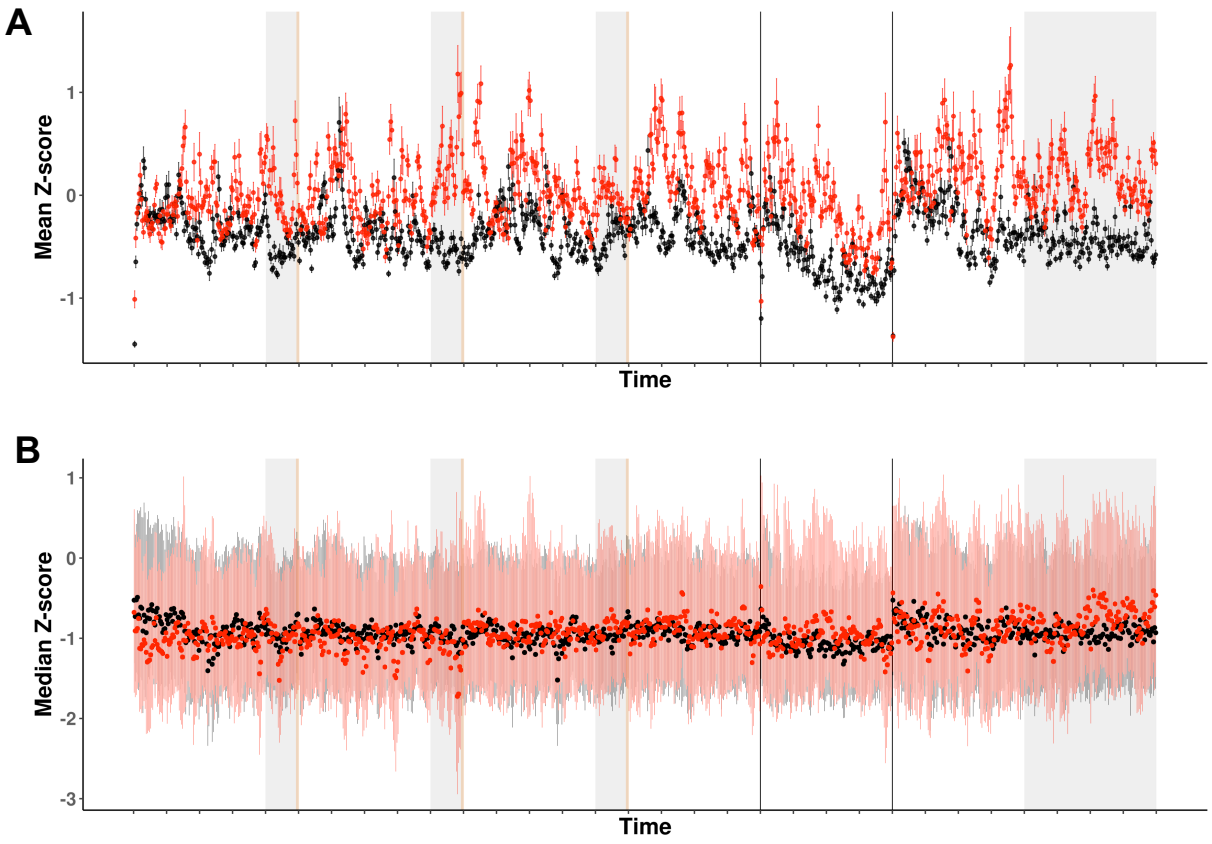

Supplementary Figure 2.1: Comparison of mean vs. median z-scores. (A) Mean z-scores (mean ± SEM) of 1-s bins suggest that cells in Cd exposed group have higher overall fluorescence. (B) Median z-scores (median ± IQR) of 1-s bins.

Supplementary Figure 2.2: Ca^{2+} traces as heatmaps. Cells are sorted by hierarchical clustering (ward.D on hclust, based on variances rather than Euclidean distances).

Chapter 3. Inducible and conditional activation of adult neurogenesis rescues cadmium-induced hippocampus-dependent memory deficits in ApoE4-KI mice

3.1 Introduction

Alzheimer's disease (AD) is a leading neurodegenerative disease characterized by progressive cognitive decline and memory loss and the leading cause of dementia accounting for an estimated 60 to 80% of cases (Alzheimer's Association, 2022). While amyloid precursor protein (*APP*), presenilin1 (*PSEN1*), and presenilin2 (*PSEN2*) genes have been identified as causal genes for early-onset AD, they account for less than 6% of AD cases (Bekris et al., 2010; Liu et al., 2013). A combination of environmental factors and genetic factors likely contribute significantly to the disease etiology for sporadic, late-onset AD (Bakulski et al., 2020; Migliore and Coppedè, 2022). Furthermore, a gene-environment interaction (GxE) between genetic factors and environmental factors may lead to increased severity or acceleration of cognitive decline.

The apolipoprotein E (*APOE*) gene is the strongest known genetic risk factor for late-onset AD. Carriers of the ε4 allele have estimates of up to 12 times higher risk compared to carriers of the more common ε3 allele (Liu et al., 2013; Michaelson, 2014). Cadmium (Cd) is a toxic heavy metal of public health concern due to ubiquitous, low-level exposures to the general population through food and smoking (Satarug et al., 2010). Recent epidemiology studies have reported associations of Cd and cognitive impairment in US adults (Ciesielski et al., 2013, 2012; Li et al., 2018). A recent report from our lab demonstrated a causal relationship between low-level Cd exposure and cognitive decline in a controlled mouse study (Wang et al., 2017). Furthermore, our lab previously utilized a humanized knock-in (KI) mouse model of AD to investigate the effect of GxE on cognition. These mice express the human ε4 (ApoE4-KI) or human ε3 alleles (ApoE3-KI) under the control of the endogenous mouse ApoE promoter; thus, the human ApoE3 or ApoE4 are expressed at physiological levels (Xu et al., 2006). Our recently published data showed that

ApoE4-KI males had earlier onset of cognitive deficits compared to ApoE3-KI males with treatment of 0.6 mg/L $CdCl_2$ in drinking water (Zhang et al., 2019). These results provide direct experimental evidence that a GxE between ApoE4 and environmental factors including heavy metals like Cd may contribute to cognitive impairment associated with AD. However, the mechanisms underlying GxE effects are largely undefined.

The process of adult neurogenesis involves the generation of neurons from a subset of neural progenitor cells (NPCs) in a quiescence state into fully differentiated neurons that integrate into existing neuronal circuits (Aimone et al., 2014; Gonçalves et al., 2016). In the adult mammalian brain, the adult NPC (aNPC) population is restricted to two neurogenic regions: the subventricular zone (SVZ), which gives rise to new inhibitory neurons in the olfactory bulb (OB), and the subgranular zone (SGZ) of the hippocampal dentate gyrus (DG), which gives rise to excitatory granular cells in the DG (Aimone et al., 2014; Gage, 2000). The integration of adult-born neurons in the hippocampus is critical in hippocampus-dependent learning and memory, with ablation or reduction of adult hippocampal neurogenesis leading to impairments in hippocampus-dependent learning and memory tasks (Anacker and Hen, 2017; Denoth-Lippuner and Jessberger, 2021; Pan et al., 2013). Our lab has previously demonstrated that Cd impairs adult neurogenesis (Wang et al., 2019) and established a causal link between Cd-induced impairment in hippocampus-dependent memory and impairment of adult neurogenesis (Wang et al., 2020). We have also previously reported an impairment of adult neurogenesis in ApoE4-KI mice congruent to the observation of earlier onset of cognitive deficits in ApoE4-KI mice compared to ApoE3-KI mice (Zhang et al., 2019).

The main goal of this study is to investigate the molecular and cellular mechanisms underlying this GxE effect of ApoE4 and Cd on hippocampus-dependent memory. We hypothesized that the GxE effect of ApoE4 and Cd on hippocampal adult neurogenesis contributes to impairment of hippocampus-dependent learning and memory. To this end, we

designed a functional rescue experiment utilizing a multi-transgenic mouse line to specifically and genetically stimulate adult neurogenesis following the observation of hippocampus-dependent memory impairment in a GxE model of humanized ApoE4-KI mice treated with Cd.

3.2 Materials and Methods

Animals

We utilized humanized ApoE3- and ApoE4-knockin (ApoE3-KI and ApoE4-KI) mice as a non-amyloid dependent genetic risk model of Alzheimer's disease. These mice were provided by Dr. Nobuyo Maeda at the University of North Carolina, Chapel Hill and maintained as homozygous lines in our animal facility.

We have previously reported that the specific and selective deletion of the extracellular signal-regulated kinase 5 (ERK5), a member of the mitogen-activated protein kinase (MAPK) family, is specifically expressed in adult neurogenic regions and is critical for the regulation of adult hippocampal neurogenesis (Pan et al., 2012). ERK5 is activated by MEK5, a specific upstream activating kinase for ERK5 which does not phosphorylate ERK1/2, JNK, or p38 even when overexpressed (English et al., 1995; Zhou et al., 1995). We generated Nestin-CreER^{TM}:caMEK5-eGFP$^{loxP/loxP}$ (simplified to caMEK5) mice to induce the activation of ERK5 through specific and selective induction of constitutively active MEK5 (caMEK5) fused with enhanced green fluorescent protein (eGFP) in the neurogenic regions of the brain (controlled by Nestin-Cre expression) to genetically and conditionally induce adult neurogenesis (Wang et al., 2014).

We bred ApoE3-KI or ApoE4-KI mice with caMEK5 mice to obtain ApoE3-KI:caMEK5 and ApoE4-KI:caMEK5 mice. To achieve these triple transgenic animals, we crossed Nestin-CreER^{TM}:caMEK5-eGFP$^{loxP/loxP}$:ApoE3-KI male mice with caMEK5-eGFP$^{loxP/loxP}$:ApoE3-KI female

mice to achieve genotypic ratio of 1:1 (Figure 3.1A). The same breeding scheme was used to obtain ApoE4-KI:caMEK5. For both breeding procedures, male animals were less than 6 months old and females were less than one year old. The ApoE3-KI:caMEK5 and ApoE4-KI:caMEK5 transgenic mouse models allow us to stimulate adult neurogenesis upon tamoxifen treatment through the expression of caMEK5 with the ApoE3-KI or ApoE4-KI background (Figure 3.1B). All animals in each experimental cohort were within 2 weeks of age. Following genotyping, male animals were randomly housed into groups of 4-5 animals per cage for the behavior cohort or 2-4 animals per cage for the cellular cohort to balance age ranges across each treatment group, assigned *a priori*. Total animal numbers for the behavior cohort were n = 13-14 per treatment per genotype at the beginning of experiment; n = 12-14 at the end of experiment. Total animal numbers for the cellular cohort were n = 6-8 per treatment per genotype at the beginning of experiment; n = 4-7 at the end of experiment.

All mice were housed under standard conditions (12 h light/dark cycle) with food (Picolab Rodent Diet 2-, Lab Diet, St. Louis, MO) and autoclaved water (tap water purified by reverse osmosis, acidified with 2.4-2.8% HCl) provided *ad libitum*. All animal care and treatments were approved by the University of Washington Institutional Animal Care and Use Committee.

Cd exposure

We have previously reported that Cd treatment with 0.6 mg/L $CdCl_2$ in drinking water yields average blood Cd levels of 0.3-0.4 µg/L in C57BL/6 mice (Wang et al., 2020) and ApoE3-KI and ApoE4-KI mice (Zhang et al., 2019), comparable to blood Cd levels in the general non-smoking US population. All mice were acclimated to water bottles for 2 weeks, then provided Cd (as 0.6 mg/L $CdCl_2$) water at 8-10 weeks of age through the end of the experiment. Water bottles were replaced weekly. Water bottle weights were recorded prior to placement in the cage and following removal from the cage. The preparation, use, and disposal of hazardous reagents were

conducted according to the guidelines from the Environmental Health and Safety Office at the University of Washington.

Study design

The study design includes a behavior cohort (Figure 3.1C) and a cellular cohort that closely follows the timeline of the behavior cohort (Figure 3.1D). For both cohorts, all animals started their Cd exposure at 8-10 weeks of age and were exposed through the end of the experiment. Because NOL deficits were expected to be observed at different time points for ApoE3-KI:caMEK5 animals and ApoE4-KI:caMEK5 animals, experimental timelines differed by genotype.

The behavioral cohort animals underwent baseline behavior tests (open field test, novel object location test) prior to Cd exposure. Following the start of Cd exposure, animals were probed for hippocampus-dependent spatial working memory using the novel object location test approximately every other week. Once NOL deficits were observed (as defined by the disappearance of significant differences between percent of time spent in the familiar vs. novel locations), the deficits were confirmed by at least two subsequent tests one week apart. Once deficits were confirmed, animals were treated with tamoxifen or vehicle to induce caMEK5 expression. Following a recovery period from tamoxifen or vehicle treatment, animals were followed up with behavior tests (open field test, novel object location test, T-maze spontaneous alternation test, and cued and contextual fear test). At the end of the experiment, brain and blood tissues were collected for Cd analysis.

The cellular cohort animals were 3 weeks younger than the behavioral cohort for ApoE4-KI:caMEK5 animals and 5 weeks younger than the behavioral cohort for ApoE3-KI:caMEK5 animals. No behavior experiments were conducted with the cellular cohorts. The timeline for tamoxifen and vehicle treatment were based on the time at which NOL deficits were confirmed in

the behavioral cohort; tissue collection coincided with the time at which NOL rescue was observed and confirmed in the behavioral cohort.

Order of experiments

For both ApoE3-KI:caMEK5 and ApoE4-KI:caMEK5 animals, tamoxifen treatment groups were assigned *a priori.* Open field (OF), novel object location (NOL) test, T-maze, and cued and contextual fear (CCF) test were conducted on animals. Baseline OF and NOL tests were conducted prior to Cd treatment (7-9 wk age). The timing of experiments differ for ApoE3-KI:caMEK5 and ApoE4-KI:caMEK5 animals due to the study design.

For ApoE3-KI:caMEK5 animals in the behavioral cohort, NOL tests were conducted at experimental weeks 2, 4, 6, 8, 10, 12, 14, 16, 18, 20, 22, 24, 26, 28, and 30, at which point NOL test deficits were confirmed. Animals underwent tamoxifen or vehicle treatment at week 32. Following treatment, NOL tests were conducted at experimental weeks 43, 45, and 47, OF at week 48, CCF at week 51, then animals were sacrificed at week 54. ApoE3-KI:caMEK5 animals in the cellular cohort were given tamoxifen or vehicle treatment at experimental week 32, then sacrificed at week 47. The T-maze test was not conducted on ApoE3-KI:caMEK5 mice.

For ApoE4-KI:caMEK5 animals in the behavioral cohort, NOL tests were conducted at experimental weeks 2, 4, 6, 8, 10, 12, 14, 16, 17, 18, and 20, at which point NOL test deficits were confirmed. Animals underwent tamoxifen or vehicle treatment at week 22. Following treatments, NOL tests were conducted at experimental weeks 32.5, 34, 38, and 39.5, OF at week 41, T-maze at week 43, CCF at week 44, then animals were sacrificed at week 49. ApoE4-KI:caMEK5 animals in the cellular cohort were given tamoxifen or vehicle treatment at experimental seek 22, then sacrificed at week 40.

Open field test

The open field test was conducted before Cd exposure and after tamoxifen administration (experiment week 48 for ApoE3-KI:caMEK5; week 41 for ApoE4-KI:caMEK5) to assess the effects of Cd on locomotor activity and anxiety. Mice were placed in a 10 x 10 x 16 inch (width x depth x height) TruScan Photo Beam Tracking arena (Coulbourn Instruments, Whitehall, PA) with clear Plexiglas sidewalls and their movement was monitored with infrared beams with a spatial resolution of 0.3 inch. Each animal was allowed to freely explore the arena without prehabituation for 20 min, and the data were collected by TruScan 2.0 software (Coulbourn Instruments). The arena was cleaned with 5% acetic acid between experimental animals. The total number of moves, moving time, and moving distance were used to assess the effects of Cd and tamoxifen on locomotor activity. The number of center entries, time spent in the center and margin, and distance traveled in the center and margin were used to assess the effects of Cd and tamoxifen on anxiety. The margin was defined as the area within 1.5 inches of the arena wall.

Novel object location test

The novel object location (NOL) test was used to assess the effects of Cd on hippocampus-dependent spatial working memory. This assay was performed as previously described (Wang et al., 2020, Zhang et al., 2019). Briefly, each mouse was placed into an open field arena (Coulbourn Instruments) with 2 identical objects placed in 2 adjacent corners. During the training session, the mouse was allowed to freely explore the arena and objects, then returned to its home cage. 1 h after training, the animal was returned to the arena with the same 2 objects with one object in the original location and the other moved to a novel location. For each week of NOL test, object locations were randomized to exclude preference of specific locations and object pairs were randomly selected from 3 distinctly different shapes, all within 1.5 and 2 inches across (custom machined brass cone, spice jars filled with sand, and small liquor bottles filled with metal

beads). Each training and test session was recorded by video cameras for later quantification. The time each animal spent actively investigating each object was manually scored and analyzed by an experimenter blinded to the animal's treatment. The data inclusion criteria for NOL assays were a minimum of 0.5 s total exploration time. The data for treatment groups within each genotype were pooled prior to tamoxifen and vehicle treatment to increase the power of the NOL test analysis and lower the possibility a type 1 error.

T-maze test

We conducted T-maze continuous alternation tests for ApoE4-KI:caMEK5 animals at the age of 43 weeks to assess spontaneous alternation as described previously with minor modifications (Spowart-Manning and van der Staay, 2004). We used a black plastic T-maze apparatus with 2 goal arms and 1 start arm (12.2 x 4.5 x 8.26 inches) placed on a table on one side of a behavior room with lighting directly above the apparatus. The test consists of a forced trial followed by 14 free-choice trials. For each trial, the animal was sequestered with a laminated black cardboard guillotine door in the distal one-third of the start arm for 5 s. In the first trial, one of the goal arms was randomly chosen to be blocked with the guillotine door, thus forcing the animal to enter one arm. In the 14 subsequent trials, no goal arm was blocked, and the mouse was allowed to enter either goal arms. Once the animal entered a goal arm, the other goal arm was immediately blocked with the guillotine door. When the animal eventually returned to the start arm, it was sequestered in the start arm with the guillotine door while the goal arms were unblocked. We allowed 30 min for each mouse to complete 14 free-choice trials. All animals completed the test in under 20 minutes. The test apparatus was cleaned with 5% acetic acid between experimental animals. We defined arm entry as the animal's whole body including tail tip entering the arm. The alternation percentage was calculated by dividing the number of times

the animal entered alternating arms by 14 (free-choice trials). All tests were scored in session by an experimenter blinded to animal treatment.

Cued and contextual fear (CCF) test

We conducted a modified cued and contextual fear conditioning test using a weak foot shock conditioning paradigm (3 x 0.3 mA, 2 s shocks with 120 s inter-trial intervals) as previously described (Engstrom et al., 2017; Pan et al., 2012) at experiment week 51 for ApoE3-KI:caMEK5, week 44 for ApoE4-KI:caMEK5. For the conditioning session, the mouse was placed into context A (10 inches x 10 inches x 16 inches arena with grid shock floor; Coulbourn Instruments) and allowed to freely explore the arena for 2 min before the presentation of a 90 dB, 30 s tone (conditioned stimulus, CS). During the last 2 s of the tone, a 0.3 mA foot shock (unconditioned stimulus, US) was delivered. This cycle was repeated two more times before the mouse was returned to its home cage. The CS and US were automatically delivered by the TruScan software (Coulbourn Instruments). 24 h after conditioning, the contextual fear memory test was conducted by placing the mouse was back into context A, but without CS or US presentation. 2 h later, the cued fear memory test was conducted by placing the mouse into context B (new behavior room; hexagonal Plexiglas arena). The mouse was allowed to freely explore the new context for 2 min, then presented with the CS for 2 min. 2 h later, the novel context test was conducted by placing the mouse into context C (new room; rat cage) and allowed to freely explore for 2 min with no presentation of CS or US. All three tests were recorded by two high-definition video cameras placed above and on the side of the test apparatus. Persistent freezing behavior (four paws on the ground, no head or body movement besides breathing) was manually quantified by for each test phase by an experimenter blinded to animal treatment.

Tamoxifen and BrdU administration

Following the confirmation of persistent spatial working memory deficits (3 consecutive deficits in NOL test), animals were administered freshly prepared tamoxifen (200 mg/kg, dissolved in corn oil with 2% glacial acetic acid; Cat: B9285; MilliporeSigma, St. Louis, MO) or vehicle (corn oil) by oral gavage once a day for 4 consecutive days in a cycle, for a total of 3 cycles with a 2-week interval between each tamoxifen treatment cycle, as previously described (Wang et al., 2014). Tamoxifen induces expression of caMEK5-eGFP in adult neural stem cells in caMEK5 mice through Cre-mediated recombination and expression of caMEK5-eGFP specifically in Nestin-expressing NPCs, allowing for the inducible and conditional activation of adult neurogenesis via caMEK5 activation of the endogenous ERK5 MAP kinase (Wang et al., 2014). To identify adult-born cells, mice in the cellular cohort received 2 intraperitoneal injections of 100 mg/kg 5-Bromo-2'-deoxyuridine (BrdU; Cat: B9285; MilliporeSigma) per day for 3 consecutive days and euthanized 2.5 weeks later. Up to 2 animals in each tamoxifen treated genotype groups in both behavioral and cellular cohorts did not survive tamoxifen treatment leading to the final animal numbers presented under the *Animals* section.

Immunohistochemistry

Mice in the cellular cohort were anesthetized with ketamine/xylazine and perfused intracardially with ice-cold solutions of 20 ml of PBS, followed by 20 ml of 4% paraformaldehyde (PFA) in PBS with heparin. Brains were collected and postfixed in 4% PFA/PBS overnight at 4 °C, followed by 30% (w/v) sucrose in PBS solution at 4 °C until brains sank. After sucrose embedding, brains were frozen at -80 °C until immunohistochemistry (IHC) processing. IHC was performed on 30 µm coronal brain sections using a free-floating antibody staining method as previously described (Pan et al., 2012, Wang et al., 2014). All primary and secondary antibodies were diluted in blocking buffer (10% donkey serum, Cat: D9663, MilliporeSigma; 1% Bovine

serum albumin, Cat: BAC61, Equitech-Bio, Kerrville, TX). The primary and secondary antibodies and dilutions used in immunohistochemistry were rat monoclonal anti-BrdU (1:500; Cat: ab6326, abcam), mouse monoclonal anti-NeuN (1:500; Cat: MAB 377, EMD Millipore), goat polyclonal anti-DCX (1:200; Cat: SC-8066, Santa Cruz Biotechnology, Dallas, TX), rabbit polyclonal anti-GFP (1:2000; Cat: A11122; Invitrogen, Carlsbad, CA), Alexa Fluor-conjugated Secondary antibodies (1:3000; A11077, A11001 or 1:500; A11055) and biotinylated goat anti-rabbit secondary antibody (1:250; BA1000, Vector Labs). After blocking and incubation with primary and secondary antibodies, tissues were incubated with 2.5 µg/ml Hoechst 33342 (Cat: H3570, Invitrogen) for 30 min, washed 3x with PBS, then mounted onto slides using anti-fade Aqua Poly/Mount (Cat: 18606, Polysciences) solution. For BrdU staining, the tissues underwent the following acid treatment prior to blocking: 10 min in 1N HCl at 4C, 30 min in 2N HCl at 37 °C, and 2x 30 min in 0.1M borate buffer. For eGFP staining, a tyramide signal amplification kit (TSA; Cat: NEL701A001KT; Akoya Biosciences, Marlborough, MA) was used as previously described (Wang et al., 2014).

Imaging and quantification of immunostained cells

One in every eight serial coronal brain sections containing the hippocampus (total of 8 to 11 sections per brain) was immunostained for doublecortin (DCX) and quantified by an experimenter blinded to genotype and treatment. All images were captured with an Olympus Fluoview-1000 laser scanning confocal microscope (Olympus, Japan) with 10x or 20x lenses or with a Leica SP8X confocal microscope (Leica Microsystems, Buffalo Grove, IL) with 10x (air), 20x (air), or 63x (oil) lenses. Optical Z-sections were processed using ImageJ2. Dendritic morphology and Sholl analyses were performed using SNT (previously Simple Neurite Tracer; v4.1.2., NIH, Bethesda, MA) in the Neuroanatomy plugin as previously described (Li et al., 2013),

with at least 40 individual neurons randomly chosen and analyzed from each genotype and treatment from 3-4 animals per group.

Blood and brain sample collection and analysis

Blood and brain samples were collected at the end of the experiment for the behavioral cohort. Mice were anesthetized with ketamine/xylazine and checked for limb reflexes prior to cardiac puncture for blood collection (> 0.3 ml/animal). Following cervical dislocation, brain samples were dissected out, separated by hemisphere using a glass slide cover, and snap frozen and stored in -80 °C until further analysis. Blood samples were stored in -20 °C until further analysis. Whole blood and right brain hemispheres were analyzed for brain Cd levels by the Environmental Health Laboratory at the University of Washington using inductively coupled plasma mass spectrometry. The experimenter who measured blood and brain Cd was blinded to the treatment and genotype of animals. The Agilent 7900 (Agilent Technologies, Santa Clara, CA) has a detection limit of approximately 0.3 ng/g per sample.

Statistical analysis

All statistical analyses and data visualizations were conducted in R (version 4.1.3). For blood and cortex Cd concentrations, open field test, T-maze test, novel object location tests, and total dendritic length, Welch's two sample t-test (α = 0.05) was used for within-genotype comparisons in each treatment group (tamoxifen vs. vehicle). Across-genotype comparisons were not performed due to timeline differences. For all figures presenting individual data points, a horizontal jitter is applied such that overlapping data points are visible without alteration in the y-axis. For all figures presenting summaries of groups, all data are expressed as mean $\pm$ SEM.

Mixed-effects linear regression using restricted maximum likelihood estimation (α = 0.05) was used for longitudinal analysis of mouse body weight, water consumption, and Sholl analysis

with random effects from mouse ID. Type III ANOVA tables were constructed with Satterthwaite's degree of freedom. *lme4, lmerTest*, and *emmeans* R packages were used for linear regression, ANOVA table construction, and for pairwise comparisons (Welch two sample t-test) at specific time points or radii with Tukey's HSD corrections.

3.3 Results

Mouse body weight and water consumption

We exposed 8–10-week-old male ApoE3-KI:caMEK5 and ApoE4-KI:caMEK5 animals to 0.6 mg/L $CdCl_2$ through the end of the experiment. Tamoxifen and vehicle treatment groups were selected *a priori*. We used 0.6 mg/L $CdCl_2$ in our study because this concentration has been used in our previous studies to study Cd neurotoxicity in mice at levels relevant to the general population (Wang et al., 2020; Zhang et al., 2019).

We recorded mouse body weights every 1-2 weeks throughout the experiment to monitor effects of tamoxifen on body weight for mice of each genotype. We did not observe an effect of tamoxifen on body weights of mice (Figure 3.2A, mixed-effects linear regression: ApoE3-KI:caMEK5, $F_{(1, 26)} = 1.14$, $p = 0.30$; Figure 3.2B, ApoE4-KI:caMEK5, $F_{(1, 25)} = 0.0002$, $p = 0.99$), and observed a significant interaction effect of experiment week and tamoxifen treatment (mixed-effects linear regression: ApoE3-KI:caMEK5, $F_{(52, 1309)} = 9.61$, $p < 2e\text{-}16$; ApoE4-KI:caMEK5, $F_{(47, 1175)} = 9.43$, $p < 2e\text{-}16$) with body weights of tamoxifen-treated animals significantly lower than vehicle-treated animals in both genotypes temporarily (Figure 3.2, Welch two sample t-test, Tukey HSD corrected: ApoE3-KI:caMEK5: $p < 0.05$ for weeks 35-49; ApoE4-KI:caMEK5: $p < 0.05$ for weeks 28-30). This suggests that tamoxifen treatment has some reversible toxicity to mice, which is consistent with the literature (Donocoff et al., 2020; Smith et al., 2022). We also recorded water consumption every week throughout the experiment in the experiment and did not observe any

effect of tamoxifen on water consumption (Figure 3.3, mixed-effects linear regression: ApoE3-KI:caMEK5, tamoxifen: $F_{(1,4)} = 0.06$, $p = 0.82$, experiment week*tamoxifen: $F_{(56,224)} = 0.86$, $p = 0.75$; ApoE4-KI:caMEK5, tamoxifen: $F_{(1, 4)} = 1.54$, $p = 0.28$, experiment week*tamoxifen: $F_{(51, 202)} = 1.25$, $p = 0.14$). These data suggest that tamoxifen treatment has no effect on water consumption.

NOL test

We performed 1-h NOL test to assess hippocampus-dependent spatial memory (Figure 3.4A). Before Cd exposure, all groups of mice spent significantly more time exploring the object in the new location (location C) compared to the old location (location A) in the testing session, suggesting that all mice had memory for the original object locations and thus were able to distinguish between the old and new locations (Figure 3.4B, Baseline). ApoE4-KI:caMEK5 mice started to show a spatial memory deficit at 16 weeks of Cd exposure, indicated by a failure to discriminate between old and new locations, and continued to show deficits at weeks 17, 18, and 20, whereas ApoE3-KI:caMEK5 mice showed spatial memory deficits later at weeks 28, 29, and 30 (Figure 3.4B, red arrowheads). This recapitulates GxE interaction effect on NOL memory reported in our previous study of ApoE3-KI and ApoE4-KI mice (Zhang et al., 2019), suggesting an effect of ApoE4 genotype on Cd-induced hippocampus dependent spatial memory even with the caMEK5 genetic background.

For each genotype, after confirming a Cd-induced memory deficit in the NOL test in at least three time points, we administered tamoxifen dissolved in corn oil to the animals via oral gavage to conditionally and selectively induce caMEK5 expression in adult neural progenitor cells. Vehicle treatment of corn oil via oral gavage was used as controls for tamoxifen. Animals were allowed to recover for 4 weeks after the last tamoxifen treatment. Tamoxifen-treated ApoE4-KI:caMEK5 mice (tamoxifen or vehicle treatment starting at week 22), exhibited a rescue in NOL

test behavior at experimental weeks 32.5, 34, 38.5, and 39.5 (3.5, 5, 9.5, and 10.5 weeks after last tamoxifen treatment, respectively) while vehicle-treated ApoE4-KI:caMEK5 mice continued to exhibit a deficit in spatial memory (Figure 3.4B, bottom, purple arrowheads). This suggests that the inducible and conditional expression of caMEK5 rescued the ApoE4-KI:caMEK5 mice from the Cd-induced impairment of hippocampus-dependent spatial working memory. Similarly, ApoE3-KI:caMEK5 mice were treated with tamoxifen or vehicle starting at week 32. Tamoxifen-treated ApoE3-KI:caMEK5 mice were able to discriminate between the old and new locations at experimental weeks 42, 45, and 47 (4, 7, and 9 weeks after the last tamoxifen treatment, respectively), while vehicle-treated ApoE3-KI:caMEK5 mice continued to exhibit a deficit in spatial memory (Figure 3.4B, top, purple arrowheads). This suggests that the inducible and conditional expression of caMEK5 also rescued ApoE3-KI:caMEK5 mice from the Cd-induced impairment of hippocampus-dependent spatial working memory.

Blood and cortex Cd concentrations

We collected blood and brain tissue for Cd analysis from the cellular cohort at sacrifice to assess Cd exposure levels, coinciding with confirmation of NOL rescue in ApoE3-KI:caMEK5 and ApoE4-KI:caMEK5 mice, respectively (experimental weeks 47 and 40). All samples had Cd levels above the detection limit. End of experiment blood Cd levels were largely within 0.2-0.4 μg/L range, comparable to blood Cd levels found in the general US population (men: 0.206– 0.255 μg/L; women: 0.263-0.304 μg/L, 2011-2018 geometric mean range; Centers for Disease Control and Prevention), with means ranging from 0.315 – 0.347 μg/L across the four treatment groups. There were no significant differences between vehicle and tamoxifen treated groups in blood Cd of ApoE3-KI:caMEK5, blood Cd of ApoE4-KI:caMEK5, or brain Cd of ApoE3-KI:caMEK5 (Figure 3.5A-C). Brain Cd levels of tamoxifen-treated ApoE4-KI:caMEK5 mice were higher compared to vehicle treated ApoE4-KI:caMEK5 mice (Figure 3.5D, Welch two sample t-test: $p = 0.03$), with

mean end of experiment brain Cd levels ranging from 1.68 – 2.01 pg/mg. These data suggest that tamoxifen treatment did not lower Cd levels in blood or brain, and that a change in Cd levels is not a likely reason for the observed NOL rescue effect.

Locomotor activity and anxiety

We used the open field test at baseline before Cd treatment to exclude any intrinsic differences in locomotor activity and anxiety between tamoxifen and vehicle groups within each genotype. There were no significant differences in the open field locomotor activity between tamoxifen and vehicle groups in either genotype prior to the Cd exposure (Figure 3.6A-C, baseline). We also used the open field test during Cd exposure and after tamoxifen or vehicle treatment to assess effects of tamoxifen on locomotor activity and anxiety at experimental weeks 48 and 41 for ApoE3-KI:caMEK5 and ApoE4-KI:caMEK5, respectively. Tamoxifen treated ApoE3-KI:caMEK5 mice spent more time moving and moved a longer distance compared to vehicle-treated ApoE3-KI:caMEK5 mice, while there were no significant differences between vehicle- and tamoxifen-treated ApoE4-KI:caMEK5 mice (Figure 3.6A-C, after). This suggests that tamoxifen treatment increased locomotor activity in ApoE3-KI:caMEK5 animals. While comparisons between ApoE3-KI:caMEK5 and ApoE4-KI:caMEK5 animals are inappropriate due to time point differences, tamoxifen treated ApoE3-KI:caMEK5 animals locomotor activity were closer to vehicle and tamoxifen treated ApoE4-KI:caMEK5 animals.

We used time and distance in the margin, center, or entries to the center to assess anxiety. There were no significant differences in anxiety behavior between tamoxifen and vehicle groups in either genotype prior to Cd exposure (Figure 3.7A-E, baseline). At week 48, tamoxifen-treated ApoE3-KI:caMEK5 mice entered the arena center more frequently and moved longer distances in the arena margin compared to vehicle-treated ApoE3-KI:caMEK5 mice (Figure 3.7A&E, E3). There were no significant differences between vehicle- and tamoxifen-treated ApoE4-KI:caMEK5

mice. Taken together with the observed increase in locomotor activity, these data suggest that tamoxifen had no effect in ApoE4-KI:caMEK5 mice, while tamoxifen may have increased anxiety levels and locomotor activity in ApoE3-KI:caMEK5 mice. Both tamoxifen-treated ApoE3-KI:caMEK5 and ApoE4-KI:caMEK5 mice exhibited NOL test recovery, thus our observed increase in locomotor activity and anxiety in tamoxifen-treated ApoE3-KI:caMEK5 mice is likely unrelated to the NOL test rescue.

Spontaneous alteration

Spontaneous alternation between two choices of maze arms is a behavior in rodents that is partially due to hippocampus-dependent spatial working memory (Spowart-Manning and van der Staay, 2004). We initially investigated the effects of caMEK5 expression on spontaneous alteration in the ApoE4-KI:caMEK5 behavioral cohort at experimental week 43 (15 weeks after last tamoxifen treatment) as their timeline in NOL deficit and tamoxifen treatment were earlier than that of ApoE3-KI:caMEK5 mice. We did not observe any differences between alternation, number of re-entry into the same arm three times (triplet), or the duration of the test between tamoxifen and vehicle treated groups in ApoE4-KI:caMEK5 mice (Figure 3.8A-C). While not statistically significant, the mean percent alternation in tamoxifen treated animals was higher than vehicle (vehicle-treated: 59.9 $\pm$ 3.5%, range: 35.7 – 78.6; tamoxifen-treated: 66.8 $\pm$ 4.3%, range: 50.0 – 100) and the number of triplets were lower in tamoxifen-treated animals (vehicle-treated: 2.5 $\pm$ 0.6, range: 0 – 7; tamoxifen-treated: 1.3 $\pm$ 0.6, range: 0 – 3). We did not obtain T-maze data for ApoE3-KI:caMEK5 mice due to constraints with the COVID-19 pandemic. These data suggest that tamoxifen may have increased spontaneous alternation in ApoE4-KI:caMEK5 mice, although the difference was not statistically significant.

Contextual fear

We conducted a cued and contextual fear conditioning test to investigate the effect of tamoxifen in Cd-treated ApoE3-KI:caMEK5 and ApoE4-KI:caMEK5 mice at experimental weeks 51 and 44, respectively. We used a weak (0.3 mA x 3) foot shock paradigm previously reported to be sensitive to changes in contextual fear memory and adult neurogenesis (Engstrom et al., 2017; Pan et al., 2012). For fear conditioning in each genotype, we observed an effect of conditioning phase on freezing behavior (mixed-effects linear regression: ApoE3-KI:caMEK5, $F_{(6, 144)} = 54.5$, $p < 2e\text{-}16$; ApoE4-KI:caMEK5, $F_{(6, 150)} = 53.0$, $p < 2e\text{-}16$) and no effect of tamoxifen or interaction effect of phase and tamoxifen (Figure 3.9A and Figure 3.10A). All groups showed minimal freezing behavior at baseline before foot shock (pre-shock freezing; mean range for all groups: 0.40 – 2.65%), and displayed increased average freezing through conditioning (Figure 3.9A and Figure 3.10A). Tamoxifen treatment did not cause any statistically significant changes in either genotype in auditory-cued (hippocampus-independent) fear memory or general freezing in a novel context as expected (Figure 3.9B and Figure 3.10B). Tamoxifen treatment did not cause any significant changes in either genotype in contextual fear memory. Group means in freezing in the contextual fear test ranged 22.9 – 35.0%. These data suggest that tamoxifen treatment had no effect on fear conditioning or contextual fear in ApoE3-KI:caMEK5 and ApoE4-KI:caMEK5 mice.

caMEK5 expression stimulates adult hippocampal neurogenesis in ApoE4 mice

We investigated the effects of tamoxifen induced expression of caMEK5 on adult hippocampal neurogenesis using a separate cohort of the mice from the same breeding group as the behavior cohort. caMEK5 is sequence tagged with eGFP in the transgenic mouse strain (see *Materials and Methods*), therefore we performed eGFP immunostaining of brain tissues collected from the cellular cohort to confirm caMEK5 expression. eGFP staining was found in the dentate

gyrus of tamoxifen treated groups in each genotype but not in vehicle treated controls (Figure 3.11). These data confirm that caMEK5 expression are conditionally induced by tamoxifen treatment and selective to aNPCs in the dentate gyrus of both ApoE3-KI:caMEK5 and ApoE4-KI:caMEK5 mice.

To investigate the effects of caMEK5 expression on aNPC survival, BrdU was administered to cellular cohort animals 2.5 weeks prior to tissue collection, which coincided with the confirmation of NOL rescue in tamoxifen-treated animals in the behavioral cohort (ApoE3-KI:caMEK5: experiment week 47; ApoE4-KI:caMEK5: experiment week 40). We quantified BrdU+ retaining cells (surviving adult-born cells) and BrdU+/NeuN+ cells (adult-born neurons). We observed no differences between tamoxifen and control groups of either genotype in the number of surviving adult-born cells, adult-born neurons, or the fraction of adult-born neurons over adult-born cells (Figure 3.12).

We further assessed the dendritic morphology, a measure of neuronal maturation, of adult-born neurons in brain sections of cellular cohort mice. We used doublecortin (DCX) immunostaining alone to visualize and trace neuronal processes of newly generated, immature neurons without performing acid treatment necessary for BrdU immunostaining, which damages neuronal processes (Figure 3.13A-B; Figure 3.14A-B). Tamoxifen treatment significantly increased the total dendritic length in both ApoE3-KI:caMEK5 and ApoE4-KI:caMEK5 mice (Figure 3.13C; Figure 3.14C: Welch two tailed t-test, ApoE3-KI:caMEK5: $p = 0.00026$; ApoE4-KI:caMEK5: $p = 4.6e\text{-}06$). For ApoE3-KI:caMEK5 mice, we did not observe an effect of tamoxifen on the number of dendritic crossings (mixed-effects linear regression: $F_{(1, 4.42)}$, $p = 0.70$), and observed a significant interaction effect of radius and tamoxifen treatment (mixed-effects linear regression: $F_{(18, 1458)} = 2.47$, $p = 0.00056$). For ApoE4-KI:caMEK5 mice, tamoxifen increased the number of dendritic crossings (mixed-effects linear regression: $F_{(1, 95)} = 22.3$, $p = 7.98e\text{-}06$), but we did observe a significant interaction effect of radius and tamoxifen treatment (mixed-effects

linear regression: $F_{(18, 1710)} = 1.90$, $p = 0.012$). Dendritic crossings of tamoxifen-treated animals were significantly higher than vehicle-treated animals in both genotypes (Figure 3.13D and Figure 3.14D; ApoE3-KI:caMEK5: 20-60 μm from soma; ApoE4-KI:caMEK5: 20-120 μm from soma). Taken together, our results suggest that tamoxifen induced caMEK5 expression in aNPCs may not increase the number of adult-born hippocampal neurons, but instead increased dendritic complexity of adult-born neurons in both ApoE3-KI:caMEK5 and ApoE4-KI:caMEK5 mice.

3.4 Discussion

There is increasing research interest in understanding the contribution of genetic and environmental risk factors in AD pathogenesis and cognitive decline (Bakulski et al., 2020; Eid et al., 2019; Finch and Kulminski, 2019). The links between Cd and AD in humans are limited to positive associations of markers of Cd exposure and mortality in AD patients in NHANES study cohorts (Min and Min, 2016; Peng et al., 2017). We have previously reported direct toxicological evidence of GxE effect of ApoE4 and environmentally relevant concentrations of Cd (Zhang et al., 2019) as well as lead (Engstrom et al., 2017) in ApoE4-KI mice. Additionally, these studies reported GxE effect of ApoE4 and heavy metals on adult neurogenesis impairment, suggesting that adult neurogenesis may be an underlying mechanism for the GxE effect on cognitive function. However, our published observation of GxE effect on cognitive function and adult neurogenesis impairments was correlative. To test our hypothesis that the GxE effect of ApoE4 and Cd on hippocampal adult neurogenesis contributes to impairment of hippocampus-dependent learning and memory, we aimed to determine if the GxE impairment of learning and memory can be reversed by a conditional genetic enhancement of adult neurogenesis. Here we designed a functional rescue experiment to specifically and genetically stimulate adult neurogenesis following the observation of hippocampus-dependent memory impairment in a GxE model of ApoE3-

KI:caMEK5 and ApoE4-KI:caMEK5 mice treated with an environmentally relevant concentration of Cd through drinking water (0.6 mg/L $CdCl_2$). This transgenic mouse model allowed us to selectively induce caMEK5 expression through treatment by tamoxifen, thereby stimulating adult neurogenesis. We focused on male animals because male ApoE4-KI mice were most sensitive to the effects of Cd exposure (Zhang et al., 2019).

We have previously utilized the NOL test for longitudinal studies of heavy metals exposures on hippocampus-dependent learning and memory (Engstrom et al., 2017; Wang et al., 2020; Zhang et al., 2019). We used the NOL test in this study to probe hippocampus-dependent spatial memory performance through Cd exposure and tamoxifen treatment. ApoE4-KI:caMEK5 mice exhibited Cd-induced deficits in the NOL test earlier than ApoE3-KI:caMEK5 (onset at experimental week 16 vs 28), suggesting that there is an effect of genotype between Cd treated ApoE3-KI:caMEK5 and ApoE4-KI:caMEK5 mice on the onset of hippocampus-dependent spatial memory impairment. This finding is consistent with our previous report of male ApoE4-KI susceptibility to Cd-induced cognitive function impairment (Zhang et al., 2019) and while we lack a Cd-treatment control, our findings still support the presence of a GxE interaction between ApoE4 and Cd. Following confirmation of NOL test impairment, we treated animals with tamoxifen or vehicle (control) to induce the expression of caMEK5 in aNPCs. The conditional and selective induction of caMEK5 was able to rescue Cd-induced NOL test impairment in ApoE4-KI:caMEK5 mice, as well as in ApoE3-KI:caMEK5 (genotype control). These findings suggest that caMEK5 expression in aNPCs is sufficient to rescue behavioral deficits, thus stimulation of adult hippocampal neurogenesis through caMEK5 expression is directly linked to the genotype differences of Cd-induced hippocampus-dependent spatial memory. The rescue effect of tamoxifen treatment on NOL test impairment in ApoE3-KI:caMEK5 mice further suggests that adult neurogenesis is directly linked to Cd-induced impairments of hippocampus-dependent

spatial memory even in our genotype control mice, consistent with our previous findings in caMEK5 mice (Wang et al., 2020).

We further analyzed histological data from the cellular cohort of mice with a Cd-exposure and tamoxifen treatment timeline parallel to the behavioral cohort to investigate the effects of caMEK5 expression on adult neurogenesis. We previously reported that aNPC survival and the number of adult-born neurons are impaired in Cd treated animals in caMEK5 mice (Wang et al., 2020) and ApoE4-KI mice (Zhang et al., 2019). We have also reported that caMEK5 expression restores aNPC survival as well as the number of adult-born neurons (Wang et al., 2020). While we did not observe any effects of caMEK5 expression on aNPC survival or the number of adult-born neurons in the present study, we reported a significant increase of the total dendritic length and dendritic crossings in both ApoE3-KI:caMEK5 and ApoE4-KI:caMEK5 mice. This is consistent with our previous findings that caMEK5 expression enhances dendritic complexity of adult-born neurons (Wang et al., 2014). Dendritic complexity is used here a proxy for adult-born neuron maturation which is critical for neuron integration into existing hippocampal networks (Engstrom et al., 2017; Wang et al., 2020, 2019). Unlike the two aforementioned studies in which we reported restoration of aNPC survival and number of adult-born neurons, we continued Cd exposure of 0.6 mg/L CdCl2 in drinking water through the end of experiments in this study. Therefore, Cd exposure may have continued to impair the survival of aNPCs and adult-born neurons, and caMEK5 expression was not sufficient to increase the number of surviving aNPCs or adult-born neurons. Our behavioral data and cellular data together suggest that the observed rescue effects are directly linked to the recovery of dendritic complexity of adult-born neurons in both ApoE3-KI:caMEK5 and ApoE4-KI:caMEK5 mice. Further, taken together with our previous report of GxE effect of ApoE4 and Cd on hippocampus-dependent memory (Zhang et al., 2019), our findings suggest a causal role of adult neurogenesis in the GxE effect of ApoE4 and Cd on hippocampus-dependent memory.

Tamoxifen treatment had no effect on locomotion or anxiety behavior in the open field test in ApoE4-KI:caMEK5 mice. On the other hand, tamoxifen treatment increased moving time and moving distance, and increased center entries and margin distance, indicating an increase in locomotion and anxiety behavior in ApoE3-KI:caMEK5 mice. It is possible that these differences are directly correlated—an increase in locomotor activity could result in increased entries to the center of the arena or increased distances moved in the center or the margin while time spent the center or margin are unaffected. Consistent with this logic, tamoxifen treated ApoE3-KI:caMEK5 mice had increased moving distance in the center (Figure 7C), although not statistically significant. Further testing for anxiety such as the elevated plus maze would help clarify these data. However, due to constraints with the COVID-19 pandemic, we were not able to further test for anxiety. While it is possible that these locomotor and anxiety effects may have impacted NOL test behavior, these differences do not fully explain the NOL test rescue effect in tamoxifen-treated ApoE3-KI:caMEK5 mice.

We observed no differences in blood or brain Cd levels except for an increase in brain Cd levels in tamoxifen-treated ApoE4-KI:caMEK5 mice. Our data suggest that changes in Cd levels do not explain the rescue effects observed following Cd-induced impairments in the NOL test. We report in the present study that 47 and 40 weeks of exposure to 0.6 mg/L $CdCl_2$ through drinking water resulted in 0.2-0.4 µg/L blood Cd levels for most ApoE3-KI:caMEK5 and ApoE4-KI:caMEK5 mice. These concentrations are within the range found in the general US population (men: 0.206–0.255 µg/L; women: 0.263-0.304 µg/L, 2011-2018 geometric mean range; Centers for Disease Control and Prevention). Furthermore, we report brain Cd levels to be approximately 1.5-2.0 pg/mg. While there are no large-scale reports of brain Cd levels in a general population to our knowledge, Cd has been detected in human brain tissue (ICP-MS: 4-30 pg/mg) in studies of autopsy tissue from general populations in a number of countries in Central Europe, Scandinavia, and Asia (Bocio et al., 2005; Lech and Sadlik, 2017; Mari et al., 2014). We previously reported

0.7-1.3 pg/mg in ApoE3-KI and ApoE4-KI mice exposed to 0.6 mg/L $CdCl_2$ through drinking water for 14 weeks (Zhang et al., 2019) and approximately 2.0 ng/g in mice exposed to 0.6 mg/L $CdCl_2$ through drinking water for 38 weeks following 29.5-32 weeks cessation of exposure, while control (0 mg/L $CdCl_2$) animals had below 0.5 ng/g Cd in the brain (Wang et al., 2020). In both studies as well as the present study, Cd exposed animals exhibited impairments in hippocampus-dependent memory through an exposure paradigm representative of exposure levels in the general US population, thus providing biological plausibility of Cd neurotoxicity. Taken together with existing epidemiology reports of negative associations of Cd levels and cognitive function, Cd may affect cognitive functions at levels prevalent in the general US population.

We further tested for spontaneous alternation and contextual fear memory to assess hippocampus function in other behavioral tests. For spontaneous alternation, there was a trend of decreased alternation by percent as well as number of triplets that suggests a rescue effect in ApoE4-KI:caMEK5 mice for spontaneous alternation, though these differences were not statistically significant. In our previous study, the GxE effect on spontaneous alternation was observed in male ApoE4-KI mice long after exposure (26 weeks after end of a 14-week Cd exposure), but not immediately (1 week) after the end of exposure (Zhang et al., 2019). For contextual fear memory, we observed no differences between tamoxifen and vehicle treated animals in either genotype. ApoE3-KI:caMEK5 and ApoE4-KI:caMEK5 mice in both tamoxifen and vehicle treatment groups had low contextual fear memory (mean percent freezing below 35%). Unfortunately, due to our study design and lack of Cd exposure control (0 mg/L $CdCl_2$) animals treated with tamoxifen or vehicle, we are not able to discern whether this 24 h context test results are indicative of Cd effect, tamoxifen effect, or neither (e.g. animal age). It is possible that continued Cd treatment through the end of the experiment in the present study affected all mice performance in these hippocampus-dependent memory tests and that what we observed are all underestimates of the therapeutic effect of caMEK5 expression. While we did not observe

behavioral rescue in spontaneous alternation and contextual fear memory, we observed a robust and persistent rescue effect in the NOL test. These discrepancies between behavioral tests may originate in the extent to which hippocampus and other brain regions are involved in each behavior that result in varying sensitivities to Cd treatment. Spontaneous alternation is a behavior due to a combination of novelty-elicited exploratory behavior as well as spatial working memory (Gerlai, 1998; Spowart-Manning and van der Staay, 2004). Contextual fear learning and memory involve the amygdala and the medial prefrontal cortex in addition to the hippocampus (Tovote et al., 2015; Xu et al., 2016). Additionally, discrepancies in behavioral data between our previous studies and this study may partly be explained by differences in genetic background, which has been well documented to affect behavioral responses in learning and memory tasks (Balogh and Wehner, 2003; Holmes et al., 2002; Seemiller et al., 2021).

While we report an exciting finding of an underlying mechanism of a GxE interaction effect, we caution against overinterpretation of our report as our study is limited to male mice and Cd treated animals only due to the logistical limitations to obtain enough animal numbers for a more complete study including both sexes and Cd treatment control (Figure 1A). Despite these limitations, we report convincing evidence utilizing a gain-of-function mouse model that demonstrate rescue of hippocampus-dependent memory and adult hippocampal neurogenesis following Cd-impairment through the induced expression of caMEK5 amid continued exposure to Cd. Our continued exposure throughout the experiment may better reflect lifelong, low-level exposures in the general population, and our study sheds light on the possibility that even in life-long exposures to Cd, there may be therapeutic benefits from stimulation of adult neurogenesis for individuals with genetic risk factors like *APOE4*.

Conclusion

Our present study found that specific and conditional stimulation of adult neurogenesis rescued Cd-induced impairments in hippocampus-dependent short-term spatial memory in a GxE model of ApoE4 and Cd, demonstrating a direct link between memory impairment and adult neurogenesis in this GxE model. Our findings provide strong evidence supporting the presence of a GxE effect and a potential underlying mechanism involving adult neurogenesis at Cd exposure levels relevant to the general US population. These findings support the hypothesis that environmental factors may have considerable impacts on cognitive function and dementia risk (Bakulski et al., 2020; Finch and Kulminski, 2019), and point to the potential benefit of interventions such as behavioral changes and policies targeting environmental factors on the cognitive health of the general population and on social burdens of AD and dementia. Furthermore, our findings highlight the potential of therapeutic interventions in mitigating age-related cognitive decline and dementia risk, particularly for individuals with elevated genetic risk, including easily accessible interventions such as exercise (Aimone et al., 2014; Ming and Song, 2011), diet (Stangl and Thuret, 2009), and lowering stress (Schoenfeld and Gould, 2012) which can stimulate adult neurogenesis.

3.5 Funding Statement

This work was supported in part by the National Institutes of Health (R01-ES-026591 to Z.X.) and the University of Washington Environmental Pathology/Toxicology Training Program (T32-ES-007032-42 to M.T.M.). We also acknowledge support from the NIH (S10 OD016240) to the W. M. Keck Center.

3.6 Acknowledgements

We would like to acknowledge previous members of the Xia lab, including Dr. Liang Zhang and Dr. Brett Mommer for their early input on this work. We are thankful to the staff at the University of Washington Environmental Health Laboratory for technical assistance with metals analysis, the staff at the University of Washington Department of Comparative Medicine for expert animal care, and to Dr. Kim Miller at the Digital Microscopy Center and Dr. Nathaniel Peters of the W. M. Keck Microscopy Center. All schematic figures were made using BioRender (biorender.com).

3.7 References

Aimone JB, Li Y, Lee SW, Clemenson GD, Deng W, Gage FH. 2014. Regulation and Function of Adult Neurogenesis: From Genes to Cognition. *Physiol Rev* **94**:991–1026. doi:10.1152/physrev.00004.2014

Alzheimer's Association. 2022. 2022 Alzheimer's Disease Facts and Figures. *Alzheimers Dement* **18**.

Anacker C, Hen R. 2017. Adult hippocampal neurogenesis and cognitive flexibility — linking memory and mood. *Nat Rev Neurosci* **18**:335–346. doi:10.1038/nrn.2017.45

Bakulski KM, Seo YA, Hickman RC, Brandt D, Vadari HS, Hu H, Park SK. 2020. Heavy Metals Exposure and Alzheimer's Disease and Related Dementias. *J Alzheimers Dis* **76**:1215–1242. doi:10.3233/JAD-200282

Balogh SA, Wehner JM. 2003. Inbred mouse strain differences in the establishment of long-term fear memory. *Behav Brain Res* **140**:97–106. doi:10.1016/S0166-4328(02)00279-6

Bekris LM, Yu C-E, Bird TD, Tsuang DW. 2010. Genetics of Alzheimer disease. *J Geriatr Psychiatry Neurol* **23**:213–227. doi:10.1177/0891988710383571

Bocio A, Nadal M, Garcia F, Domingo JL. 2005. Monitoring metals in the population living in the vicinity of a hazardous waste incinerator. *Biol Trace Elem Res* **106**:41–50. doi:10.1385/BTER:106:1:041

Centers for Disease Control and Prevention. 2022. National Report on Human Exposure to Environmental Chemicals: Data Table Viewer. https://www.cdc.gov/exposurereport/

Ciesielski T, Bellinger DC, Schwartz J, Hauser R, Wright RO. 2013. Associations between cadmium exposure and neurocognitive test scores in a cross-sectional study of US adults. *Environ Health* **12**. doi:10.1186/1476-069X-12-13

Ciesielski T, Weuve J, Bellinger DC, Schwartz J, Lanphear B, Wright RO. 2012. Cadmium Exposure and Neurodevelopmental Outcomes in U.S. Children. *Environ Health Perspect* **120**:758–763. doi:10.1289/ehp.1104152

Denoth-Lippuner A, Jessberger S. 2021. Formation and integration of new neurons in the adult hippocampus. *Nat Rev Neurosci* **22**:223–236. doi:10.1038/s41583-021-00433-z

Donocoff RS, Teteloshvili N, Chung H, Shoulson R, Creusot RJ. 2020. Optimization of tamoxifen-induced Cre activity and its effect on immune cell populations. *Sci Rep* **10**:15244. doi:10.1038/s41598-020-72179-0

Eid A, Mhatre I, Richardson JR. 2019. Gene-environment interactions in Alzheimer's disease: A potential path to precision medicine. *Pharmacol Ther* **199**:173–187. doi:10.1016/j.pharmthera.2019.03.005

English JM, Vanderbilt CA, Xu S, Marcus S, Cobb MH. 1995. Isolation of MEK5 and Differential Expression of Alternatively Spliced Forms. *J Biol Chem* **270**:28897–28902. doi:10.1074/jbc.270.48.28897

Engstrom AK, Snyder JM, Maeda N, Xia Z. 2017. Gene-environment interaction between lead and Apolipoprotein E4 causes cognitive behavior deficits in mice. *Mol Neurodegener* **12**. doi:10.1186/s13024-017-0155-2

Finch CE, Kulminski AM. 2019. The Alzheimer's Disease Exposome. *Alzheimers Dement* **15**:1123–1132. doi:10.1016/j.jalz.2019.06.3914

Gage FH. 2000. Mammalian Neural Stem Cells. *Science* **287**:1433–1438. doi:10.1126/science.287.5457.1433

Gerlai R. 1998. A new continuous alternation task in T-maze detects hippocampal dysfunction in mice: A strain comparison and lesion study. *Behav Brain Res* **95**:91–101. doi:10.1016/S0166-4328(97)00214-3

Gonçalves JT, Schafer ST, Gage FH. 2016. Adult Neurogenesis in the Hippocampus: From Stem Cells to Behavior. *Cell* **167**:897–914. doi:10.1016/j.cell.2016.10.021

Holmes A, Wrenn CC, Harris AP, Thayer KE, Crawley JN. 2002. Behavioral profiles of inbred strains on novel olfactory, spatial and emotional tests for reference memory in mice. *Genes Brain Behav* **1**:55–69. doi:10.1046/j.1601-1848.2001.00005.x

Lech T, Sadlik JK. 2017. Cadmium Concentration in Human Autopsy Tissues. *Biol Trace Elem Res* **179**:172–177. doi:10.1007/s12011-017-0959-5

Li H, Wang Z, Fu Z, Yan M, Wu N, Wu H, Yin P. 2018. Associations between blood cadmium levels and cognitive function in a cross-sectional study of US adults aged 60 years or older. *BMJ Open* **8**. doi:10.1136/bmjopen-2017-020533

Liu C-C, Kanekiyo T, Xu H, Bu G. 2013. Apolipoprotein E and Alzheimer disease: risk, mechanisms and therapy. *Nat Rev Neurol* **9**:106–118. doi:10.1038/nrneurol.2012.263

Mari M, Nadal M, Schuhmacher M, Barbería E, García F, Domingo JL. 2014. Human Exposure to Metals: Levels in Autopsy Tissues of Individuals Living Near a Hazardous Waste Incinerator. *Biol Trace Elem Res* **159**:15–21. doi:10.1007/s12011-014-9957-z

Michaelson DM. 2014. APOE ε4: The most prevalent yet understudied risk factor for Alzheimer's disease. *Alzheimers Dement* **10**:861–868. doi:10.1016/j.jalz.2014.06.015

Migliore L, Coppedè F. 2022. Gene–environment interactions in Alzheimer disease: the emerging role of epigenetics. *Nat Rev Neurol* 1–18. doi:10.1038/s41582-022-00714-w

Min J, Min K. 2016. Blood cadmium levels and Alzheimer's disease mortality risk in older US adults. *Environ Health* **15**. doi:10.1186/s12940-016-0155-7

Ming G, Song H. 2011. Adult Neurogenesis in the Mammalian Brain: Significant Answers and Significant Questions. *Neuron* **70**:687–702. doi:10.1016/j.neuron.2011.05.001

Pan Y-W, Chan GCK, Kuo CT, Storm DR, Xia Z. 2012. Inhibition of Adult Neurogenesis by Inducible and Targeted Deletion of ERK5 Mitogen-Activated Protein Kinase Specifically in Adult Neurogenic Regions Impairs Contextual Fear Extinction and Remote Fear Memory. *J Neurosci* **32**:6444–6455. doi:10.1523/JNEUROSCI.6076-11.2012

Pan Y-W, Storm DR, Xia Z. 2013. Role of adult neurogenesis in hippocampus-dependent memory, contextual fear extinction and remote contextual memory: New insights from ERK5 MAP kinase. *Neurobiol Learn Mem*, MCCS 2013 **105**:81–92. doi:10.1016/j.nlm.2013.07.011

Peng Q, Bakulski KM, Nan B, Park SK. 2017. Cadmium and Alzheimer's disease mortality in U.S. adults: Updated evidence with a urinary biomarker and extended follow-up time. *Environ Res* **157**:44–51. doi:10.1016/j.envres.2017.05.011

Satarug S, Garrett SH, Sens MA, Sens DA. 2010. Cadmium, Environmental Exposure, and Health Outcomes. *Environ Health Perspect* **118**:182–190. doi:10.1289/ehp.0901234

Schoenfeld TJ, Gould E. 2012. Stress, stress hormones, and adult neurogenesis. *Exp Neurol*, Special Issue: Stress and neurological disease **233**:12–21. doi:10.1016/j.expneurol.2011.01.008

Seemiller LR, Mooney-Leber SM, Henry E, McGarvey A, Druffner A, Peltz G, Gould TJ. 2021. Genetic background determines behavioral responses during fear conditioning. *Neurobiol Learn Mem* **184**:107501. doi:10.1016/j.nlm.2021.107501

Smith BM, Saulsbery AI, Sarchet P, Devasthali N, Einstein D, Kirby ED. 2022. Oral and Injected Tamoxifen Alter Adult Hippocampal Neurogenesis in Female and Male Mice. *eNeuro* **9**. doi:10.1523/ENEURO.0422-21.2022

Spowart-Manning L, van der Staay FJ. 2004. The T-maze continuous alternation task for assessing the effects of putative cognition enhancers in the mouse. *Behav Brain Res* **151**:37–46. doi:10.1016/j.bbr.2003.08.004

Stangl D, Thuret S. 2009. Impact of diet on adult hippocampal neurogenesis. *Genes Nutr* **4**:271–282. doi:10.1007/s12263-009-0134-5

Tovote P, Fadok JP, Lüthi A. 2015. Neuronal circuits for fear and anxiety. *Nat Rev Neurosci* **16**:317–331. doi:10.1038/nrn3945

Wang H, Abel GM, Storm DR, Xia Z. 2019. Cadmium Exposure Impairs Adult Hippocampal Neurogenesis. *Toxicol Sci* **171**:501–514. doi:10.1093/toxsci/kfz152

Wang H, Matsushita MT, Zhang L, Abel GM, Mommer BC, Huddy TF, Storm DR, Xia Z. 2020. Inducible and Conditional Stimulation of Adult Hippocampal Neurogenesis Rescues Cadmium-Induced Impairments of Adult Hippocampal Neurogenesis and Hippocampus-Dependent Memory in Mice. *Toxicol Sci Off J Soc Toxicol* **177**:263–280. doi:10.1093/toxsci/kfaa104

Wang H, Zhang L, Abel GM, Storm DR, Xia Z. 2017. Cadmium Exposure Impairs Cognition and Olfactory Memory in Male C57BL/6 Mice. *Toxicol Sci*. doi:10.1093/toxsci/kfx202

Wang W, Pan Y-W, Zou J, Li T, Abel GM, Palmiter RD, Storm DR, Xia Z. 2014. Genetic Activation of ERK5 MAP Kinase Enhances Adult Neurogenesis and Extends Hippocampus-Dependent Long-Term Memory. *J Neurosci* **34**:2130–2147. doi:10.1523/JNEUROSCI.3324-13.2014

Xu C, Krabbe S, Gründemann J, Botta P, Fadok JP, Osakada F, Saur D, Grewe BF, Schnitzer MJ, Callaway EM, Lüthi A. 2016. Distinct Hippocampal Pathways Mediate Dissociable Roles of Context in Memory Retrieval. *Cell* **167**:961-972.e16. doi:10.1016/j.cell.2016.09.051

Xu Q, Bernardo A, Walker D, Kanegawa T, Mahley RW, Huang Y. 2006. Profile and Regulation of Apolipoprotein E (ApoE) Expression in the CNS in Mice with Targeting of Green Fluorescent Protein Gene to the ApoE Locus. *J Neurosci* **26**:4985–4994. doi:10.1523/JNEUROSCI.5476-05.2006

Zhang L, Wang H, Abel GM, Storm DR, Xia Z. 2019. The Effects of Gene-Environment Interactions Between Cadmium Exposure and Apolipoprotein E4 on Memory in a Mouse Model of Alzheimer's Disease. *Toxicol Sci* kfz218. doi:10.1093/toxsci/kfz218

Zhou G, Bao ZQ, Dixon JE. 1995. Components of a New Human Protein Kinase Signal Transduction Pathway. *J Biol Chem* **270**:12665–12669. doi:10.1074/jbc.270.21.12665

3.8 Figures

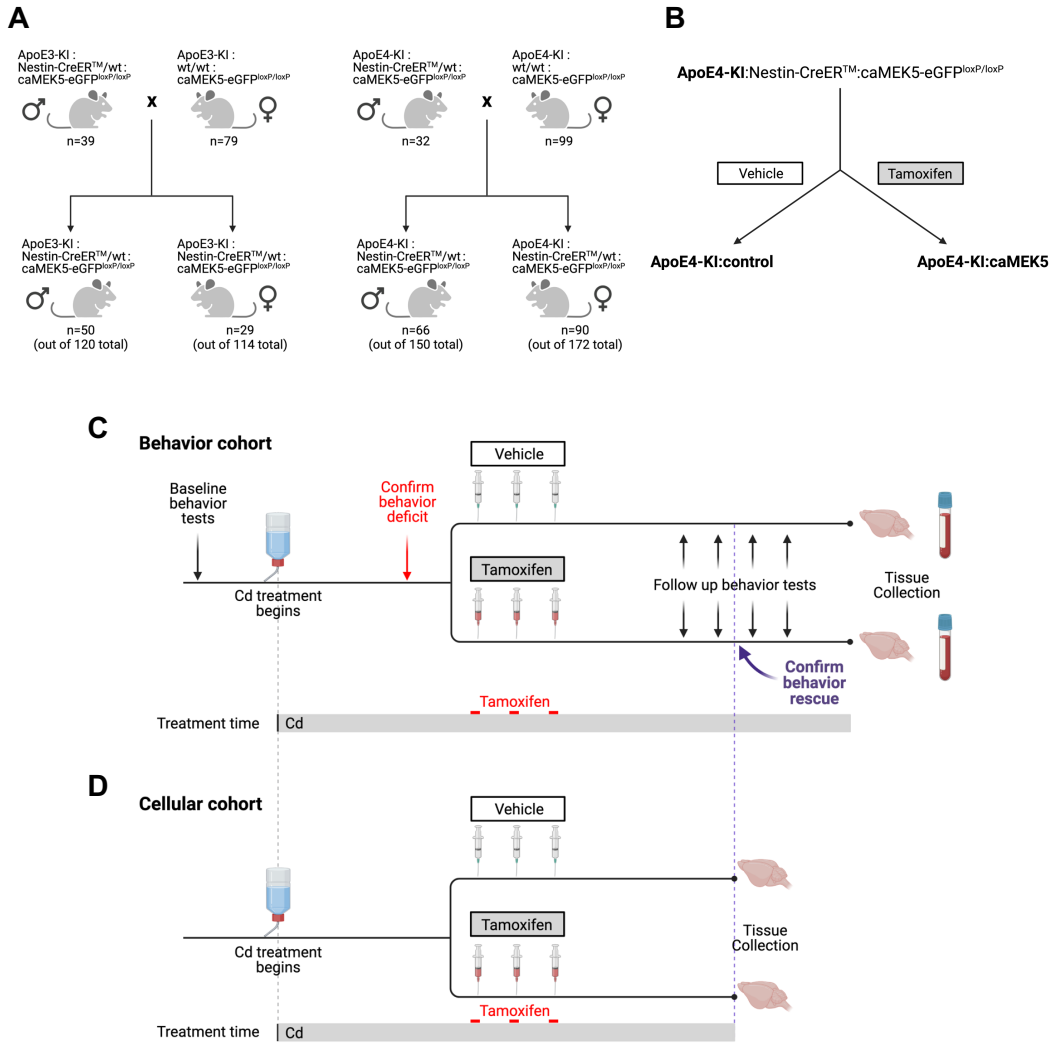

Figure 3.1. Study design for the caMEK5 rescue experiment. (A) Breeding scheme. (B) Schematic diagram for generation of transgenic mice through tamoxifen treatment. Tamoxifen-treated animals express constitutively active MEK5 (caMEK5) in adult neurogenic regions (under the Nestin-CreER^{TM} promoter) with ApoE4-KI background (ApoE4-KI:caMEK5); control animals have the same genetic background but do not express caMEK5 (ApoE4-KI:control). The same strategy was used to generate ApoE3-KI:caMEK5 and control mice. (B-C) Study design for the caMEK5 rescue experiment within each genotype in the behavior and cellular cohorts. (C) Prior to Cd treatment, baseline behavior was assessed with the open field and novel object location (NOL) tests. Animals began Cd treatment through drinking water (0.6 mg/L $CdCl_2$) at 8-10 weeks of age. Cognitive function was probed every other week with NOL test. Once memory deficits were confirmed by NOL test at three consecutive time points, animals were given tamoxifen or vehicle (n=12-15/group) treatment to induce caMEK5 expression. Follow up behavior tests were performed to assess cognitive function after tamoxifen or vehicle treatment. At the end of the experiment, blood and one brain hemisphere were collected for Cd analysis. The other brain hemisphere was fixed and frozen for histology. (D) Tissue collection in the cellular cohort was based on NOL rescue confirmation in the behavior cohort.

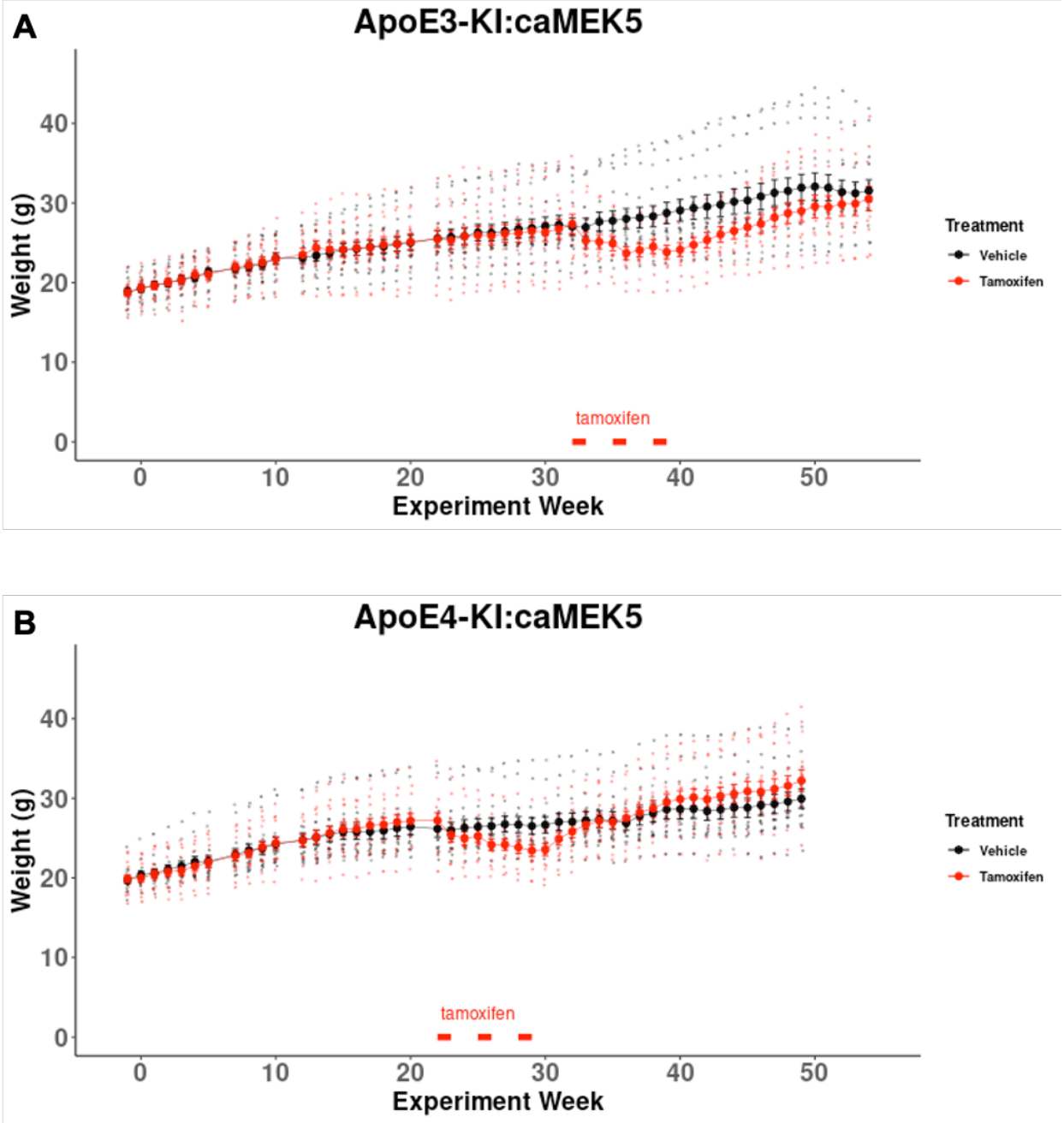

Figure 3.2. Behavioral cohort animal weights for (A) ApoE3:caMEK5 and (B) ApoE4:caMEK5. Bars (blue) indicate tamoxifen treatment. Data are presented as mean+/- SEM.

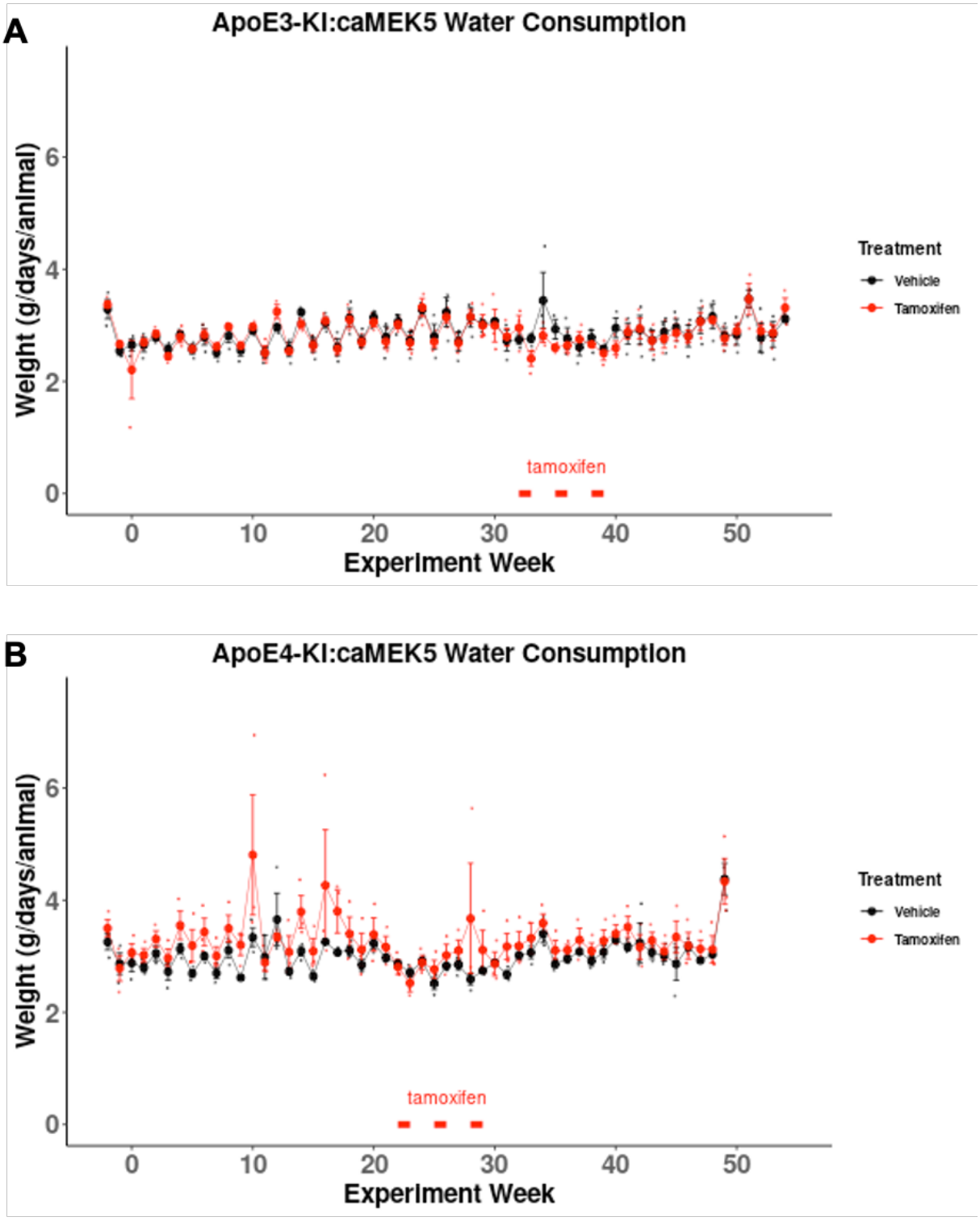

Figure 3.3. Behavioral cohort water consumption for (A) ApoE3:caMEK5 and (B) ApoE4:caMEK5. Bars (blue) indicate tamoxifen treatment. Data are presented as mean+/- SEM.

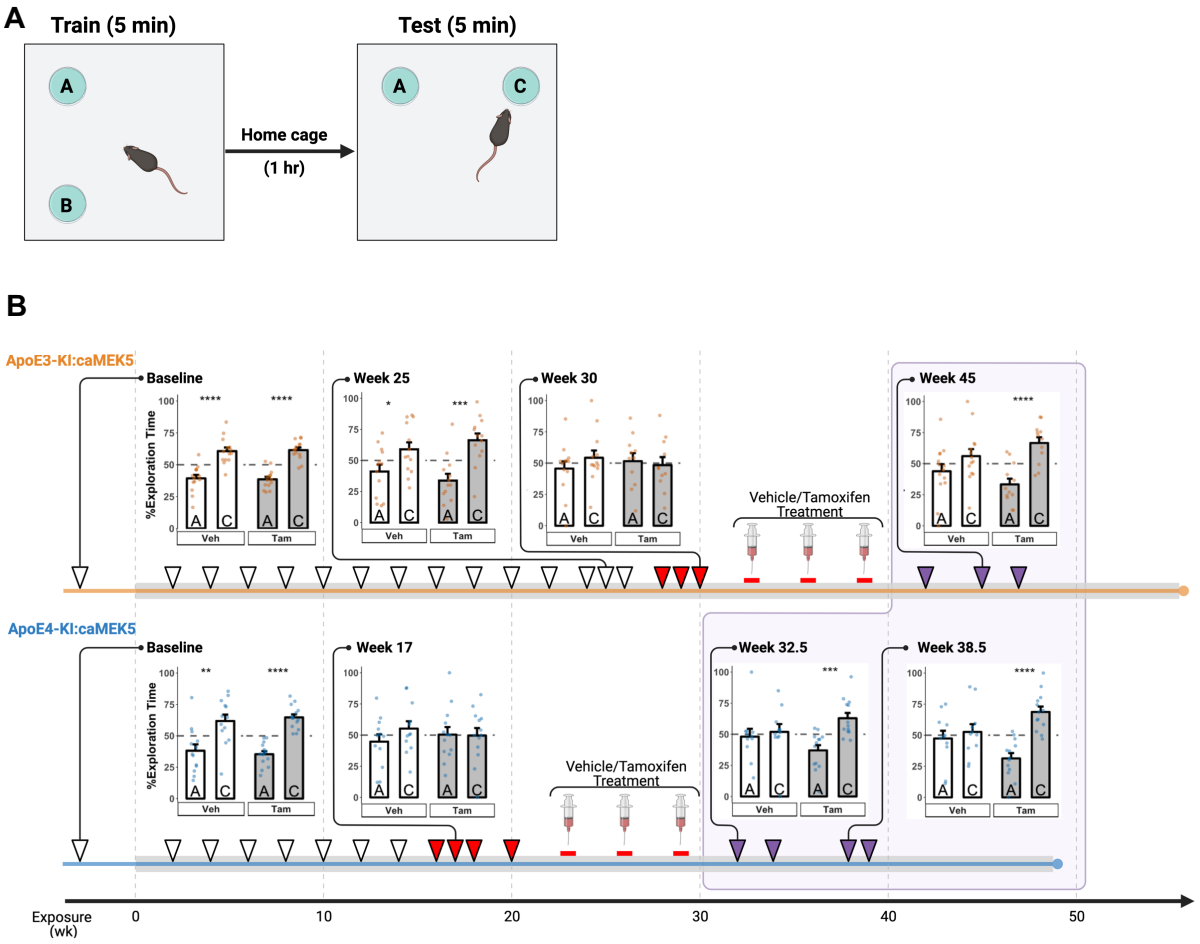

Figure 3.4. Effects of Cd exposure on hippocampus-dependent short-term spatial memory in the novel object location (NOL) test. Cd treatment lasted throughout the experiment (gray box); each test time point is indicated with an arrowhead. (A) Schematic of NOL test. The duration of time each mouse spent exploring identical objects in the old location A and novel location C was quantified. (B) ApoE3-KI and ApoE4-KI mice were unable to distinguish between the old and new locations starting at 28 and 16 weeks, respectively. Observed NOL impairments are indicated in red. Time points after vehicle/tamoxifen treatment is boxed in light purple. Both ApoE3-KI:caMEK5 and ApoE4-KI:caMEK5 mice were able to distinguish between the old and new locations following tamoxifen treatment. ApoE3-KI:control and ApoE4-KI:control mice continued to be unable to distinguish between old and new locations. Data are presented as mean+/- SEM. Welch's two tailed t-test: *p <= .05, **p <= 0.01, ***p <= 0.001, ****p <= 0.0001

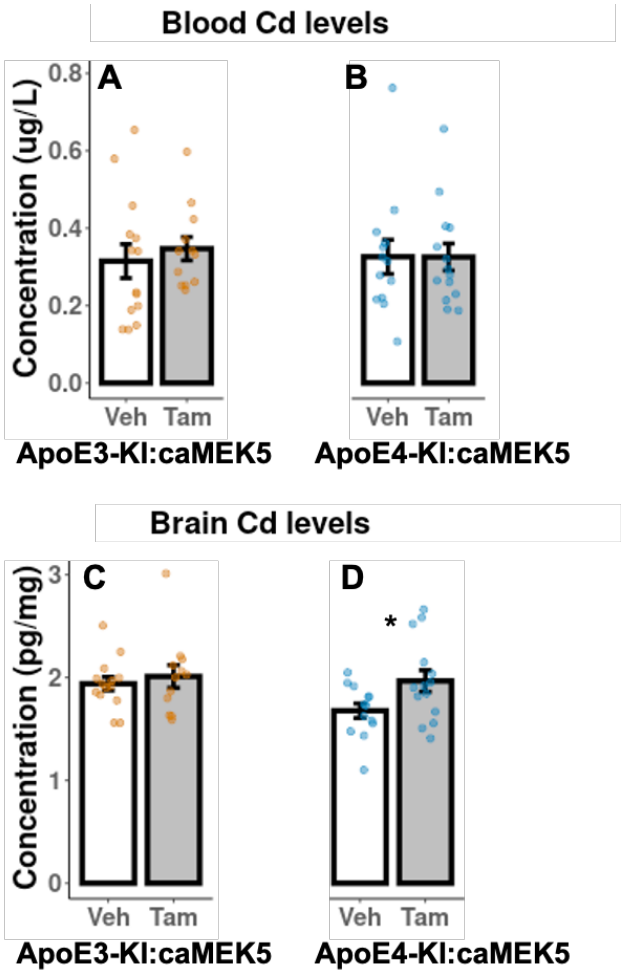

Figure 3.5. Cd concentrations in mouse blood and brain hemisphere at the end of experiment, after 54 weeks of exposure (ApoE3-KI:caMEK5) or 49 weeks of exposure (ApoE4-KI:caMEK5). There were no significant differences between vehicle and tamoxifen treated groups in (A) blood Cd of ApoE3-KI, (B) blood Cd of ApoE4-KI, or (C) brain Cd of ApoE3-KI. (D) Tamoxifen treated ApoE4-KI mice had significantly higher brain Cd levels compared to vehicle treated ApoE4-KI mice. Data are presented as mean+/- SEM. Welch's two tailed t-test: *p <= .05

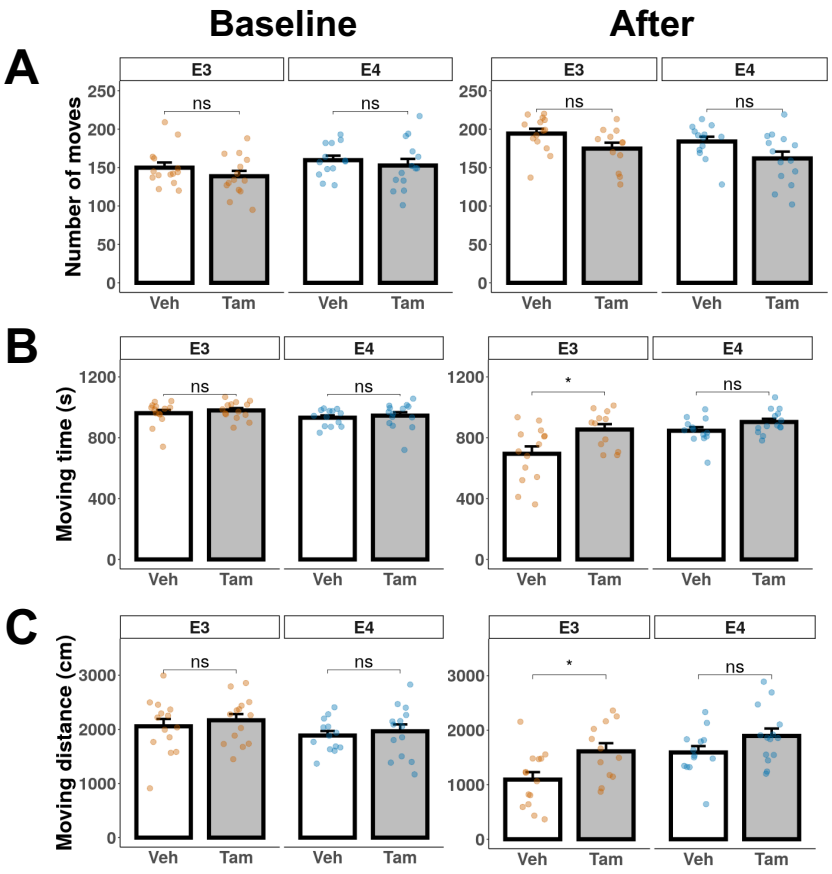

Figure 3.6. Locomotor activity of ApoE3-KI and ApoE4-KI mice (n=12-15/group) measured in the open field test at baseline and after Cd + Veh/Tam treatment. There were no significant difference between Veh and Tam treated ApoE3-KI mice in the (A) number of moves. Tam treated ApoE3-KI mice showed in increase in (B) total moving time, (C) total moving distance, and (D) speed. There was no significant difference between Veh and Tam treated ApoE4-KI mice in the (A) number of moves, (B) total moving time, (C) total moving distance, (D) speed, or (E) rest time. Data are presented as mean+/- SEM. Welch's two tailed t-test: *p <= .05

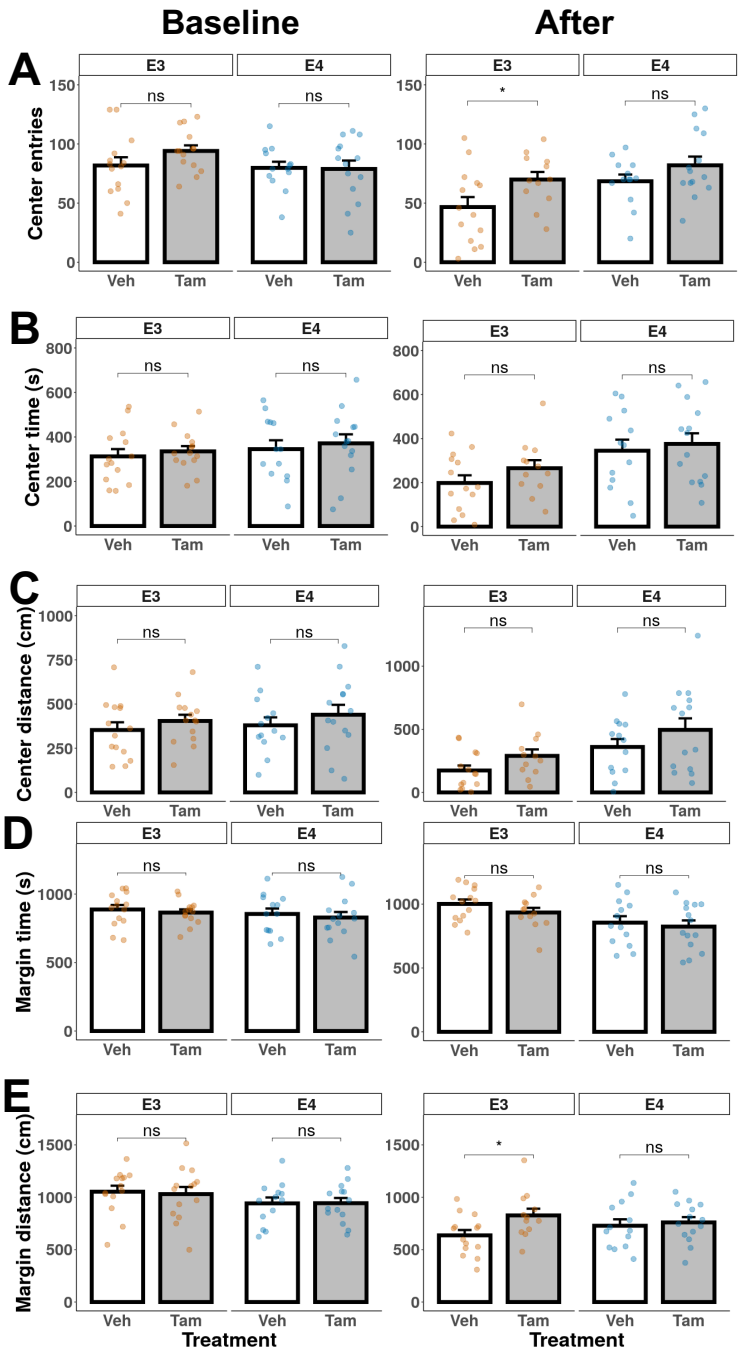

Figure 3.7 Anxiety behavior of ApoE3-KI and ApoE4-KI mice (n=12-15/group) measured in the open field test at baseline and after Cd + Veh/Tam treatment. There were no significant difference between Veh and Tam treated ApoE3-KI mice in the (B) center time, (C) center distance, and (D) margin time. Tam treated ApoE3-KI mice exhibited increased (A) number of entries to center, and increased (E) margin distance. There was no significant difference between Veh and Tam treated ApoE4-KI mice in the (A) number of entries to center, (B) center time, (C) center distance, (D) margin time, or (E) margin distance. Data are presented as mean+/- SEM. Welch's two tailed t-test: *p <= .05

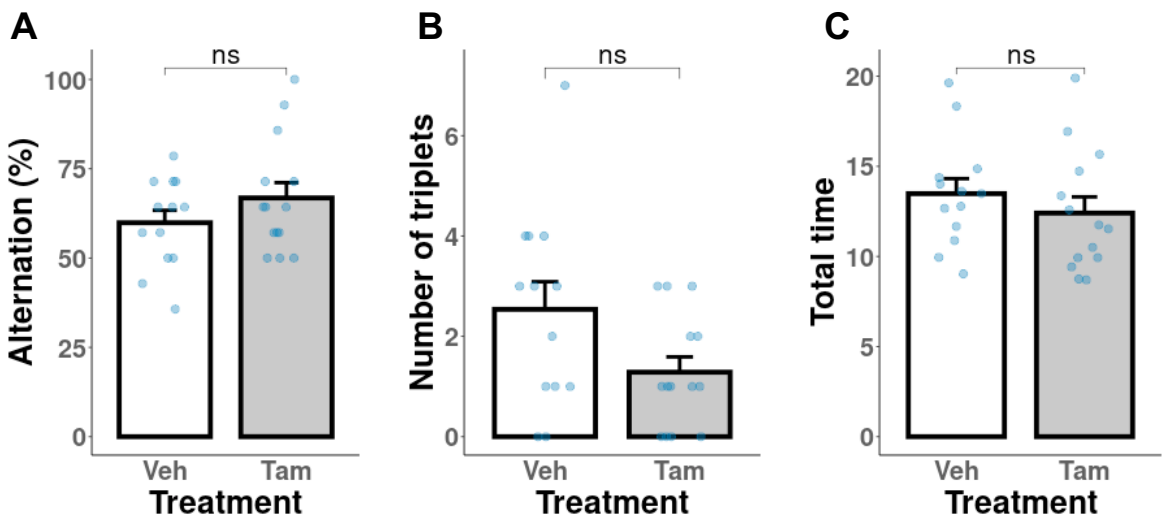

Figure 3.8. Spontaneous alternation in ApoE4-KI:caMEK5 mice in the T-maze test after tamoxifen treatment. There were no significant differences between the tamoxifen and vehicle treated group in (A) percent of alternation, (B) number of triplets, or (C) total duration of the test.

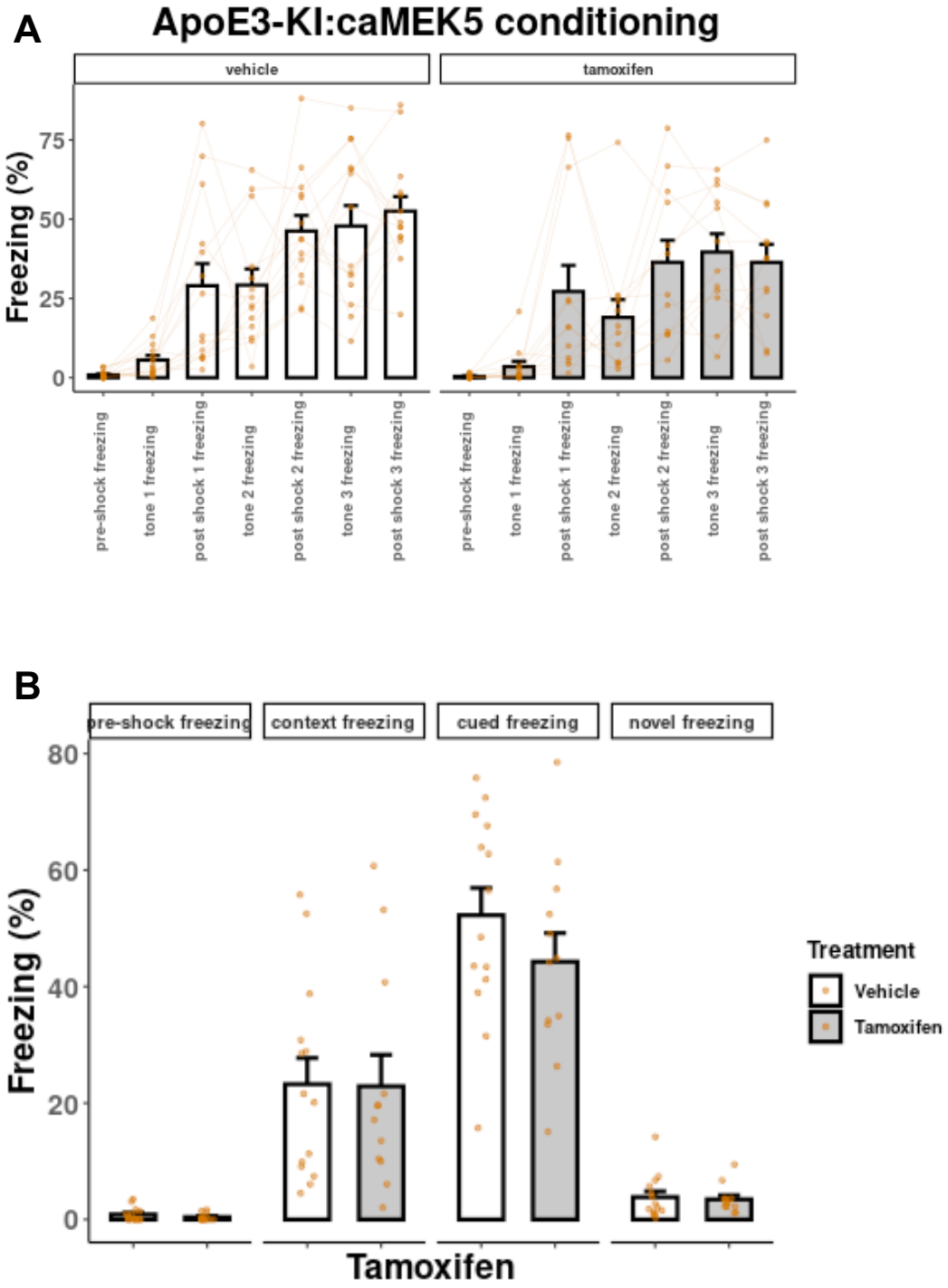

Figure 3.9. Cued and contextual fear conditioning in ApoE3-KI:caMEK5 after tamoxifen treatment during conditioning (A) and in contextual, cued, and novel freezing tests (B).

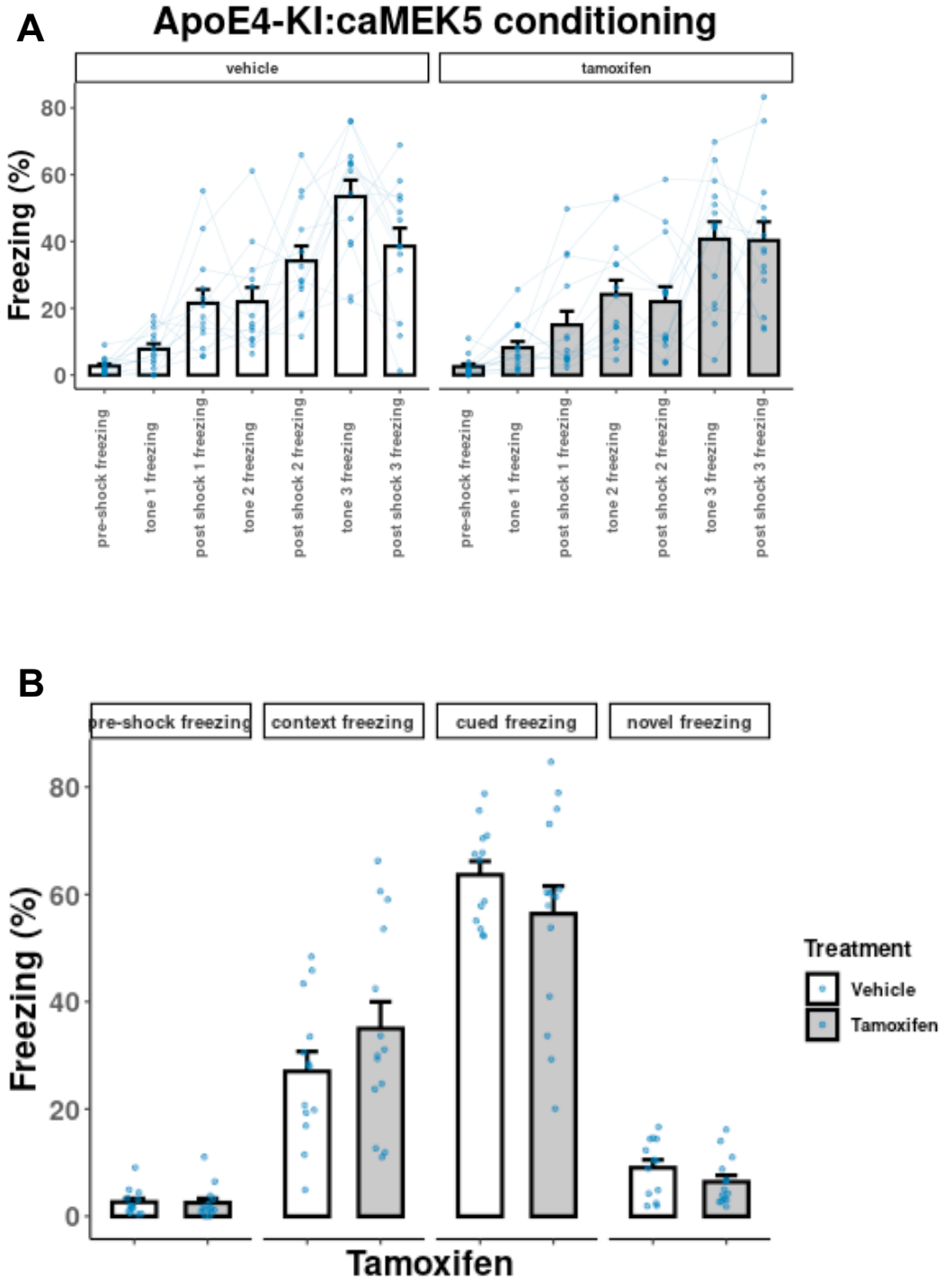

Figure 3.10. Cued and contextual fear conditioning in ApoE4-KI:caMEK5 after tamoxifen treatment during conditioning (A) and in contextual, cued, and novel freezing tests (B).

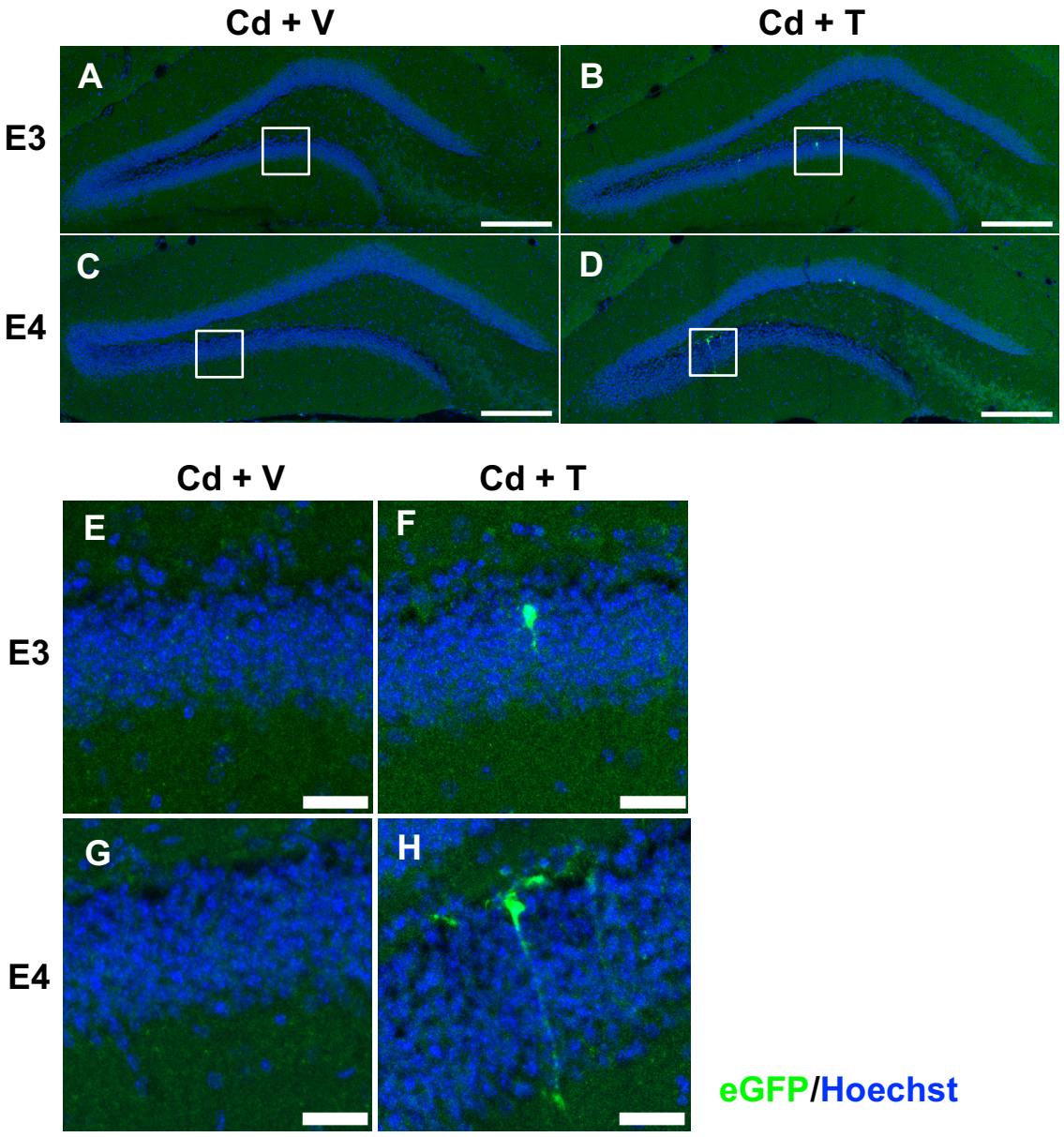

Figure 3.11. Representative images of TSA signal amplified caMEK5-eGFP signal. Full dentate gyrus field images were taken on a 20x objective and stitched in LAS X (A-D); scale bar: 200 µm. (E-H) Zoomed in images from ROI shown in A-D; scale bar: 30 µm.

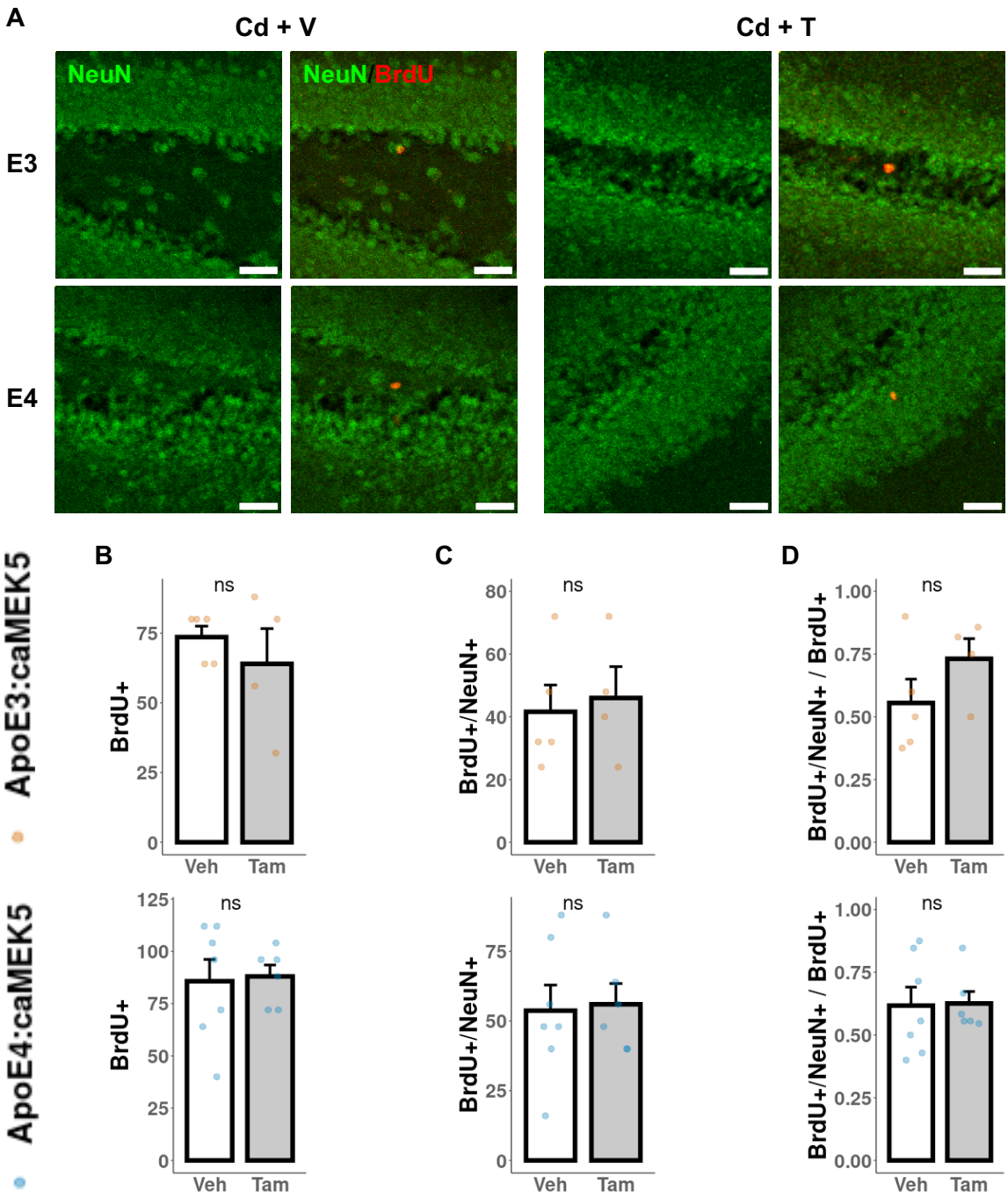

Figure 3.12. Quantification of adult-born neurons that differentiated into mature neurons in the DG. (A) Representative images of BrdU+ and NeuN+ staining in the DG. Scale bar, 30 μm. Quantification of (B) total number of BrdU+ cells, (C) total number of BrdU+ and NeuN+ cells, and (D) ratio of BrdU+ and NeuN+ cells to BrdU+ cells for tamoxifen or vehicle treated ApoE3-KI:caMEK5 (n = 4-5) and ApoE4-KI:caMEK5 (n = 6-7) mice. Data are presented as mean +/- SEM.

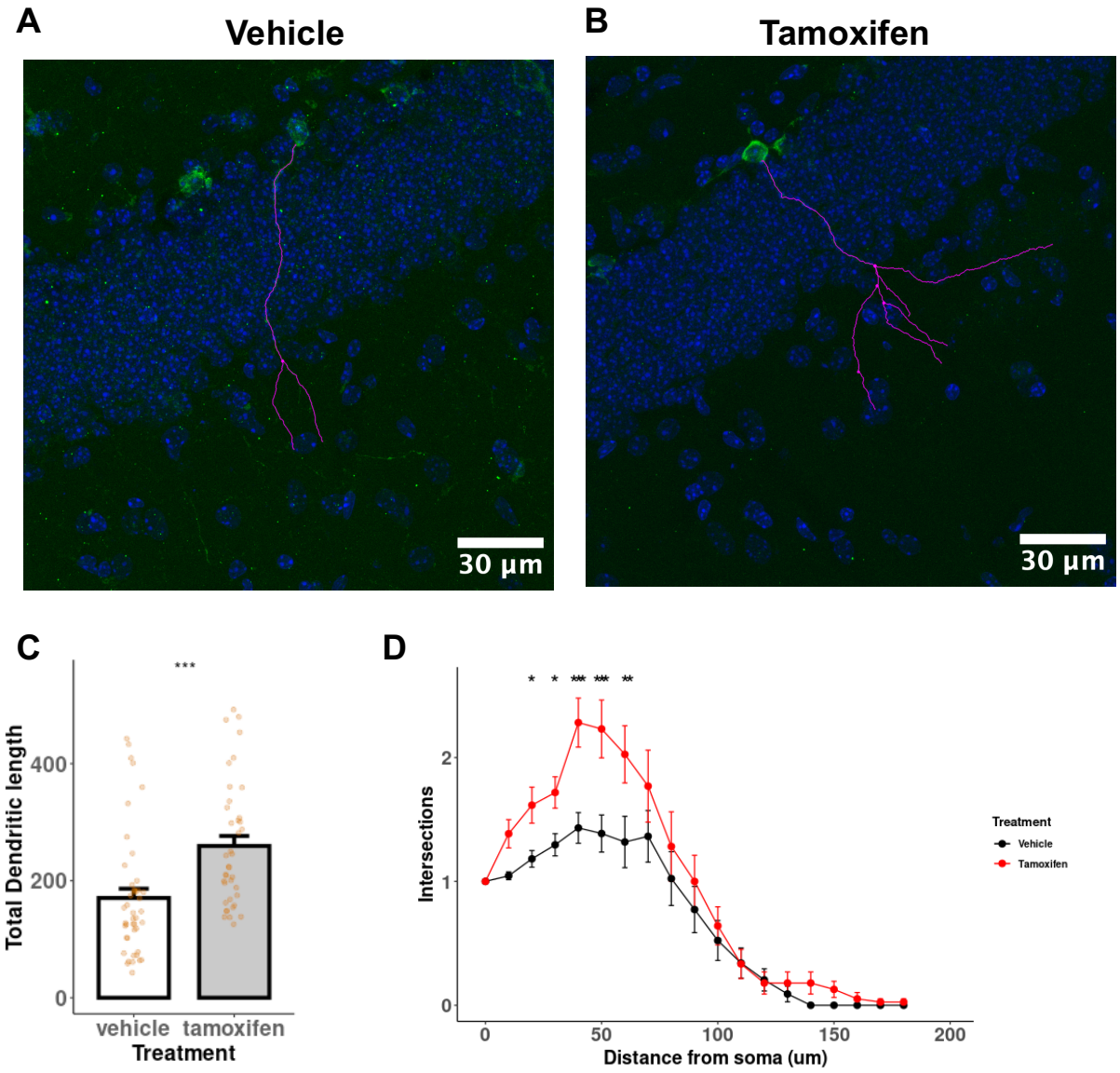

Figure 3.13. Dendritic branching of DCX+ cells in ApoE3-KI:caMEK5 mice. (A-B) Representative images of traced cells for vehicle-treated (A) and tamoxifen-treated (B) animals. (C) Tamoxifen-treated animals have significantly increased total dendritic length compared to vehicle-treated animals. Welch's two tailed t-test: p = 0.00026. (D) Tamoxifen-treated animals have significantly increased numbers of intersections compared to vehicle-treated animals. Pairwise comparisons at each experimental week were based on estimates from mixed-effects linear regression, with Tukey HSD correction: *p <= .05, ** p <= 0.01, *** p <= 0.001. N = 3-4 animals per group, >= 40 cells per group.

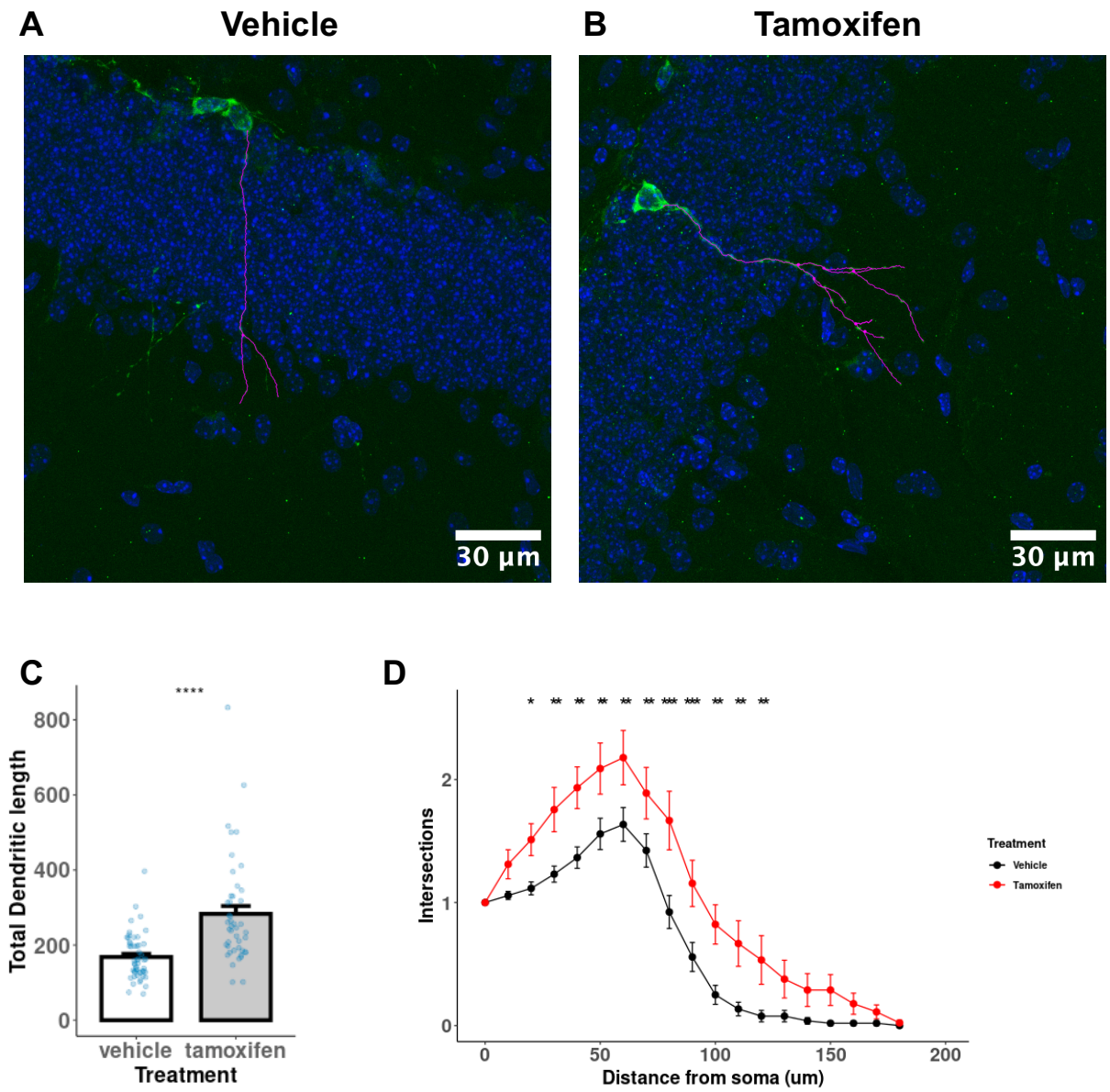

Figure 3.14. Dendritic branching of DCX+ cells in ApoE4-KI:caMEK5 mice. (A-B) Representative images of traced cells for vehicle-treated (A) and tamoxifen-treated (B) animals. (C) Tamoxifen-treated animals have significantly increased total dendritic length compared to vehicle-treated animals. Welch's two tailed t-test: p = 4.6e-06. (D) Tamoxifen-treated animals have significantly increased numbers of intersections compared to vehicle-treated animals. Pairwise comparisons at each experimental week were based on estimates from mixed-effects linear regression, with Tukey HSD correction: *p <= .05, ** p <= 0.01, *** p <= 0.001. N = 3-4 animals per group, >= 40 cells per group.

Chapter 4. Conclusions and Future Directions

Neurological effects of acute cadmium (Cd) exposures have been reported as early as the 1970s with descriptions of occupational and accidental exposures in humans and toxicology studies in rodents (ATSDR, 2012). While the 2012 ATSDR report concluded that there is not enough evidence of neurological effects of Cd exposure, the body of literature that followed its publication converge on the potent neurotoxic effects of Cd. Epidemiologic and toxicological studies, including those from our laboratory, report findings that Cd is a potent neurotoxicant at exposure levels relevant to the US general population (Ciesielski et al., 2013; Li et al., 2018; Wang et al., 2020, 2019, 2018). However, the mechanisms underlying low level Cd neurotoxicity are not yet well understood. Cd is in the top 10 of the ATSDR Substance Priority List due to its ubiquitous commercial and industrial use and high waste accumulation (ATSDR, 2019). Despite gradually decreasing trends of markers of Cd exposure in the general population (Centers for Disease Control and Prevention, 2022; Tellez-Plaza Maria et al., 2012), Cd remains a public health concern due to the persistence and lifetime accumulation of Cd as a result of its long biological half-life of 10-30 years (Suwazono et al., 2009) combined with its ubiquity. This dissertation describes mouse model studies to address cellular and molecular mechanisms underlying Cd impairment on memory by combining behavior paradigms with state-of-the-art *in vivo* calcium (Ca^{2+}) imaging and transgenic mouse models.

Chapter 2 describes experiments utilizing a state-of-the-art *in vivo* Ca^{2+} imaging method to investigate the effects of Cd exposure on calcium activity in hippocampal neurons *in vivo* in freely behaving mice. Cd has been described to mimic Ca^{2+} and to disrupt Ca^{2+}-dependent signaling through direct interference with signaling molecules as well as indirect interference through changes in intracellular Ca^{2+} levels (Templeton and Liu, 2018; Thévenod et al., 2018). Transient increases in intracellular Ca^{2+} levels in the brain, including the CA1 region of the

hippocampus, are necessary for learning and memory (Sabatini et al., 2002; Wang and Storm, 2003; Zamorano et al., 2018; Zhang et al., 2019). In our study, Ca^{2+} activity in excitatory neurons in CA1 was recorded *in vivo* in animals treated with Cd during acquisition and recall of fear memory. We found that fewer neurons are activated in Cd-treated groups compared to control during fear memory conditioning and recall, suggesting that Cd may contribute to learning and memory deficit by reducing activity of neurons. We observed these effects at Cd exposure levels that result in blood Cd levels comparable to the general US population levels. This provides a molecular mechanism for Cd interference of learning and memory at exposure levels relevant to US adults. To our knowledge, our study is the first to describe Cd effects on brain Ca^{2+} activity *in vivo* in freely behaving mice.

Chapter 3 describes a functional rescue experiment utilizing a transgenic mouse model that allows for conditional and specific genetic activation of adult neurogenesis in a mouse model of Alzheimer's disease to investigate the link between impairment of adult neurogenesis and memory impairment in a GxE model of ApoE4 and Cd. Our data from both behavior and cellular experiments support a causal link between adult neurogenesis and memory impairment. This provides a cellular mechanism for Cd impairment of memory in a GxE model at exposure levels relevant to US adults. This study also highlights the therapeutic potential of enrichment of adult neurogenesis both through pharmacological targets as well as through accessible stimuli such as physical exercise and environmental enrichment to ameliorate or prevent cognitive decline.

The works presented in this dissertation support the idea that Cd is neurotoxic at levels relevant to the general population and more importantly, at levels currently considered to be safe. Further research is required to understand the underlying mechanisms of low-level Cd neurotoxicity and how recent findings in toxicological studies translate to and integrate with epidemiology studies. Current regulatory and advisory limits should be revisited based on the body of work published within the last decade to protect public health.

Future directions

Limitations with time and resources made explorations of the connection between Chapters 2 and 3 outside of the scope of this dissertation. Nevertheless, there are several potential connections between Ca^{2+} signaling, AD, and adult neurogenesis that warrant future study. Dysregulation of Ca^{2+} homeostasis and impairments in Ca^{2+} signaling have been implicated in AD (Alzheimer's Association Calcium Hypothesis Workgroup, 2017). Adult-born neurons are sensitive to signals from a diverse set of cells in their environment and may be particularly sensitive to disruption of Ca^{2+} signals (Aimone et al., 2014; Danielson et al., 2016). Impairment of hippocampal adult neurogenesis is highly correlated with the progression of AD in human patients (Moreno-Jiménez et al., 2019). These connections can be teased apart through studies integrating *in vivo* imaging methods with mouse models of AD (e.g. ApoE4-KI), Cre-driver mouse lines (e.g. Nestin-Cre), and Cre-dependent GCaMP6 virus.

Recent advances in technology facilitates never-before possible studies of complex crosstalk between the central nervous system with other organs and their interactions with toxicants and the host genetics. My early graduate work during a rotation in Dr. Julia Cui's laboratory contributed to research that described profound modification of the gut-liver axis in ApoE4-KI male mice, which were most susceptible to Cd-induced memory impairments (Zhang et al., 2021). I expect that integration of system biology and -omics methods into studies of environmental neurotoxicants in both novel toxicology systems such as three-dimensional *in vitro* models from human-induced pluripotent cells in future studies (Yin et al., 2018) and *in vivo* models have the capacity to open exciting and highly insightful mechanistic research in Cd neurotoxicity.

4.1 References

Aimone JB, Li Y, Lee SW, Clemenson GD, Deng W, Gage FH. 2014. Regulation and Function of Adult Neurogenesis: From Genes to Cognition. *Physiol Rev* **94**:991–1026. doi:10.1152/physrev.00004.2014

Alzheimer's Association Calcium Hypothesis Workgroup. 2017. Calcium Hypothesis of Alzheimer's disease and brain aging: A framework for integrating new evidence into a comprehensive theory of pathogenesis. *Alzheimers Dement J Alzheimers Assoc* **13**:178-182.e17. doi:10.1016/j.jalz.2016.12.006

ATSDR. 2019. 2019 Substance Priority List. https://www.atsdr.cdc.gov/spl/index.html

ATSDR (Agency for Toxic Substances and Disease Registry). 2012. Toxicological Profile for Cadmium.

Centers for Disease Control and Prevention. 2022. National Report on Human Exposure to Environmental Chemicals: Data Table Viewer. https://www.cdc.gov/exposurereport/

Ciesielski T, Bellinger DC, Schwartz J, Hauser R, Wright RO. 2013. Associations between cadmium exposure and neurocognitive test scores in a cross-sectional study of US adults. *Environ Health* **12**. doi:10.1186/1476-069X-12-13

Danielson NB, Kaifosh P, Zaremba JD, Lovett-Barron M, Tsai J, Denny CA, Balough EM, Goldberg AR, Drew LJ, Hen R, Losonczy A, Kheirbek MA. 2016. Distinct Contribution of Adult-Born Hippocampal Granule Cells to Context Encoding. *Neuron* **90**:101–112. doi:10.1016/j.neuron.2016.02.019

Li H, Wang Z, Fu Z, Yan M, Wu N, Wu H, Yin P. 2018. Associations between blood cadmium levels and cognitive function in a cross-sectional study of US adults aged 60 years or older. *BMJ Open* **8**:e020533. doi:10.1136/bmjopen-2017-020533

Moreno-Jiménez EP, Flor-García M, Terreros-Roncal J, Rábano A, Cafini F, Pallas-Bazarra N, Ávila J, Llorens-Martín M. 2019. Adult hippocampal neurogenesis is abundant in neurologically healthy subjects and drops sharply in patients with Alzheimer's disease. *Nat Med* **25**:554–560. doi:10.1038/s41591-019-0375-9

Sabatini BL, Oertner TG, Svoboda K. 2002. The Life Cycle of Ca2+ Ions in Dendritic Spines. *Neuron* **33**:439–452. doi:10.1016/S0896-6273(02)00573-1

Suwazono Y, Kido T, Nakagawa H, Nishijo M, Honda R, Kobayashi E, Dochi M, Nogawa K. 2009. Biological half-life of cadmium in the urine of inhabitants after cessation of cadmium exposure. *Biomarkers* **14**:77–81. doi:10.1080/13547500902730698

Tellez-Plaza Maria, Navas-Acien Ana, Caldwell Kathleen L., Menke Andy, Muntner Paul, Guallar Eliseo. 2012. Reduction in Cadmium Exposure in the United States Population, 1988–2008: The Contribution of Declining Smoking Rates. *Environ Health Perspect* **120**:204–209. doi:10.1289/ehp.1104020

Templeton DM, Liu Y. 2018. Interactions of Cadmium with Signaling Molecules In: Thévenod F, Petering D, M. Templeton D, Lee W-K, Hartwig A, editors. Cadmium Interaction with Animal Cells. Cham: Springer International Publishing. pp. 53–81. doi:10.1007/978-3-319-89623-6_3

Thévenod F, Petering D, M. Templeton D, Lee W-K, Hartwig A, editors. 2018. Cadmium Interaction with Animal Cells. Cham: Springer International Publishing. doi:10.1007/978-3-319-89623-6

Wang H, Abel GM, Storm DR, Xia Z. 2019. Cadmium Exposure Impairs Adult Hippocampal Neurogenesis. *Toxicol Sci* **171**:501–514. doi:10.1093/toxsci/kfz152

Wang H, Matsushita MT, Zhang L, Abel GM, Mommer BC, Huddy TF, Storm DR, Xia Z. 2020. Inducible and Conditional Stimulation of Adult Hippocampal Neurogenesis Rescues Cadmium-Induced Impairments of Adult Hippocampal Neurogenesis and Hippocampus-Dependent Memory in Mice. *Toxicol Sci Off J Soc Toxicol* **177**:263–280. doi:10.1093/toxsci/kfaa104

Wang H, Storm DR. 2003. Calmodulin-Regulated Adenylyl Cyclases: Cross-Talk and Plasticity in the Central Nervous System. *Mol Pharmacol* **63**:463–468. doi:10.1124/mol.63.3.463

Wang H, Zhang L, Abel GM, Storm DR, Xia Z. 2018. Cadmium Exposure Impairs Cognition and Olfactory Memory in Male C57BL/6 Mice. *Toxicol Sci Off J Soc Toxicol* **161**:87–102. doi:10.1093/toxsci/kfx202

Yin F, Zhu Y, Wang Y, Qin J. 2018. Engineering Brain Organoids to Probe Impaired Neurogenesis Induced by Cadmium 8.

Zamorano C, Fernández-Albert J, Storm DR, Carné X, Sindreu C. 2018. Memory Retrieval Re-Activates Erk1/2 Signaling in the Same Set of CA1 Neurons Recruited During Conditioning. *Neuroscience*, Molecular and Cellular Mechanisms of Cognitive Function **370**:101–111. doi:10.1016/j.neuroscience.2017.03.034

Zhang A, Matsushita M, Zhang L, Wang H, Shi X, Gu H, Xia Z, Cui JY. 2021. Cadmium exposure modulates the gut-liver axis in an Alzheimer's disease mouse model. *Commun Biol* **4**:1–16. doi:10.1038/s42003-021-02898-1

Zhang L, Chen X, Sindreu C, Lu S, Storm DR, Zweifel LS, Xia Z. 2019. Dynamics of a hippocampal neuronal ensemble encoding trace fear memory revealed by in vivo Ca2+ imaging. *PLoS ONE* **14**. doi:10.1371/journal.pone.0219152